

Aus dem Institut für Klinische Neuroimmunologie  
der Ludwig-Maximilians-Universität München  
Direktor: Prof. Dr. med. Martin Kerschensteiner



**Calcium and structural dynamics of the axonal  
endoplasmic reticulum in animal models of  
spinal cord injury and multiple sclerosis**

Dissertation  
zum Erwerb des Doktorgrades der Medizin  
an der Medizinischen Fakultät der  
Ludwig-Maximilians-Universität zu München

vorgelegt von  
Jonas Lehmitz  
aus Hamburg

2021

---

Mit Genehmigung der Medizinischen Fakultät  
der Universität München

Berichterstatter: Prof. Dr. med. Martin Kerschensteiner

Mitberichterstatter: Prof. Dr. med. Jochen Herms

PD Dr. med. Astrid Blaschek

Prof. Dr. rer. nat. Christian Behrends

Mitbetreuung durch den

promovierten Mitarbeiter: Prof. Dr. med. Thomas Misgeld

Dekan: Prof. Dr. med. Thomas Gudermann

Tag der mündlichen Prüfung: 16.12.2021

# Table of Contents

<b>List of Figures</b> .....	<b>IV</b>
<b>List of Tables</b> .....	<b>IV</b>
<b>List of Abbreviations</b> .....	<b>V</b>
<b>Zusammenfassung</b> .....	<b>IX</b>
<b>Summary</b> .....	<b>XI</b>
<b>1. Introduction</b> .....	<b>1</b>
1.1. Multiple Sclerosis .....	1
1.1.1. Epidemiology and aetiology .....	1
1.1.2. Diagnosis and clinical course .....	2
1.1.3. Pathomechanism .....	3
1.1.4. Animal models .....	6
1.2. Spinal cord injury .....	8
1.2.1. Epidemiology and aetiology .....	8
1.2.2. Pathomechanism .....	8
1.2.3. Animal models .....	13
1.3. Endoplasmic Reticulum .....	14
1.3.1. Organisation of neuronal ER .....	14
1.3.2. Functions of neuronal ER .....	15
1.3.3. ER calcium homeostasis .....	18
1.3.4. Structural dynamics of the ER .....	21
1.4. Axon degeneration .....	23
1.4.1. Patterns and mechanisms of axon degeneration .....	23
1.4.2. Role of calcium in axon degeneration .....	28
1.4.3. Role of ER calcium in axon degeneration .....	30
1.5. In vivo imaging of neuronal calcium levels .....	31
1.5.1. Genetically encoded calcium indicators .....	32
1.5.2. In vivo microscopy of the nervous system .....	34
<b>2. Materials and Methods</b> .....	<b>37</b>
2.1. Reagents .....	37
2.1.1. Surgery and in vivo imaging .....	37

2.1.2.	Immunization.....	38
2.1.3.	Tissue processing / immunohistochemistry.....	38
2.2.	Materials .....	39
2.2.1.	Surgery and in vivo imaging.....	39
2.2.2.	Tissue processing / immunohistochemistry.....	40
2.3.	Technical devices .....	40
2.3.1.	Surgery and in vivo imaging.....	40
2.3.2.	Microscopy.....	41
2.3.3.	Tissue processing / immunohistochemistry.....	41
2.4.	Data analysis / software.....	41
2.5.	Experimental animals .....	42
2.6.	Methods.....	42
2.6.1.	Tissue processing and immunohistochemistry.....	42
2.6.2.	In vivo microscopy .....	43
2.6.3.	Pharmacological experiments .....	44
2.6.4.	EAE induction and in vivo imaging.....	45
2.6.5.	Spinal cord contusion model .....	46
2.6.6.	Image processing and data analysis.....	46
<b>3.</b>	<b>Contributions of other lab members to the thesis project .....</b>	<b>48</b>
<b>4.</b>	<b>Objectives .....</b>	<b>50</b>
<b>5.</b>	<b>Results .....</b>	<b>51</b>
5.1.	Imaging ER calcium in spinal cord axons of Thy1-TwitchER mice .....	51
5.1.1.	Evaluation of Twitch2B 54S+ ER expression pattern and intracellular localization.....	51
5.1.2.	Optimization of in vivo imaging conditions for ER calcium measurements .....	53
5.1.3.	Pharmacological characterization of Thy1-TwitchER mice .....	54
5.2.	Imaging structural and calcium dynamics of the ER in models of axon degeneration.....	56
5.2.1.	ER calcium release and fragmentation after contusion injury .....	56
5.2.2.	Absence of ER calcium release in early stages of FAD .....	59
5.2.3.	Spatial regulation of ER calcium levels along stage 1 axons .....	60
5.2.4.	Absence of temporal ER calcium fluctuations in FAD .....	62
5.2.5.	Relation of ER and cytoplasmic calcium levels in spinal cord axons .....	63

<b>6. Discussion</b> .....	<b>66</b>
6.1. In vivo imaging of ER calcium signals in axons .....	66
6.1.1. Evaluation of Twitch2B 54S+ ER .....	66
6.1.2. Morphological characterization of Thy1-TwitchER mice .....	68
6.1.3. Functional characterization of Thy1-TwitchER mice .....	69
6.2. Structural and calcium dynamics of the ER in axon degeneration .....	71
6.2.1. Evaluation of the used animal models .....	71
6.2.2. ER dynamics in traumatic axon injury .....	74
6.2.3. ER calcium release in EAE .....	76
6.2.4. Sources of elevated intra-axonal calcium in EAE.....	79
6.3. Concluding remarks and outlook .....	84
<b>7. References</b> .....	<b>87</b>
<b>Acknowledgements</b> .....	<b>108</b>
<b>Affidavit / Eidesstattliche Versicherung</b> .....	<b>109</b>

## List of Figures

Figure 1: Inflammation in Multiple Sclerosis .....	4
Figure 2: Pathophysiology of Spinal Cord Injury.....	9
Figure 3: Calcium signalling of neuronal ER.....	19
Figure 4: FAD in EAE and MS .....	25
Figure 5: Mechanisms of axon degeneration.....	26
Figure 6: Increased cytoplasmic calcium predicts axonal fate in EAE .....	29
Figure 7: Twitch2B 54 S+ ER expression pattern and colocalization with GRP78/BiP .....	51
Figure 8: Introducing a 1:30 h waiting time post-surgery increases ER calcium levels in Thy1-TwitchER mice .....	53
Figure 9: Response of Thy1-TwitchER mice to ER calcium depleting agents .....	55
Figure 10: Temporal dynamics of ER calcium and structure after contusion injury ..	57
Figure 11: ER calcium release only occurs late in FAD .....	59
Figure 12: ER calcium levels are similar in swollen and non-swollen sections of stage 1 axons .....	61
Figure 13: No temporal ER calcium release events occur in healthy control and EAE mice.....	62
Figure 14: Caffeine-mediated ER calcium depletion does not cause measurably increases of cytoplasmic calcium .....	64
Figure 15: Extracellular calcium is responsible for elevated cytoplasmic calcium levels and axon degeneration.....	80

## List of Tables

Table 1: EAE clinical scoring scale.....	45
--	----

## List of Abbreviations

2-APB	2-Aminoethoxydiphenyl borate
4-CEP	4-Chloro-3-ethylphenol
AAD	Acute axon degeneration
aCSF	Artificial cerebrospinal fluid
AIF	Apoptosis-inducing factor
AMPA	$\alpha$ -amino-3-hydroxy-5-methyl-4-isoxazolepropionic acid
APP	Amyloid precursor protein
ASIC	Acid-sensing ion channel
ATF6	Activating transcription factor 6
ATL	Atlastin
ATP	Adenosine triphosphate
BAPTA	1,2-Bis(o-aminophenoxy)ethane-N,N,N',N'-tetraacetic acid
BiP/GRP78	Binding immunoglobulin protein / glucose-regulated protein 78
Ca <sup>2+</sup>	Calcium
CAMKII	Ca <sup>2+</sup> / calmodulin-dependent protein kinase II
CFP	Cyan fluorescent protein
CICR	Calcium-induced calcium release
CIS	Clinically isolated syndrome
Climp-63	Cytoskeleton-linking membrane protein 63
CNS	Central nervous system
CPA	Cyclopiazonic acid
CSD	Cortical spreading depolarization
CSF	Cerebrospinal fluid
DiIc	(5)-DS (1,1'-Dioctadecyl-3,3,3',3'-Tetramethylindodicarbocyanine-5,5'-Disulfonic acid)
DIS	Dissemination in space
DIT	Dissemination in time
DMD	Disease-modifying drug
DMSO	Dimethyl sulfoxide
DNA	Deoxyribonucleic acid
DRG	Dorsal root ganglion
EAE	Experimental autoimmune encephalomyelitis
EBV	Epstein-Barr virus
EGTA	(Ethylene glycol-bis( $\beta$ -aminoethyl ether)-N,N,N',N'-tetraacetic acid
ER	Endoplasmic reticulum
ERp57	Endoplasmic reticulum resident protein 57

FAD	Focal axonal degeneration
fMRI	Functional magnetic resonance imaging
FP	Fluorescent protein
FRET	Förster resonance energy transfer
GABA	Gamma-aminobutyric acid
GECI	Genetically encoded calcium indicator
GFP	Green fluorescent protein
GluR	Glutamate receptor
GTP	Guanosine triphosphate
HLA	Human leukocyte antigen
HyD	Hybrid detector
ICD	International classification of diseases
IP <sub>3</sub>	Inositol trisphosphate
IP <sub>3</sub> R	Inositol trisphosphate receptor
IRE1 $\alpha$	Inositol-requiring enzyme 1 alpha
JNK	c-Jun N-terminal kinase
K <sup>+</sup>	Potassium
K <sub>d</sub>	Dissociation constant
KO	Knockout
KX	Ketamine, xylazine
LiSCI	Laser-induced spinal cord injury
MAC	Membrane attack complex
MAM	Mitochondria-associated ER membrane
MBP	Myelin basic protein
Mg <sup>2+</sup>	Magnesium
MMF	Medetomidine, midazolam and fentanyl
MOG	Myelin oligodendrocyte glycoprotein
mPTP	Mitochondrial permeability transition pore
MRI	Magnetic resonance imaging
mRNA	Messenger ribonucleic acid
MRS	Magnetic resonance spectroscopy
MS	Multiple sclerosis
N.A.	Numeric aperture
Na <sup>+</sup>	Sodium
NAA	N-acetylaspartic acid
NAD	Nicotinamide adenine dinucleotide
NCX	Sodium-calcium exchanger
NE	Nuclear envelope
NMDA	N-methyl-D-aspartic acid

NMNAT	Nicotinamide mononucleotide adenylyltransferase
NO	Nitric oxide
OSER	Organized smooth endoplasmic reticulum
PBS	Phosphate-buffered saline
PERK	Protein kinase R-like endoplasmic reticulum kinase
PFA	Paraformaldehyde
PLP	Proteolipid protein
PM	Plasma membrane
PNS	Peripheral nervous system
PPMS	Primary progressive multiple sclerosis
Ptx	Pertussis toxin
REEP	Receptor expression-enhancing protein
RER	Rough endoplasmic reticulum
RNS	Reactive nitrogen species
ROCK	Rho-associated protein kinase
ROI	Region of interest
ROS	Reactive oxygen species
RRMS	Relapsing-remitting multiple sclerosis
Rtn	Reticulon
RyR	Ryanodine receptor
SCI	Spinal cord injury
SD	Standard deviation
SER	Smooth endoplasmic reticulum
SERCA	Sarco/endoplasmic reticulum calcium ATPase
Smac/DIABLO	Second mitochondria-derived activator of caspase / Diablo homolog
SOCE	Store-operated calcium entry
SOD	Superoxide dismutase
SPMS	Secondary progressive multiple sclerosis
STIM	Stromal interaction molecule
TAC	Tip-attachment complex
TG	Thapsigargin
TMEM170A	Transmembrane protein 170A
TnC	Troponin C
TNF $\alpha$	Tumor necrosis factor alpha
TRPC	Transient receptor potential cation channel
TwER	Thy1-TwitchER
UPE4B	Ubiquitin conjugation factor E4 B
UPR	Unfolded protein response

US	United States
VGCC	Voltage-gated calcium channel
WD	Wallerian degeneration
Wld <sup>s</sup>	Wallerian degeneration slow
YFP	Yellow fluorescent protein
Yop1	Yersinia enterocolitica outer membrane protein 1

## Zusammenfassung

Bei der Multiplen Sklerose und der traumatischen Rückenmarksverletzung handelt es sich um Erkrankungen des zentralen Nervensystems, bei denen die irreversiblen neurologischen Einschränkungen maßgeblich durch bleibende axonale Schäden bedingt sind. Vorarbeiten in unserem Labor konnten zeigen, dass erhöhte intraaxonale Kalziumkonzentrationen das Schicksal der Axone in neuroinflammatorischen und traumatischen Läsionen bei Mäusen bestimmen. Das endoplasmatische Retikulum (ER), ein bedeutender zytoplasmatischer Kalziumspeicher, ist in der Literatur als mögliche Quelle für den schädlichen Kalziumanstieg in Axonen beschrieben worden und könnte daher wesentlich zur axonalen Degeneration beitragen. Aus diesem Grund wurde in unserem Labor eine transgene Mauslinie namens Thy1-TwitchER generiert, die den genetisch kodierten ratiometrischen Kalziumindikator Twitch2B 54S+ in Nervenzellen exprimiert.

Aufbauend auf diesen Vorarbeiten habe ich in der vorliegenden Arbeit zuerst das Expressionsmuster in dieser neuen Mauslinie charakterisiert und bestätigt, dass der Kalziumsensor in Neuronen und Axonen des Rückenmarks exprimiert wird. Nach der Optimierung des in vivo Mikroskopieprotokolls für die Thy1-TwitchER Mäuse konnte die richtige Funktionsweise des Twitch2B 54S+ Sensors unter in vivo Bedingungen nachgewiesen werden, indem mittels verschiedener Pharmaka schnelle und langsame Kalziumfreisetzungen aus dem ER ausgelöst wurden. In einem spinalen Kontusionsmodell konnte ich in der Folge zeigen, dass es unmittelbar nach dem Trauma zu einer inkompletten ER-Kalzium Entleerung und ER-Fragmentierung kommt. Diese beiden Prozesse verliefen unabhängig voneinander und konnten sich im weiteren Zeitverlauf teilweise wieder zurückbilden. Im Gegensatz dazu kam es in der Experimentellen Autoimmunen Enzephalomyelitis (EAE), einem Mausmodell der Multiplen Sklerose, in degenerierenden Axonen zu keinen Veränderungen im Kalziumgehalt des ER. Lediglich in bereits fragmentierten Nervenfasern, die kein Regenerationspotential mehr besitzen, konnte ich eine ER-Kalzium Freisetzung beobachten. Überraschenderweise konnte ich zudem beobachten, dass die in vivo Applikation von Koffein, zwar wie erwartet eine Depletion des gesamten ER-Kalziumgehaltes induziert, dies aber zu keiner messbaren Erhöhung der intraaxonalen Kalziumkonzentration beiträgt. Daraus ließ sich schließen, dass Kalziumfreisetzungen aus dem ER nicht ursächlich für den zytoplasmatischen Kalziumanstieg sind, der das

Fortschreiten der axonalen Degeneration bedingt. Weitere Experimente unserer Arbeitsgruppe identifizierten komplementierend Schäden der Plasmamembran als Eintrittspforte für Kalzium aus dem extrazellulären Raum.

Diese Ergebnisse erweitern den aktuellen Wissensstand über die Dynamiken des ER in Mausmodellen der Multiplen Sklerose und der traumatischen Rückenmarksverletzung. Zukünftig könnten Untersuchungen mit der Thy1-TwitchER Mauslinie weitere Erkenntnisse über die Physiologie und Pathologie des ER liefern und eventuell auch neue Therapieansätze für neurodegenerative Erkrankungen ermöglichen.

## Summary

Multiple sclerosis (MS) and spinal cord injury (SCI) are both diseases of the central nervous system where persistent axonal loss is a major contributor to the irreversible neurological disability. Preceding studies in our laboratory could reveal that intra-axonal calcium increases are responsible for determining the axonal fate in experimental autoimmune encephalomyelitis (EAE) and after spinal cord contusion in mice. The endoplasmic reticulum (ER), a major intracellular calcium store, has been considered to be a source for such detrimental cytoplasmic calcium increases and could thus play an important role in axon degeneration. Therefore, the transgenic mouse line Thy1-TwitchER with the genetically encoded ratiometric calcium indicator Twitch2B 54S+ was generated in our laboratory.

Based on this preceding work I first characterized the expression pattern of this new mouse line in this thesis and could confirm that the used calcium sensor is correctly located in neurons and axons of the spinal cord. After optimizing the in vivo microscopy protocol for Thy1-TwitchER mice, the proper functionality of the Twitch2B 54S+ sensor in the in vivo approach was verified using several pharmacological agents which induce slow or fast ER calcium depletions. In the spinal cord contusion model I could subsequently show the occurrence of a partial depletion of ER calcium and ER fragmentation immediately after the trauma. Both processes appeared to be independent from each other and capable of recovery over the time course. However, in EAE axons undergoing focal axon degeneration I could not detect an ER calcium release. Depletions of ER calcium could only be found in fragmented axons whose fate was already determined. Surprisingly, I could also observe that the in vivo application of caffeine, which leads to the expected complete ER calcium depletion, does not cause measurable increases of intra-axonal calcium concentrations. Consequently, a calcium release from the ER as a source for intra-axonal calcium elevations, which trigger axon degeneration, could be ruled out. Further studies in our laboratory could however demonstrate that plasma membrane ruptures trigger the detrimental calcium influx from the extracellular space.

These results expand the current knowledge about ER dynamics in mouse models of MS and SCI. In the future, research with the novel Thy1-TwitchER mouse line could lead to further insights about the physiology and pathology of this organelle and potentially to new therapeutic approaches for neurodegenerative diseases.

# 1. Introduction

The degeneration of the neuron and its processes plays an important role in different groups of neurological diseases, including degenerative, traumatic and inflammatory central nervous system (CNS) disorders. Each of these has its own distinct aetiology but some aspects of the pathomechanism that lead to neuronal loss might be similar. Prominent examples of the classic degenerative CNS disorders are Alzheimer's disease, Parkinson's disease and Amyotrophic lateral sclerosis. Traumatic SCI, also being one of the first models, in which the degeneration process of axons has been studied, leads to neurodegeneration after partial or complete disruption of axonal fibre tracts. Neurological disabilities in MS, probably the best investigated inflammatory CNS disease, have been shown to be also determined by axon degeneration and neuronal loss (Lingor et al. 2012; Correale et al. 2019). As this thesis focuses on the pathomechanisms of axon degeneration in MS and SCI, these neurological diseases will be discussed in detail in the following paragraphs

## 1.1. Multiple Sclerosis

### 1.1.1. Epidemiology and aetiology

"She was very fit, she was a non-smoker, non-drinker, and I say all of this because of course then for her to be diagnosed at 35 with an illness that would kill her was just the most enormous shock to us and everyone who knew her."(Joanne K. Rowling, 2014)

Multiple sclerosis, the chameleon of neurological diseases, was first described by Jean-Martin Charcot in 1868 and has since then been in the focus of many researchers due to its still unknown exact cause, variable disease course and symptoms as well as the lack of a cure. The mean age of a MS diagnosis is in the late twenties to early thirties, but even children or people over the age of 60 diagnosed with MS can rarely be seen. The female to male sex ratio has increased in the last decades and is now at about 3:1 (F:M) (Orton et al. 2006). There is an increasing prevalence and incidence of MS, only partly attributable to the improved diagnosis and higher survival, which results in relevant economic and social problems (Browne et al. 2014; Flachenecker et al. 2017).

Until today, the exact aetiology of MS is still unclear, however epidemiological studies have identified several genetic and environmental risk factors. The fact that about one

out of eight MS patients has a positive family history as well as the concordance excess of monozygotic over dizygotic twins underline the genetic influence of MS susceptibility (Harirchian et al. 2018; Willer et al. 2003). This genetic risk has been shown to be associated with the HLA-DRB1 locus, however more genes have already been identified by genome-wide association studies (Hollenbach und Oksenberg 2015; Jager et al. 2009; International Multiple Sclerosis Genetics Consortium 2019a, 2019b). Regarding environmental risk factors studies have shown that nearly all MS patients have been infected with EBV, with individuals having high titres of anti-EBV antibodies and / or having a history of infectious mononucleosis being at an increased risk to develop MS (Levin et al. 2005; Nielsen et al. 2007). Furthermore, low Vitamin D levels and smoking are associated with an increased hazard for MS (Sintzel et al. 2018; Palacios et al. 2011).

### 1.1.2. Diagnosis and clinical course

In 2013 the National Multiple Sclerosis Society has published a revised form of the definition of clinical courses of MS, defining four different types:

A clinically isolated syndrome (CIS) describes the first clinical episode of symptoms suggestive of inflammatory demyelination in the CNS, indicating the possibility of MS, until the criteria of dissemination in space (DIS) and time (DIT) have been proven in order to finally diagnose MS. This means that the affection of multiple different CNS areas at different timepoints is required, fulfilled by clinical evidence (e.g. second episode or at least another clinical objective lesion), MRI or cerebrospinal fluid (CSF) analysis. These requirements are implemented in the McDonald criteria for MS diagnosis, that have been revised for the third time in 2017 (Thompson et al. 2018). Conversion rates from CIS into clinically definite MS range around 60%, with the likelihood depending on the CNS location of the first presentation of demyelination (Fisniku et al. 2008). Here, early treatment of CIS patients has been shown to be effective in delaying the conversion into MS (Comi et al. 2009).

Relapsing-remitting MS (RRMS) describes a clinical course defined by unpredictable acute periods of neurological symptoms (relapses) and their disappearance (remission), where the deficits that appeared during the relapse might recover or symptoms may persist. However, in between each relapse there is no progression of the disease. This type represents the initial disease course of 80% of MS patients, but

around 90% of RRMS patients will have developed a secondary progressive (SPMS) course after 20 to 25 years of onset (Trojano et al. 2003). This continuous disease progression can still be superimposed with intermittent relapses and minor remissions. Around 15 to 20% of MS patients suffer from primary progression from the onset of the disease without any previous relapses, thus named primary progressive MS (PPMS). The mean age of onset of this form of the disease is at 40 years and therefore around ten years later than in RRMS (Miller und Leary 2007). Yet, no matter if patients showed secondary progression after RRMS or had a primarily progressive clinical course, the median age of disease progression and the time course of disability progression is comparable. In addition, the prognosis of MS, meaning progression of irreversible disability, seems to be more dependent on the age of onset, rather than the initial clinical disease course (Confavreux und Vukusic 2006). These findings suggest that there are presumably common underlying pathomechanisms for the different clinical disease courses.

### 1.1.3. Pathomechanism

Primarily assumed to be a neuroinflammatory disease, there are currently two different models to explain the pathomechanism of MS: The outside-in model states that a dysregulated immune system leads to CNS injury, the inside-out model argues that a primary nervous system damage initiates a secondary inflammatory response. However, current knowledge cannot fully contradict either of these models, thus there is a dualistic approach in research focusing on inflammation and neurodegeneration (Stys et al. 2012).

#### 1.1.3.1 Inflammation

The inflammatory process is thought to be initiated by a loss of self-tolerance with the activation of autoreactive T cells in the periphery, that, after migrating across the blood-brain barrier, get reactivated in the CNS by local antigen-presenting cells presenting CNS autoantigens. This process leads to the recruitment and activation of T cells, B cells, macrophages and microglia, which damage the myelin sheaths. While peripheral T cells are supposed to be activated by a phenomenon known as molecular mimicry (Wucherpfennig und Strominger 1995), the subsequent myelin damage results in a release of further CNS autoepitopes that leads to the activation of more self-reactive T

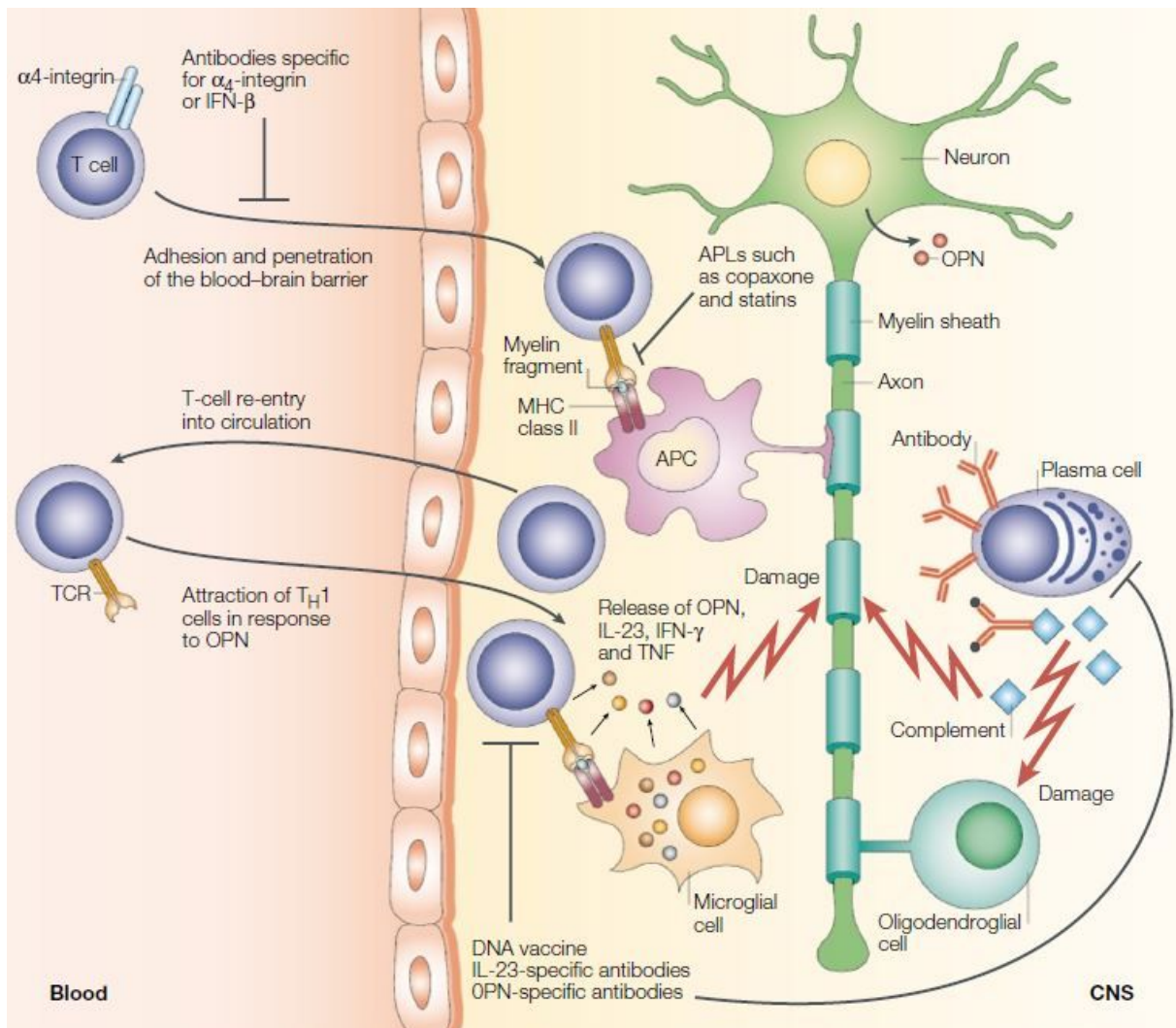


**Figure 1: Inflammation in Multiple Sclerosis**

Autoreactive T cells diapedese into the CNS via  $\alpha_4$ -integrin and get activated by antigen-presenting cells leading to recirculation, recruitment and activation of more T cells, B cells, macrophages and microglia. Release of cytokines damages oligodendroglial cells and the insulating myelin sheaths around the axon. Activated B cells (plasma cells) secrete antibodies against myelin proteins which recruit the complement system and further damage axonal myelination. Figure from and caption modified from (Steinman und Zamvil 2003)

cells and thus a wider autoimmune response (Miller et al. 1997). Patients with MS have been shown to have a larger amount of  $CD8^+$  T cells and  $CD4^+$  T cells with a proinflammatory Th1 and Th17 phenotype compared to healthy patients (Crawford et al. 2004; Tzartos et al. 2008; Li et al. 2017). On top of that B cells have been in the focus of intense research, as not only B cells themselves and autoantibodies directed against targets such as MBP, PLP, MOG and axonal proteins have been found in the CNS and CSF of MS patients (Warren und Catz 1994; Stich et al. 2016), but also meningeal B cell aggregates that exhibit a more severe cortical pathology in secondary progressive MS (Figure 1) (Howell et al. 2011). This relevance of B cells in MS can be

supported by the fact that B cell targeted immunotherapies have shown to be successful and were therefore implemented into the guidelines for MS therapy (Hauser et al. 2017; Montalban et al. 2017).

#### 1.1.3.2 Demyelination

A central element of disease pathology in MS is the formation of demyelinating lesions in the CNS caused by the dysregulated cells of the immune system. By now, neuropathological studies have discovered four different patterns of demyelination in MS tissue. Pattern I and II show similar features, as both are induced by T cells and macrophages. Yet, in Pattern II additional antibodies and complement mediate the myelin damage. The lack of those suggests a damage process via products released by activated macrophages, such as TNF $\alpha$  in pattern I. Pattern III lesions, which in contrast to pattern I and II lesions are not located around inflamed vessels, are distinguished by a loss of oligodendrocytes due to apoptosis. If demyelination appears with oligodendrocyte degeneration through DNA fragmentation, a lesion is categorized as pattern IV (Lucchinetti et al. 2000).

#### 1.1.3.3 Axonal Damage

With acute inflammatory lesions being the major driver for the relapses in RRMS it is interesting to note that the likelihood and time of onset of MS progression is independent of the number of relapses in the relapse-remitting phase (Scalfari et al. 2010). On top of that the current therapy strategies with disease-modifying drugs (DMD) that target the inflammatory autoimmune activity are close to unsuccessful in delaying disease progression in PPMS and SPMS (Lublin et al. 2016; Kapoor et al. 2018). Hence, there must be another underlying pathological feature that is responsible for this phenomenon, which is the irreversible neuroaxonal damage.

Several studies have brought up evidence that axonal injury occurs already at disease onset, where damaged axons can be found in active lesions. In histopathology, axonal pathology has been visualized by the abundance of amyloid precursor protein (APP). Normally being transported by fast axonal transport, it accumulates in injured axons due to the breakdown of the cytoskeleton. APP accumulations and thus axonal loss has been demonstrated in acute MS lesions and in active border of less acute lesions (Ferguson et al. 1997). Another histopathological marker for axon injury is SMI-32

which stains non-phosphorylated neurofilaments. Intense SMI-32 immunoreactivity also revealed axonal loss and axonal end bulbs as indicators for transected axons in MS lesions (Trapp et al. 1998). In a more recent study, whole post mortem spinal cords of MS patients with a disease duration of nearly 30 years were analysed. Here, a 60% reduction of the axonal density in the corticospinal tract, equally affecting large and small axons, could be found, supporting the hypothesis that axonal damage is a major contributor to disease progression (Petrova et al. 2018).

Axonal injury has also been detected by magnetic resonance spectroscopy (MRS) of the CNS by measuring a reduction of N-acetyl-aspartate (NAA), which is a neuronal/axonal marker. MRS studies of spinal cords of MS patients showed a reduction of NAA levels by 30% in moderately affected and by over 50% in paralyzed patients (Bjartmar et al. 2000; Blamire et al. 2007). Another study has combined MRS with fMRI in MS patients without impairment of their hand motor function, revealing a strong correlation between reduced NAA levels and an increased activation of the sensorimotor cortex after simple hand movements compared to healthy controls. Thus, axonal damage has been linked to the progressive disability in MS, starting in the early stages of the disease. In the beginning this damage can be compensated by adaptive cortical changes, but cumulation of axonal loss will most likely lead to functional impairments (Reddy et al. 2000).

#### 1.1.4. Animal models

In order to study the main pathological processes and to develop potential therapies, different animal models have been developed. Yet, none of them is capable of modelling the exact stages and clinical presentation of MS. Besides virus-induced demyelination and demyelination models induced by toxins such as ethidium bromide, lysolecithin or cuprizone, which are very useful for studying the de- and remyelination processes, EAE is the most utilized animal model for MS pathology. EAE is an inflammatory, demyelinating disease of the CNS, which was first described in primates by Thomas M. Rivers. Since then modifications and variations of EAE have been developed so that mice have become the standard species to investigate EAE and different models now exist for focusing on single aspects of the pathomechanism of MS (Bjelobaba et al. 2018). In general, two main EAE induction methods can be separated: actively induced EAE (aEAE) and passive EAE (pEAE).

In aEAE mice obtain subcutaneous injections of immunogenic myelin proteins, such as myelin oligodendrocyte glycoprotein (MOG) or myelin basic protein (MBP), emulsified in complete Freund's adjuvant, combined with additional injections of pertussis toxin. This initiates a strong immune response, increased blood brain barrier permeability and eventually inflammation, demyelination and axonal damage in the CNS (Stromnes und Goverman 2006a). Passive EAE uses the adoptive transfer of myelin antigen-specific T cells into naïve mice, which is beneficial for studying the role and function of T cells, as they can be labelled prior to injection or manipulated in order to alter their effector function (Stromnes und Goverman 2006b)

The genetic background of mice and the specific myelin antigen has an impact on the disease form of EAE. Immunization with proteolipid protein peptide (PLP) in SJL mice or MOG in Biozzi ABH mice induces a relapsing-remitting disease, whereas C57BL/6 mice injected with MOG develop acute monophasic or chronic forms of EAE (Gold et al. 2006; Bjelobaba et al. 2018).

Despite EAE being the best studied and most commonly used animal model for MS, it is important to note that it also has its downsides and fails to completely recapitulate the pathomechanism of MS. On the one hand, it is obvious that the above described EAE models do not feature the spontaneity of MS, as it is required to induce the disease in the animal model. However, to capture this feature, spontaneous EAE models based on different genetic manipulations have been developed (Goverman et al. 1993; Krishnamoorthy et al. 2006). On the other hand, EAE mostly affects the spinal cord with a high lesion load, which is different from MS where patients often present with inflammatory lesions in the brain and optic nerve. Further, more than thousand therapeutic interventions have been tested in EAE and being stated to be successful in treating EAE. But unfortunately, this success could in many cases not be translated into clinical practice (Baker et al. 2011). However, some disease-modifying drugs, such as natalizumab or mitoxantrone have first been shown to be effective in EAE and are now part of the standard therapy regimen for MS patients (Yednock et al. 1992; Ridge et al. 1985). In summary, animal models, even if different from the actual human disease, have demonstrated to be helpful understanding the biology of MS and bear the possibility to discover new treatment options.

## **1.2. Spinal cord injury**

### **1.2.1. Epidemiology and aetiology**

SCI is a devastating traumatic event, which results in severe neurological impairments, psychological and social problems in patients and a high financial burden. Hence, it has been intensively studied in the last few decades. Epidemiological data reveal differences in prevalence and incidence of SCI between studied countries and regions within them. The highest prevalence has been reported in the United States of America with around 900 cases per million (DeVivo et al. 1980), compared to the lowest prevalence of 280 per million in Finland (Dahlberg et al. 2005). In the US the annual incidence for SCI is at 54 per one million inhabitants (Jain et al. 2015), a high difference of incidence exists between Taipei City and Hualien County in Taiwan. The variation in numbers can be explained by actual differences due to e.g. higher motorcycle usage, alcoholism or violence, however, differences in data collection and ICD coding also have to be taken into account (Lan et al. 1993; Singh et al. 2014).

The mean age of incidence in the US is at 42 years, with the peak age ranging between 15 to 30 years. Japan shows an exception in this trend, where there is a larger proportion of elderly people that experience SCI (Singh et al. 2014). Here, it is important to note that due to the aging of the world's population the number of elderly patients suffering from SCI will increase, forcing healthcare systems to adapt (Fehlings et al. 2013). There is a high male-to-female ratio, in the US 80% of new SCI patients were male.

In general, the primary cause for SCI were traffic accidents followed by falls. Other common causes include gunshot or stab wounds, sports and suicide (Singh et al. 2014).

### **1.2.2. Pathomechanism**

#### **1.2.2.1 Injury Phases**

The pathophysiology of SCI can be divided into a primary and a secondary injury phase, which itself consists of temporally subsequent phases: immediate ( $\leq 2$  hours), early acute ( $\leq 48$  hours), secondary subacute ( $\leq 14$  days), intermediate ( $\leq 6$  months) and chronic ( $\geq 6$  months) (Rowland et al. 2008).

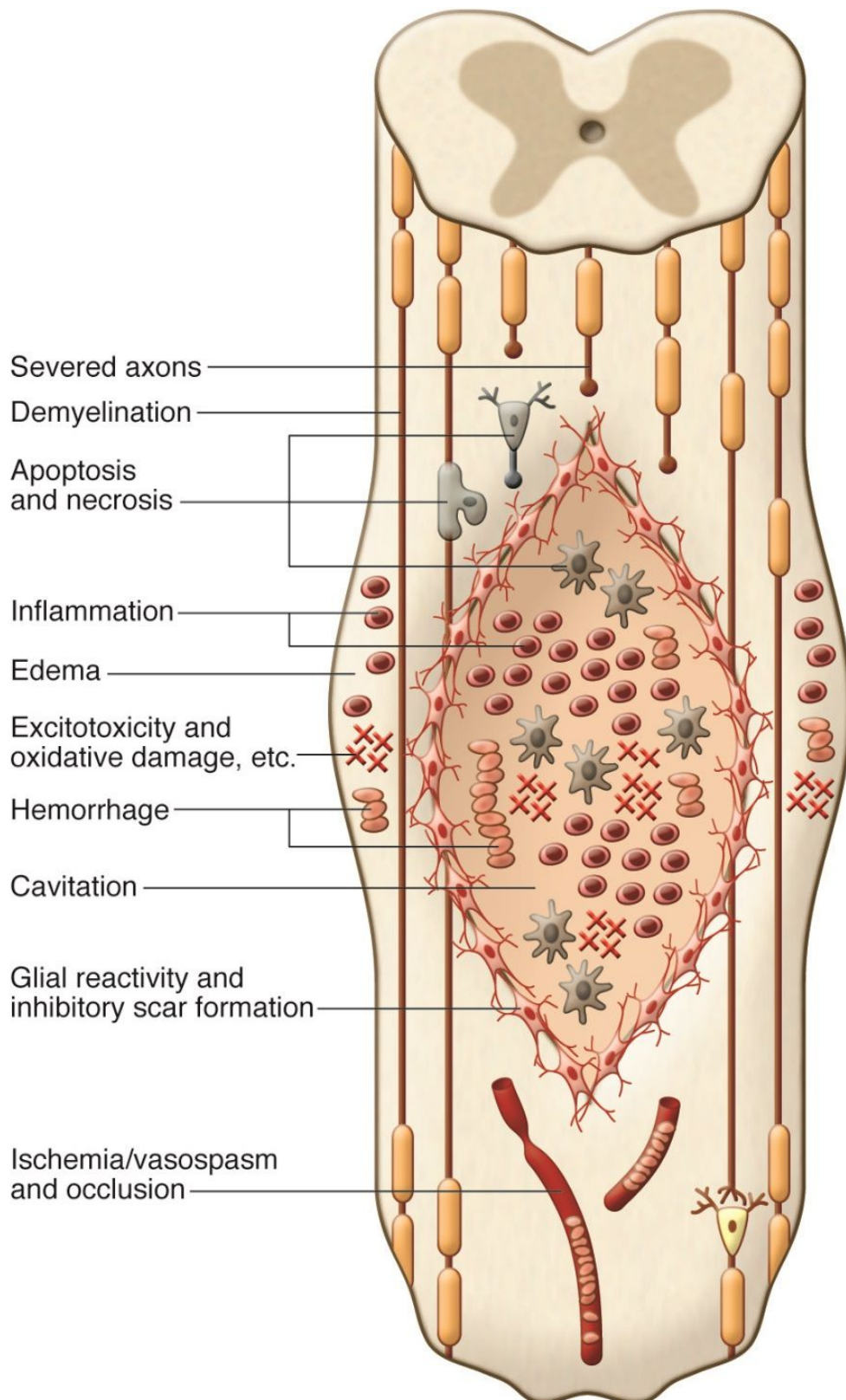


**Figure 2: Pathophysiology of Spinal Cord Injury**

The initial mechanical damage to the spinal cord causes axonal disruption and swelling, haemorrhage and oedema. Secondary to that infiltrating immune cells, microglia and astrocytes initiate an inflammatory response leading to further neuronal damage but also allow regeneration processes. Hypertrophic astrocytes then start forming a glial scar which acts as a blockade for axonal sprouting. Figure modified and caption adapted from (Mothe und Tator 2012)

The primary injury phase is described by the mechanical destruction of CNS tissue by the injury itself. This normally does not lead to a complete transection of the spinal cord, but causes neuronal and glial death, as well as axonal disruption and swelling, due to the disruption of cell membranes. Clinically this results in a phenomenon called spinal shock characterized by the absence of reflexes, paralyzed muscles, neurosensory failure and autonomic abnormalities caudal to the SCI site (Rowland et al. 2008; Ditunno et al. 2004). However, a study in a mouse model has shown that injured axons can be rescued if membranous integrity is regained and degeneration programs are interrupted (Williams et al. 2014). Pathophysiological processes provoked by the primary injury event are part of the secondary injury mechanisms, which lead to further tissue damage and loss.

Besides the direct mechanical damage in the first two hours after injury, major pathophysiological events are haemorrhage, due to the disruption of small vessels, and swelling. This results in CNS ischemia and thus in further necrotic cell death. Already in the first hour post injury microglial activation and the release of proinflammatory cytokines have been described in animal studies (Pineau und Lacroix 2007; Donnelly und Popovich 2008). In addition to abovementioned pathological processes, excitotoxicity and ionic imbalances, oxidative stress and an inflammatory response play important roles in inducing further neuroaxonal damage. Glutamate levels increase after injury causing an influx of sodium and calcium into neurons which leads to swelling and cell death through calpain activation, mitochondrial dysfunction and oxidative stress (Rowland et al. 2008; Rungta et al. 2015). Another critical contributor for secondary damage is oxidative stress as free oxygen radical levels, for instance nitric oxide, superoxide, hydrogen peroxide and peroxynitrite have been shown to be increased in animal models, accompanied with decreased levels of antioxidative agents, such as glutathione. The production of free radicals is thought to be a result of glutamate excitotoxicity, ischemia and following subsequent reperfusion and leads to neuronal death through protein oxidation and lipid peroxidation. As a result mitochondrial membranes are damaged followed by mitochondrial dysfunction and disturbed intracellular ionic homeostasis (Hall et al. 2016; Visavadiya et al. 2016). The highly complex inflammatory response involves activated microglia and astrocytes, infiltrated immune cells and an increased production cytokines and chemokines. Their effects however are complex and can shift over time, as the release of neurotoxic factors results in neuronal death, but the concomitant release of trophic

factors leads to repair processes and axonal sprouting (Figure 2) (Schwab et al. 2014). The following subacute period is characterized by a pronounced phagocytic response that clears the local cell debris and might enhance axon growth. However, intralésional hypertrophic astrocytes begin to form a glial scar, which acts as a barrier to the regeneration processes (Rowland et al. 2008). In contrary to that, studies in mice have revealed that reactive astrocytes also exert a beneficial role by limiting the inflammatory response (Herrmann et al. 2008). In the following phases the glial scar continues to mature and develops cysts which represents the final stage of the SCI lesion (Figure 2). Additionally, axonal sprouting and plasticity processes take place and lead to minor functional recovery (Rowland et al. 2008).

#### 1.2.2.2 Complications

SCI patients suffer from a variety of complications that reduce life quality and increase morbidity and mortality. Damage to motoneurons and corresponding fibre tracts leads to muscle paralysis and after the initial spinal shock to increased muscle tone, exaggerated tendon reflexes and spasticity. This inactive state further causes catabolism of the bones characterized by bone demineralization, hypercalciuria and renal stones. Thus, there is an increased risk for renal failure and bone fractures after SCI (Dudley-Javoroski und Shields 2008).

Disruption of the sympathetic nervous systems after cervical and high thoracic SCI results in reduced cardiac blood return and abnormalities in the cardiac rhythm, such as bradyarrhythmia and ectopic beats. Due to this, hypotension is a common problem in SCI patients which stresses the necessity of adequate cardiovascular monitoring and therapy as low blood pressure can aggravate spinal cord ischemia (Hagen 2015; Rogers und Todd 2016).

Due to physical inactivity and an increased procoagulative state, there is a higher risk of deep vein thrombosis (~17%), potentially leading to pulmonary embolism (Agarwal und Mathur 2009). Other relatively common life-threatening complications are infections, with pneumonia and bloodstream infections being responsible for about one third of deaths in SCI patients. Here, mobilizing patients has proven to be useful for reducing the risk of pneumonia (Garcia-Arguello et al. 2017).

### 1.2.2.3 Axon degeneration

Neurological deficits and disability after SCI mainly depend on the number of remaining axons and their functional state at the lesion site. Direct damage and secondary disease mechanisms are responsible for the disturbance of their integrity.

A spinal cord contusion injury study in mice has identified that axons at the injury site undergo a process of axonal swelling in the first hours post contusion before they eventually break down. This is accompanied by elevated intra-axonal calcium levels, due to the mechanical rupture of the axonal membrane, that trigger degeneration processes. However, axons that succeed in resealing their plasma membrane can restore their intra-axonal calcium levels and thus protect themselves from further axon degeneration (Williams et al. 2014).

Chronic SCI models have shown electrophysiological changes in injured axons with lower excitability, increased refractory period and reduced conduction speed. Concomitant morphological changes included thinner myelin sheaths and an increase in the mean axonal diameter, which can be explained by the appearance of swollen axons and terminal end bulbs (Nashmi und Fehlings 2001). These changes in morphology have also been described in post-mortem human tissue (Puckett et al. 1997). Moreover, human MRI studies in chronic SCI patients ( $\geq 14$  years) have revealed a decrease in the spinal cord cross-sectional area representing spinal atrophy due to long term neuroaxonal degeneration. Diffusion tensor imaging parameters are also altered in the spinal cord illustrating axonal degeneration and demyelination and thus, reduced white matter integrity (Freund et al. 2013).

Until today many studies have focused on neurorestorative processes, such as neuroaxonal repair and cell replacement with neuronal stem cells, embryonic stem cells or olfactory ensheathing cells. Despite these therapeutic approaches of facilitating plasticity have been shown to be beneficial, they might also account for harmful events, like intensifying pain pathways or neuropathic pain (Onifer et al. 2011). These insights stress the importance of focusing research onto neuropreservative interventions, in order to maintain as many axonal projections as possible to reduce neurological disability.

### 1.2.3. Animal models

The era of animal models for experimental SCI was introduced in 1911 with Allen's experiment where a mass was dropped onto a canine's dorsal dura. Since then several different disease models in a variety of animal species have been developed to study SCI.

The most commonly used species are rodents, especially rats, followed by mice. Already the choice of the experimental animal is important, as for example rats develop cystic cavities at the lesion site, resembling the human pathophysiological processes. However, the injury site in mice gets smaller over time without cyst development. This is the reason for rats being more suitable for preclinical studies or testing potential pharmacological treatments. For studying basic pathophysiological processes of SCI mice are equally applicable. Due to significant differences in nervous system complexity and responses between rodents and humans, non-human primates have been used for experimental SCI and advanced our knowledge regarding CNS plasticity, behavioural recovery and the therapeutic potential of brain-machine-interface devices (Lee und Lee 2013).

In most experimental animals, injuries are induced in the dorsal thoracic spinal cord. However, SCI in patients most frequently occurs at the anterior cervical site. Hence, more cervical injury animal models have been developed to achieve a better reflection of the human pathology (Zhang et al. 2014; Pearse et al. 2005).

Furthermore, different types of injury induction exist, with contusion being the most common, followed by transection and compression models. Non-mechanical models, such as ischemic models, induced by temporary aortic occlusion, are rarely used but suitable for studying SCI caused by ischemia/reperfusion and aortic diseases. Spinal cord contusion can be performed by a mass weight drop, a New York university impactor or an Infinite Horizons impactor, that has a good precision and reproducibility (Sharif-Alhoseini et al. 2017; Nardone et al. 2017). For simulating human spinal cord occlusion, or investigating surgical decompression after SCI, compression models are widely used. Finally, in transection models complete or targeted interruption of the spinal cord or specifically selected axonal pathways can be conducted. These models are appropriate for studying regeneration, tissue engineering, plasticity or the role of neuronal circuitries. Withal, in clinical SCI transections can only rarely be seen making

transection models disadvantageous for mimicking the exact pathophysiology of human SCI (Zhang et al. 2014; Sharif-Alhoseini et al. 2017).

### **1.3. Endoplasmic Reticulum**

After first being described as ergastoplasm by C. Garnier in 1897 and E. Veratti's discovery of the sarcoplasmic reticulum in muscle fibres in 1902, the endoplasmic reticulum (ER) was rediscovered in 1945 using electron microscopy. It was described as a "lace-like reticulum" in chicken embryo fibroblasts and due to its endoplasmic enrichment (non-spreading region of fibroblasts) and network structure it was given its current name in 1953 (Porter et al. 1945; Porter 1953). The ER network consists of sheets and tubules and is highly conserved in every eukaryotic cell. Earlier studies in guinea pig pancreas cells have shown that the rough-surfaced ER takes up 22% of the total volume and around 60% of the total membrane surface area (Bolender 1974). Therefore, it is understandable that the ER is vital for every cell, with neurons being no exception, in which the ER even has additional functions.

#### **1.3.1. Organisation of neuronal ER**

Neuronal ER, like the ER in every other cell type, can be divided into three different subdomains: the nuclear envelope (NE), ribosome-rich rough ER (RER) and mostly ribosome-free smooth ER (SER). It is a reticular system consisting of lipids and proteins and has been shown to be continuous throughout the whole neuronal cell body, dendrites and axons. This finding has been achieved by labelling rat Purkinje and hippocampal neurons with 1,1'-dihexadecyl-3,3',3'-tetramethylindocarbocyanine perchlorate (DiIC), which is supposed to spread within a continuous lipid bilayer, and has also been confirmed by other cell studies, where green fluorescent protein (GFP) molecules could diffuse within the ER lumen into areas, which have been photobleached before (Terasaki et al. 1994; Subramanian und Meyer 1997). The NE in neurons, also referred to as the nuclear membrane, consists of a double lipid bilayer without any ribosomes. Its thinner outer membrane has fine undulations and tubular protrusions reaching into the cytoplasm and is connected with the RER network formed out of flat sheets organized in stacks, enriched with ribosomes and interconnected by tubules. This structure, which is abundant in the soma, spreading into the dendrites but is missing in the axon hillock, resembles the Nissl bodies in the equally named

staining (Palay und Palade 1955). The SER in neurons is mostly devoid of ribosomes and predominantly exists in distal dendrites, dendritic spines and in the axon is constituted of differently sized tubules (Wu et al. 2017).

Despite being a continuous network throughout the whole neuron, the ER shows a local heterogeneity in function and morphology. In the soma the ER consists of tubules and cisternae that form a tightly woven reticular structure in the cytoplasm and around other organelles such as mitochondria, lysosomes, vesicles and has contacts to the plasma membrane (PM). The latter, also named cortical ER, provides for around 12,5% of the PM surface and is formed by cisternae with a variable thickness. Thin cortical ER cisternae are devoid of ribosomes (Wu et al. 2017; Rosenbluth 1962). In dendrites smooth and rough ER exists and its structure is mostly tubular with some cisternae. As in the soma, here the ER also forms ER-PM contacts suggesting a frequent interaction. Additionally, the ER reaches into dendritic spines, with 50% of small spines and over 80% of large mushroom spines containing SER. If no ER structure is found in small spines, there are ER tubules reaching into the neck of the spine. In large spines the ER forms stacks of cisternae, called spine apparatus, that frequently connect to the PM (Wu et al. 2017; Spacek und Harris 1997). The existence of ER in dendritic spines suggests a contribution to the synaptic activity. Interestingly, synaptic signalling can lead to reversible morphological alterations of the ER, resulting in consequences for intra-ER protein mobility and calcium signalling (Kucharz et al. 2009). In axons ER appearance is heterogenous, with larger myelinated or non-myelinated axons consisting of large, anastomosed tubules of SER, whereas small axons only contain a single thin tubule. ER tubules size varies between 15 and 30 nm, compared to non-neuronal cells where tubules show a diameter of around 60 nm. Close to synaptic varicosities and at nodes of Ranvier ER tubules widen or form small cisternae that assemble contacts to mitochondria and other organelles. Compared to the soma, axonal ER has a higher amount of contact sites to mitochondria than to the PM (Wu et al. 2017; Tsukita und Ishikawa 1980; Terasaki 2018).

### 1.3.2. Functions of neuronal ER

Most of the functions of the neuronal ER are similar to those of the ER in every other eukaryotic cell, but the fact that neurons are excitable cells combined with their distinct polarized morphology with dendrites and long-distance axons makes neuronal ER

unique. Besides the synthesis of proteins and lipids and the interaction with multiple other cell organelles, the ER in neurons plays an important role in cellular calcium dynamics, which, due to the focus of this research project, will be highlighted in a separate chapter.

Most secreted and transmembrane proteins, proteins of the secretory and endocytotic pathway, as well as ER resident proteins all pass the ER during their synthesis. The nascent polypeptides of these proteins contain a signal recognition particle that binds to the ER membrane leading to the co-translational translocation of the proteins into the ER lumen. Already during the process of translation and post translation proteins receive modifications in the ER and the Golgi apparatus, before they are transported to their site of action (Hong und Tang 1993). This process is controlled by ER resident chaperones that precisely fold new proteins and promote the degradation of misfolded proteins, which is necessary for cellular health and functioning. However, several conditions such as neuronal aging, neuroinflammation, calcium dysregulation, oxidative stress and many more lead to the accumulation and aggregation of misfolded proteins that trigger ER stress followed by the unfolded protein response (UPR) with the aim to either mitigate the stress or induce apoptosis. The UPR is initiated by three transmembrane ER proteins: inositol-requiring protein 1 $\alpha$  (IRE1 $\alpha$ ), activating transcription factor-6 (ATF6) and protein-kinase RNA-like ER kinase (PERK). IRE1 $\alpha$  and ATF6 lead to pro-survival processes via XBP1 inducing ER-associated degradation, whereas IRE1 $\alpha$  also activates apoptotic pathways. PERK inhibits further protein synthesis and initiates the expression of pro-survival genes. If the damage to the cell is too severe, ATF4, a molecule downstream in the PERK pathway, induces cell death. Mutant SOD1 in amyotrophic lateral sclerosis, tau and amyloid  $\beta$  oligomers in Alzheimer's disease and aggregations of  $\alpha$ -synuclein in Parkinson's disease have been shown to trigger the UPR (Hetz und Saxena 2017). Furthermore, an increased expression of UPR proteins has been identified in oligodendrocytes, astrocytes and inflammatory cells in MS and EAE lesions. Examinations of MS and EAE tissue have found elevated levels of proteins linked to ER stress in neurons, which result in mitochondrial dysfunction and neuronal death (Stone und Lin 2015; Haile et al. 2017). In summary, the ER plays an important role in regulating cellular stress by first trying to restore normal function and if impossible initiating cell death.

The main hub for protein synthesis is localized in the soma and the proximal dendritic compartment, where lots of RER can be found. However, distal dendrites and axons

mainly contain SER, hence, the question remains how membrane or secreted proteins are synthesized or transported to their specific location. Currently there are two different theories for protein-trafficking into dendrites. In the canonical pathway proteins are produced in the somatic ER, sorted by the Golgi apparatus and then transported via axonal transport to their target location (Ramírez und Couve 2011). Other studies have shown that mRNA is translated locally in the dendritic ER, which is modulated by synaptic activity and neurotransmitters and is of relevant importance for long-term potentiation and long-term depression. For this purpose, mRNAs are transported to dendrites along microtubules and stored until their translation is initiated (Bramham und Wells 2007). Studying GABAB receptor (GABABR) trafficking into dendrites has revealed another possible mechanism for protein transport involving the ER. GABABR subunits are synthesized in the somatic ER and after transportation along ER membranes locally assemble in the dendritic ER to form the full heteromeric GABABR (Ramírez et al. 2009). The possibility of the local synthesis of transmembrane or secreted proteins in axons is currently under debate. However, there is evidence for the accumulation of mRNA and axonal ribosomes for axonal protein synthesis after damage or during development (Hirai et al. 2017; Shigeoka et al. 2016).

Besides protein synthesis the ER is also important for lipid synthesis. Neuronal ER is capable of synthesizing phospholipids, such as phosphatidylcholine, which makes up more than 50% of the neuronal lipid content, sphingomyelin and other fatty acids (Vance et al. 1991). About 23% of our body's cholesterol is comprised in the brain, mostly in myelin sheaths, but also in neurons, where membrane rafts, enriched in cholesterol, are supposed to contribute to synaptic function. Despite the importance of cholesterol, neurons mostly rely on the import of this component from astrocytes, possibly to save energy, as cholesterol synthesis, involving the ER, is highly energy-consuming (Martín et al. 2014; Pfrieger 2003).

The ER facilitates many contacts with other organelles, including mitochondria, endosomes, peroxisomes, the Golgi apparatus and the plasma membrane (PM), to exert its functions. At ER-PM contact sites lipid compositions of both membrane compartments can be controlled which is achieved by tethering proteins evading vesicle formation and fusion. By this means, newly synthesized lipids can be transferred from the ER to the PM, and lipid metabolites can be returned to the ER for further metabolization and recycling (Chung et al. 2015). Additionally, ER-PM contacts

are essential for calcium signalling via store-operated calcium entry (SOCE), enabled by the coupling of ER-localized stromal interaction molecule (STIM1, 2) and the PM calcium channel Orai1 (Stefan et al. 2013). This pathway will be described in further detail in the following chapter. Other important contact sites are mitochondria-associated membranes (MAM), where subdomains of the ER couple with mitochondria. These MAMs make up about 5-20% of the mitochondrial surface and are crucial for neuronal survival and functioning (Rizzuto et al. 1998). As in ER-PM contact sites, MAMs enable the regulation of the lipid metabolism, as enzymes of both organelles are needed for the synthesis of phosphatidylethanolamine from phosphatidylserine, which can then be further metabolized in the ER into other essential phospholipids (Vance 1990). Furthermore, MAMs are involved in cellular calcium homeostasis forming microdomains for efficient calcium transfer from the ER to mitochondria. Calcium regulated metabolic enzymes of the tricarboxylic acid cycle get stimulated by a moderate mitochondrial calcium increase and lead to an increased ATP synthesis. Thus, perturbations of MAMs have negative effects on ER homeostasis and the general energy state of the neuron (Rizzuto et al. 2012). On top of that MAMs contribute to mitochondrial fission by marking the scission site (Friedman et al. 2011). Moreover, they play a role in the transport of mitochondria along microtubules (Friedman et al. 2010).

### 1.3.3. ER calcium homeostasis

The neuronal cytoplasmic calcium concentration ( $[Ca^{2+}]_{cyt}$ ) is very low, ranging between 10-100 nM, which is lower by four orders of magnitude in comparison to the extracellular calcium levels. However, neurons contain calcium stores, the mitochondria representing one of them, with calcium concentrations of about 220 nM at rest and possible high calcium increases that are relevant for regulating their energy metabolism (Ivannikov und Macleod 2013). The ER serves as the other important cellular calcium store with intraluminal ER calcium concentrations ( $[Ca^{2+}]_{ER}$ ) of 164  $\mu$ M in the neuronal soma and 156  $\mu$ M in the axon (Juan-Sanz et al. 2017). This calcium store plays an important role in regulating neuronal calcium homeostasis and is

necessary for synaptic activity and intraneuronal signalling processes, but also the induction of cell death signals.

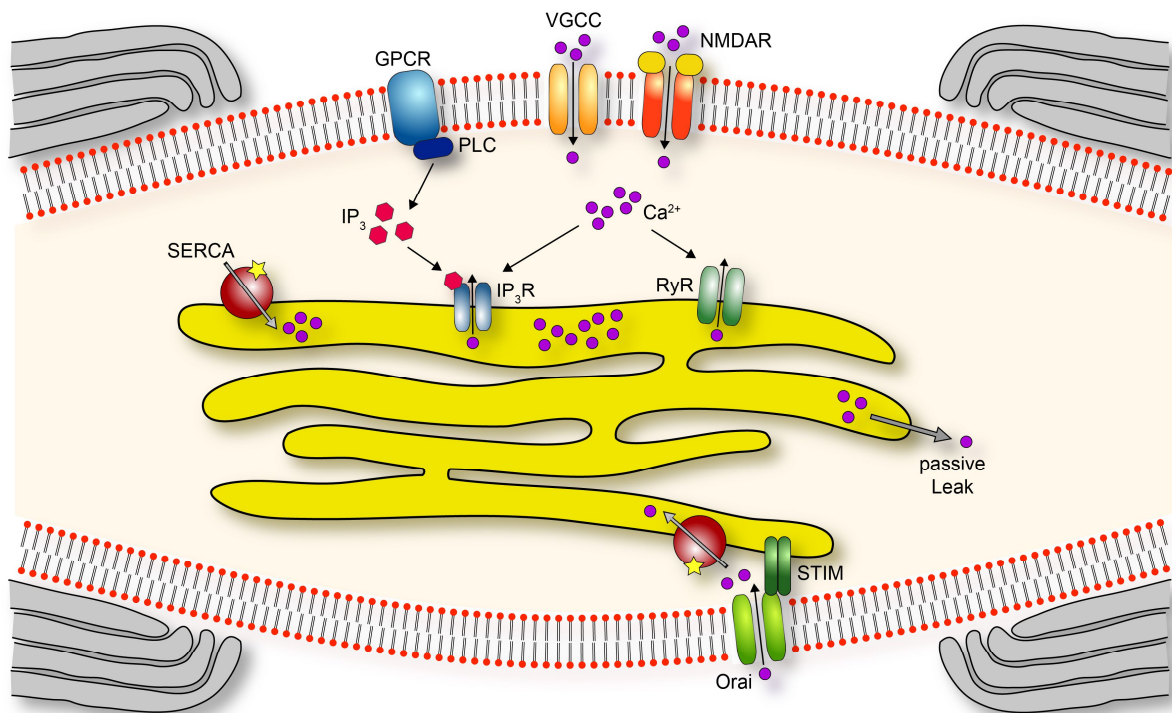


**Figure 3: Calcium signalling of neuronal ER**

A passive Ca<sup>2+</sup> leak leads to ER Ca<sup>2+</sup> depletion which is counteracted by SERCAs. Ca<sup>2+</sup> release appears through IP<sub>3</sub> receptors activated by Ca<sup>2+</sup> or IP<sub>3</sub> which is generated by phospholipase C (PLC) associated with G protein-coupled receptors (GPCR). Ca<sup>2+</sup> influx through voltage-gated calcium channels (VGCCs) or NMDA receptors (NMDARs) induces Ca<sup>2+</sup> induced calcium release (CICR) via ryanodine receptors (RyR). ER Ca<sup>2+</sup> depletion sensed by STIM proteins activate Orai channels for the replenishment of Ca<sup>2+</sup> stores (SOCE).

One important mechanism for balancing [Ca<sup>2+</sup>]<sub>ER</sub> is a constant calcium leak, which is a slow process and responsible for the investigated ER calcium depletion when blocking the counteracting pumps that fill up ER calcium stores. Studies have shown that this leakage is potentially happening through the translocon, the pore complex which is essential for co-translational translocation during protein synthesis (Flourakis et al. 2006). On top of that, pannexins, gap junction molecules and presenilins, which are linked to Alzheimer's disease, are implicated to drive the passive calcium leak from the ER (Vanden Abeele et al. 2006; Tu et al. 2006). This process is counterbalanced by sarcoplasmic-endoplasmic reticulum Ca<sup>2+</sup> ATPases (SERCA), that pump calcium against the electrochemical gradient from the cytosol into the ER by adenosine triphosphate (ATP) hydrolysis (Figure 3). From the currently known seven isoforms, SERCA2b is the one ubiquitously expressed in the brain. Its activity is tightly controlled by the free intraluminal [Ca<sup>2+</sup>]<sub>ER</sub>. This is monitored by the calcium-binding proteins

calreticulin and ERp57 which can sense  $[Ca^{2+}]_{ER}$  and activate the SERCA directly or, the latter, through altering the redox state of the pump (John et al. 1998; Li und Camacho 2004).

Intraluminal ER calcium is buffered by a variety of calcium binding proteins, with calreticulin being the most abundant. This protein has 20-50 binding sites with low affinity for calcium. Other low-affinity calcium binding proteins including calsequestrin, endoplasmic reticulum chaperone, BiP/GRP78 and calumenin also partake in ER calcium buffering (Michalak et al. 2002). It is important to note, that calcium buffering in the cytosol and within the ER is significantly different. Cytosolic calcium buffers have high affinities for calcium which enables very localized calcium signals because calcium diffusion is restricted. In comparison, ER calcium buffers enable intraluminal calcium diffusion and high levels of free calcium, so that multiple calcium signalling processes can quickly be generated (Mogami et al. 1999).

Depletion of ER calcium stores results in a process called store-operated calcium entry (SOCE), which is promoted by the interaction of the PM-associated calcium channels Orai and transient receptor potential channels (TRPC) with stromal interaction molecule 1 (STIM1). STIM1 is an ER membrane protein that can sense drops in  $[Ca^{2+}]_{ER}$  with its EF-hand motif and thereby gets transported to ER-PM contact sites. There STIM1 activates Orai channels and TRPC that trigger a calcium influx into the cytoplasm which subsequently replenishes the ER calcium stores (Figure 3) (Wegierski und Kuznicki 2018). Another STIM protein, STIM2, is characterized by a lower calcium affinity compared to STIM1 and thus can sense smaller ER calcium depletions. For this reason, STIM2 is supposed to play a central role in the tight regulation of ER and cytosolic calcium levels (Brandman et al. 2007).

The ER calcium stores are mobilized by the activation of two types of receptors, the ryanodine receptor (RyR) and the inositol 1,4,5 trisphosphate receptor (IP<sub>3</sub>R). For each there are different isoforms, of which RyR2 and IP<sub>3</sub>R1 are the predominant forms that can be found in neuronal tissue (Fujino et al. 1995). The RyR is mainly activated by calcium, so that a calcium influx through the PM facilitates a further calcium release from the ER into the cytoplasm, a process called calcium induced calcium release (CICR) (Figure 3). Very high cytosolic calcium concentrations (> 10 mM), however, lead to an inhibition of the RyR. Additionally, elevations in  $[Ca^{2+}]_{ER}$  increase the sensitivity of RyRs to binding agonists. Pharmacological agents that activate RyRs are

caffeine and low concentrations of ryanodine, whereas high concentrations of the latter inhibit the receptor's activity (Fill und Copello 2002).

IP<sub>3</sub>Rs get activated by IP<sub>3</sub>, which, besides diacylglycerol, is a hydrolysis product of phosphatidylinositol bisphosphate. Thus, the binding of any extracellular ligand to its respective receptor, which is coupled to phospholipase C, will lead to the activation of the ER calcium pool (Figure 3). Similar to RyRs, the activity of IP<sub>3</sub>Rs is modulated by calcium, so that a calcium release from one channel can trigger more release waves from neighbouring IP<sub>3</sub>Rs or RyRs. This potentiating mechanism can create temporally and spatially confined calcium signals or regenerative calcium increases that can propagate through the whole neuron (Berridge 1997).

#### 1.3.4. Structural dynamics of the ER

As previously described the ER is a complex network of interconnected sheets and tubules. Thus, this leaves the question, how such a reticular system can stably exist, be newly formed or disassembled and move around during physiological and pathological processes. Here, several protein families come into play.

ER tubules are formed by reticulons (Rtns) and receptor expression-enhancing proteins (REEPs, Yop1 in yeasts), which are ER membrane proteins, that make up around 10% of the whole membrane surface area of the ER. Due to their distinct morphology of two hydrophobic transmembrane hairpins, they are capable of forming wedge-like structures inside the lipid layer which results in the curvature of the tubules (Hu et al. 2008). Rtns and REEPs have been shown to also be involved in shaping ER sheets by concentrating to the sheet edges and forming a curvature, so that the two opposing membranes of an ER sheet get into close proximity. The membrane protein Climp-63 is supposed to act as a luminal spacer to determine the luminal width of ER sheets (Shibata et al. 2010). In addition, TMEM170A is an ER membrane protein that induces sheet formation and counteracts the activity of Rtn4. Upregulation of the sheet promoting proteins Climp-63 and TMEM170A results in an abundance of ER sheets, whereas overexpression of Rtns and REEPs leads to the formation of elongated tubules and a higher tubule-to-sheet ratio. Hence, a balance between sheet or tubular promoting ER membrane proteins is needed to facilitate a physiological ER morphology (Christodoulou et al. 2016).

In order to form a network, ER tubules need to be fused, which is mainly mediated by atlastins (ATLs), proteins with GTPase activity and part of the dynamin protein family. GTP bound ATLs of nearby tubules form dimers and pull the two membranes together after their hydrolysis of GTP, which enables the fusion of both tubules (Liu et al. 2012). Further studies have demonstrated that ATL inactivation causes the network to disassemble resulting in long, unconnected tubules. Thus, ATLs are needed to form and preserve the three-dimensional ER network and stabilize it at its junctions (Wang et al. 2016). These findings also have clinical relevance, because mutations of ATL1 and REEP1 in humans are frequent causes for hereditary spastic paraplegia, a disease characterized by degeneration of corticospinal axons (Salinas et al. 2008).

Besides having a complex morphology, the ER is also a highly dynamic organelle. ER tubules elongate via sliding along microtubules or by the tip attachment complex (TAC), where the tip of an ER tubule is attached to the plus end of a microtubule and moves depending on its length variation (Waterman-Storer und Salmon 1998). Furthermore, the ER is supposed to move along the actin network and network junctions are capable of sliding along a tubule, to rearrange the ER structure (Bridgman 1999; Lee und Chen 1988).

For the following paragraph and the rest of this thesis it is important to note that the terms ER fission and ER fragmentation, with the latter being used for the morphological changes of the ER in this thesis, most likely represent comparable mechanisms. Thus, they can be regarded as synonyms. More extensive alterations in ER structure have been found in studies of fertilized star fish eggs. Prior to fertilization, injected GFP targeted to the ER rapidly diffuses in the ER network. However, after fertilizing the eggs ER structures seemed to be disrupted with a decreased possibility of freely moving GFP molecules in the ER lumen (Terasaki et al. 1996). In cultured hippocampal neurons glutamate stimulation and potassium-induced depolarisation leads to rapid fission of the continuous ER into small vesicles. Some of those appear to form clusters, which might occur due to dendritic swelling in cases of severe damage. The fission process does not depend on ER calcium release but on a cytoplasmic calcium increase mediated by NMDA and AMPA receptors and voltage gated calcium channels (VGCC). In addition to that, ER fission appears to be reversible and can also be attenuated by blocking NMDA receptor activity with an antagonist (Kucharz et al. 2009; Kucharz et al. 2011a). These findings have been confirmed in *in vivo* mouse studies where brain ischemia has been induced by cardiac arrest. Under ischemic conditions the lack of

proper energy supply results in elevated cytoplasmic calcium levels and thus in rapid ER fission (Kucharz et al. 2011b). A more recent study has brought more light into this intriguing process. Synaptic activity due to somatosensory stimulation induces ER fission in single dendritic spines, whereas cortical spreading depolarization (CSD), a phenomenon responsible for migraine aura and as well existent after stroke, traumatic brain injury and brain haemorrhage, leads to ER fission in the whole dendrites. Both processes are again reversible and during the loss of ER continuity synaptic function is reversibly decreased. Fission occurs due to NMDA receptor gated calcium increases, which subsequently activate calcium/calmodulin-dependent protein kinase II (CAMKII), whereas the refusion of ER fragments is mediated by dynamin GTPases. Furthermore, inhibiting the fission process with blockers of CAMKII mitigates the reduction of synaptic activity (Kucharz und Lauritzen 2018).

This process of ER fission leaves many questions unanswered concerning its significance and role for neuronal cell biology. Given the fact that, under normal conditions, the ER is a continuous network, which allows free intraluminal diffusion of calcium, ER fragmentation might create isolated ER vesicles with a restricted amount of releasable calcium. This could have relevant implications on synaptic functions and the prevention of neuronal damage. Additionally, ER fragments can help to segregate damaged proteins, in order to avoid the activation of a generalized unfolded protein response (Kucharz et al. 2009; Kucharz und Lauritzen 2018).

## **1.4. Axon degeneration**

### **1.4.1. Patterns and mechanisms of axon degeneration**

Axons, the largest units of neurons with lengths of sometimes more than a meter, conduct electrical impulses from the neuronal soma towards its target cells. Thus, it is no surprise that the loss of this entity will have significant effects on the integrity of the nervous system. However, axonal degeneration is not only a process that takes place in neurological diseases but is also crucial for the development and plasticity of the nervous system (Luo und O'Leary 2005).

The first pattern of axonal degeneration was discovered by August Waller in 1850, hence called Wallerian degeneration (WD), who described that the distal part of an axon undergoes a degradation process after axotomy. After axonal transection, during the lag phase, the distal stump first remains morphologically intact for one to three days with visible accumulation of material in the proximal end. Subsequently, the

fragmentation process begins resulting in the complete elimination of the distal axon. The degeneration of the axon triggers macrophages and other glia cells to remove the debris to enable regeneration and repair (Lingor et al. 2012; Chen et al. 2015). The discovery of a mutated mouse strain, called *Wld<sup>s</sup>*, revealed more insight into the mechanism of Wallerian degeneration, as axons in these mice survived for several weeks after axotomy (Lunn et al. 1989). Genetic analysis of this mouse strain showed that the protein responsible for slowing down WD is a chimeric product which consists of a fragment of an E4-type ubiquitin ligase (UBE4b) and nicotinamide adenyltransferase 1 (NMNAT1). The latter, a protein relevant in the nicotinamide-adenine dinucleotide+ (NAD<sup>+</sup>) salvage pathway, has been unveiled to promote the neuroprotective phenotype as local overexpression of NMNAT1 in axons prolonged axonal survival after transection (Sasaki et al., 2009). Other isoforms of NMNAT, the more labile NMNAT2 and the mitochondrial NMNAT3, have been shown to have comparable effects on axonal degeneration (Yan et al. 2010; Yahata et al. 2009).

Directly after axotomy another pattern of axonal degeneration is triggered, therefore called acute axonal degeneration (AAD). For about 10 to 20 minutes after transection axons stay morphologically intact but then undergo rapid fragmentation affecting both the proximal and the distal stump. Being a distinct mode of axonal degeneration, AAD still has morphological and mechanistic features resembling WD, as this degeneration process is also delayed by the *Wld<sup>s</sup>* mutation. It is hypothesized that the transection causes a sudden calcium influx resulting in elevated axoplasmic calcium levels, which activates the calcium dependent protease calpain that is responsible for the cytoskeletal degradation. Within a day after the lesion the proximal axon stumps start to sprout again but do not manage to reach their distal targets in the CNS (Kerschensteiner et al. 2005; Knöferle et al. 2010).

Another distinct pattern of axonal degeneration has been described in the animal model of multiple sclerosis, EAE, and was termed focal axonal degeneration. Here, in inflammatory CNS lesions three morphologically distinguishable stages of axons have been identified: normal appearing (stage 0), swollen (stage 1) and disrupted (stage 2) axons (Figure 4). Interestingly all different stages of FAD can already be found at the onset of EAE, where the demyelination process has not even started. Furthermore, the fate of swollen stage 1 axons is undetermined, meaning that they can remain in their current stage, degenerate or recover, so that stage 1 axons might represent a crucial therapeutic target point. Ultrastructural analysis of axons in inflammatory lesions

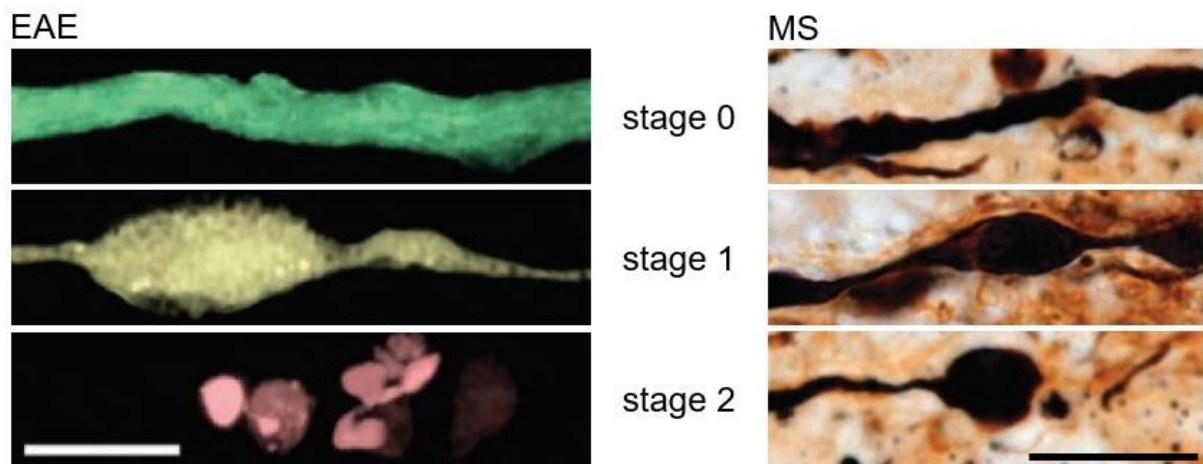


**Figure 4: FAD in EAE and MS**

Exemplary images of axon morphology of normal-appearing stage 0, swollen stage 1 and fragmented stage 2 axons in EAE (left panels) and in a human MS lesion with Bielschowsky staining (right panels). Scale bars 10  $\mu\text{m}$ . Figure adapted from (Nikić et al. 2011)

showed that mitochondria appeared to be swollen and functionally impaired in stage 1 and even in some healthy appearing stage 0 axons, indicating that mitochondrial damage might be an early event in the axon degeneration process. These morphology stages of axon degeneration have also been found in biopsies of human MS lesions (Figure 4) (Nikić et al. 2011).

Further studies of these different modes of axonal degeneration have revealed more insight into the underlying molecular mechanisms that will be reviewed in the following paragraphs (Figure 5).

Experiments in progressive motor neuronopathy mice with alterations in the neuronal microtubule network, colchicine treatment or malfunctioning neurofilament proteins have shown to result in WD-like degeneration processes implicating that the disruption of axonal transport can trigger axonal degeneration (Martin et al. 2002; Julien 1999). As already described, APP accumulation can be used as a marker for impaired axonal transport as it accumulates in axonal spheroids. Accumulated APP has first been found in axons affected by traumatic brain injury, but later also been described in acute multiple sclerosis lesions, Alzheimer's dementia and other neurodegenerative diseases (Gentleman et al. 1993; Ferguson et al. 1997). In acute EAE activated immune cells release reactive oxygen and nitrogen species that cause pervasive axonal transport dysfunction by altering microtubule functions. During chronic inflammation these transport deficits persist, leading to a lack of relevant organelles in the distal parts of axons and thus end in axonal degeneration (Sorbara et al. 2014).

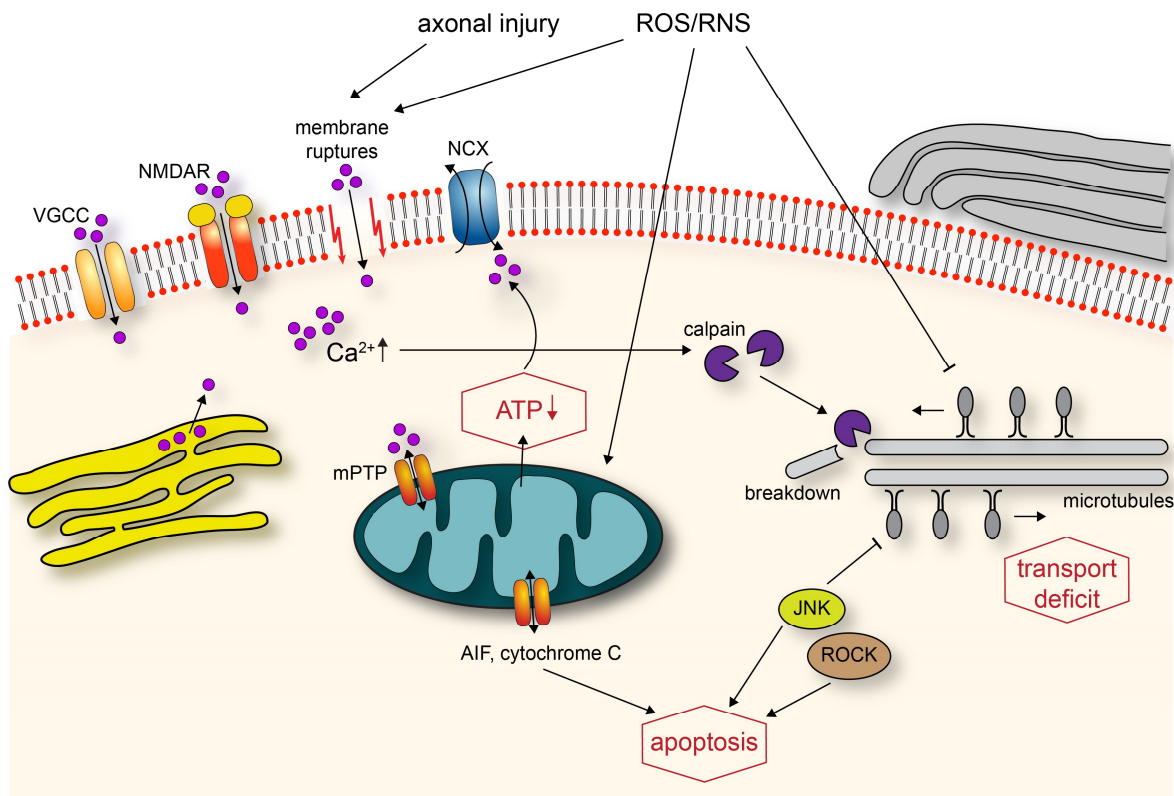


**Figure 5: Mechanisms of axon degeneration**

Depicted are possible mechanisms of axon degeneration caused by axonal injury and/or oxidative stress to the axon. Intra-axonal calcium levels increase due to an influx of extracellular calcium via calcium channels (VGCC, NMDAR) and membrane ruptures as well as the depletion of intracellular calcium stores (ER and mitochondria). Energetic failure after mitochondrial impairment leads to a reverse functioning of the Na<sup>+</sup>-Ca<sup>2+</sup> exchanger (NCX) which further elevates cytoplasmic calcium. Axonal transport is perturbed by reactive oxygen and nitrogen species (ROS/RNS), activation of c-Jun N-terminal kinase (JNK) or cytoskeletal breakdown via calpain which gets activated upon the intra-axonal calcium increase. Apoptotic pathways, which are still questionable to exist in axons (Dubois-Dauphin et al. 1994; Finn et al. 2000), are initiated by the release of apoptosis inducing factor (AIF) along with cytochrome C from damaged mitochondria and by the activation of JNK and the Rho-associated coiled coil containing protein kinase (ROCK).

Several different kinases have been implicated to play a crucial role in the execution of axonal degeneration. One of such is the c-Jun N-terminal kinase (JNK) which upon activation mediates manifold processes including apoptotic pathway activation and the inhibition of axonal transport (Davis 2000; Stagi et al. 2006). The involvement of JNK in axonal degeneration has been studied in spinal cord injury where activated JNK could be found in high numbers in axons of the corticospinal tract after hemisection. Inhibiting JNK and a knockout of JNK reduced APP accumulation, axonal retraction and thereby improved motor recovery after injury (Yoshimura et al. 2011). The Rho-associated coiled-coil containing protein kinase (ROCK) has been shown to hinder axonal regeneration and promote axonal degeneration in the CNS (Liu et al. 2015;

Karnezis et al. 2004). Inhibiting ROCK with Fasudil in acute and chronic experimental models of MS resulted in a decrease of immune cell infiltration, demyelination and axonal degeneration (Sun et al. 2006).

Mitochondria have long been known to be the “power-houses” of nearly every cell providing the energy needed for cellular homeostasis and functions. However, they are also involved in calcium signalling processes, activating apoptotic pathways and the production of reactive oxygen species (ROS). Given that, it is no surprise that mitochondrial dysfunction, which is associated with many neurological diseases, is another underlying cause for axon degeneration. Mitochondria can get damaged by different means such as Tau accumulation and amyloid beta in Alzheimer’s disease (Cummins et al. 2019; Casley et al. 2002), increased intra-axonal calcium levels after axonal injury (Wolf et al. 2001) or ROS and RNS generated by activated immune cells in neuroinflammatory lesions (Nikić et al. 2011). Mitochondrial dysfunction leads to a lack of ATP in the axon resulting in a reduced activity of the Na<sup>+</sup>/K<sup>+</sup>-ATPase and subsequently in axon membrane depolarization. Consequently, the increase of intra-axonal sodium induces a reverse operation of the Na<sup>+</sup>-Ca<sup>2+</sup> exchanger (NCX) and thus a further increase in axoplasmic calcium which effect will be reviewed later (Stys et al. 1992). Upon damage mitochondria release pro-apoptotic factors including cytochrome c, Smac/DIABLO or apoptosis inducing factor (AIF) which can be facilitated by Bcl-2 proteins or the formation and opening of the mitochondrial permeability transition pore (mPTP). In addition to activating apoptotic pathways, this opening, which can be caused by an increased level of mitochondrial calcium or high quantities of ROS and RNS, brings about a loss of the inner mitochondrial membrane potential and thus a reduction in ATP synthesis (Cabral-Costa und Kowaltowski 2019). The production of mitochondrial ROS occurs during oxidative phosphorylation but is well buffered by non-enzymatic (glutathione, coenzyme Q) and enzymatic (glutathione peroxidase, manganese superoxide dismutase catalase) in the healthy state. However, these antioxidant buffers decrease when mitochondria get damaged resulting in increased levels of ROS that can further harm mitochondria and cause oxidative stress to other axonal components (Lin und Beal 2006). These processes only sum up some of the involvement of mitochondria in axon degeneration but highlight the importance of these organelles as therapeutic targets in neurological diseases.

#### 1.4.2. Role of calcium in axon degeneration

Calcium is a key second messenger in cellular processes and regulates cell proliferation, differentiation, metabolism, cell death as well as neuronal activity. Nonetheless, with the importance of neuronal calcium levels being tightly regulated, calcium overload does have detrimental effects on the state of axons. Increase of axonal calcium levels results in the activation of proteases – most importantly calpain, which is responsible for the cytoskeletal degradation – lipases and nucleases, as well as mitochondrial dysfunction and ER stress all leading to axon degeneration (Ureshino et al. 2019). This raises the question how an axoplasmic calcium increase is generated upon axonal damage. Here, the influx from the extracellular and the intracellular calcium compartment, consisting of mitochondrial and ER calcium stores, seem to be plausible answers, with the latter being reviewed in the next chapter. Extracellular calcium is likely to have a significant contribution as scavenging of these ions in the extracellular space using ethylene glycol-bis( $\beta$ -aminoethyl ether)-N,N,N',N'-tetraacetic acid (EGTA) prevents an intra-axonal calcium rise and further injury to axons in experimental models for traumatic axonal injury and EAE (Wolf et al. 2001; Williams et al. 2014; Witte et al. 2019). Voltage-gated calcium channels (VGCCs) represent important channels for neuronal calcium signalling and have been described to be partially causative for the calcium influx after axonal injury. Blockade of this class of calcium channels using cobalt, cadmium, amlodipine or verapamil reduced the extent of axonal degeneration (Agrawal et al. 2000; Knöferle et al. 2010). However, in vivo mice experiments of SCI and EAE of our group did not support this theory as a mixture of VGCC blockers did not affect axonal calcium levels in vivo (Williams et al. 2014; Witte et al. 2019). Glutamate receptors (Kainate, AMPA and NMDA) have been proposed to be another possible entry pathway for calcium given the relevance of glutamate excitotoxicity in CNS disease. Experiments have shown that glutamate receptors are indeed expressed along axons in the spinal cord and the binding of receptor agonists result in an increase of intra-axonal calcium (Ouardouz et al. 2009b). However, the involvement of glutamate receptors for calcium-induced axon degeneration in our in-vivo paradigms of SCI and EAE could not be confirmed in our in vivo calcium imaging experiments (Williams et al. 2014; Witte et al. 2019). Other experiments have suggested a sodium dependent influx of calcium, since the expression of neuronal sodium channels has been described to be upregulated after neuronal injury (Hains et al. 2003). Consequent to axonal injury sodium entries into the

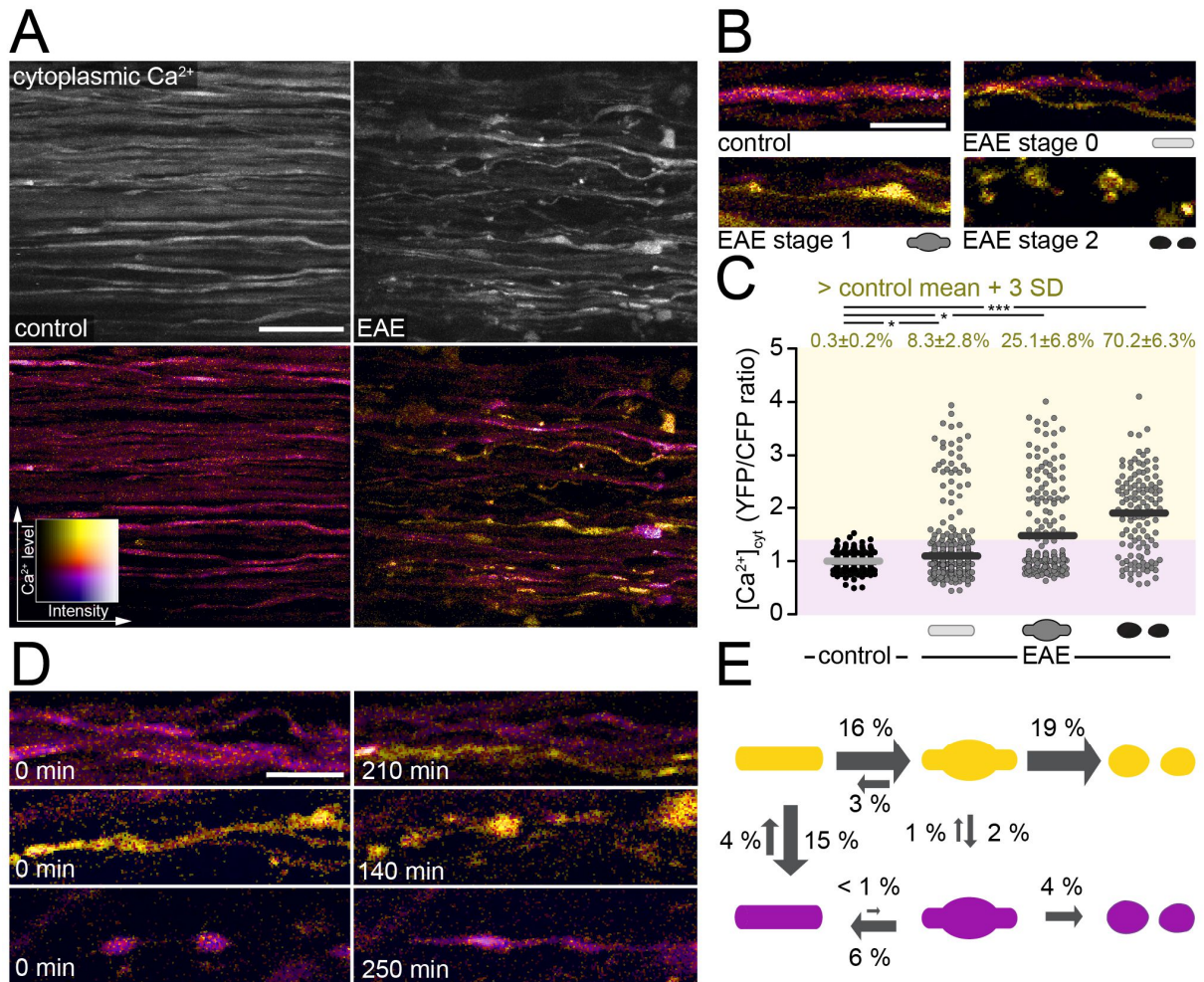


**Figure 6: Increased cytoplasmic calcium predicts axonal fate in EAE**

(A) In-vivo projection images of the spinal cord of healthy control (left) and EAE (right) Thy1-CerTN-L15 mice. Top row: greyscale image of the YFP channel, bottom row: colour-coded images for  $[Ca^{2+}]_{cyt}$ . (B) Exemplary ratiometric (YFP/CFP) images of healthy control axons (upper left), normal-appearing stage 0 (upper right), swollen stage 1 (lower left) and fragmented stage 2 (lower right) axons in acute EAE lesions. (C) Axonal  $[Ca^{2+}]_{cyt}$  (YFP/CFP ratio normalized to the mean of control axons) in healthy control mice and the different stages of FAD in EAE (pre and post application of 50 mM caffeine). Bars indicate means, percentages (above) display fraction of axons with increased  $[Ca^{2+}]_{cyt} > \text{control mean} + 3 \text{ SD}$ . Mann-Whitney U test for control vs. EAE stages 0, 1, 2.  $N = 6$  control mice,  $n = 11$  EAE mice. (D) Ratiometric time-lapse images of a stage 0 axon rising in  $[Ca^{2+}]_{cyt}$  (top), a high  $[Ca^{2+}]_{cyt}$  stage 0 axon undergoing fragmentation (middle) and a recovery from stage 1 to stage 0 in a low  $[Ca^{2+}]_{cyt}$  axon. (E) Depiction of transition probabilities of different morphological stages of high  $[Ca^{2+}]_{cyt}$  (yellow) and low  $[Ca^{2+}]_{cyt}$  (purple) axons per observed axon hour ( $n = 307$  axons, 8 mice, 1201 axon hours). Scale bars in (A) 25  $\mu\text{m}$ , in (B) and (D) 10  $\mu\text{m}$ . \* $P < 0.05$ , \*\*\* $P < 0.001$ . Figure and caption adapted from (Witte et al. 2019). Experimenter: Adrian-Minh Schumacher

axon through its respective channels leading to increased intra-axonal sodium levels and thus to a depolarization of the membrane. This induces a reverse operation of the NCX and the activation of VGCCs and finally results in increased axonal calcium levels (Wolf et al. 2001). While inhibiting sodium influx, the NCX and VGCCs in in vitro models

for axonal injury, our in vivo experiments could not confirm this mechanism for SCI and EAE.

Having ruled out several possible entry pathways for extracellular calcium into the axon, what alternative mechanisms could explain this phenomenon? For both studied paradigms of axonal injury – SCI and EAE – elevated intra-axonal calcium levels have been shown to predict the fate of axons resulting in a higher rate of fragmentation than recovery (Figure 6). Work in our lab then revealed an alternative entry way for extracellular calcium through nano-ruptures of the axonal plasma membrane. This has been demonstrated by the usage of fluorescent dyes that get taken up by membrane-damaged axons in traumatic and inflammatory lesions and the presence of which correlates with the elevated intra-axonal calcium levels (Williams et al. 2014; Witte et al. 2019).

#### 1.4.3. Role of ER calcium in axon degeneration

Apart from the extracellular calcium compartment intra-axonal calcium stores do exist. Both, mitochondria and the ER, store higher amounts of calcium and are involved in neuronal calcium signalling. As my thesis is focussed on the role of the ER in axon degeneration, I will first review the existing literature on ER calcium after axon injury in this chapter.

The first experiments on ER calcium release were performed in models of ischemic injury to neurons. Early studies could demonstrate that chelating extracellular calcium does not fully prevent the degeneration of dorsal column axons, whereas buffering intracellular calcium is protective, leading to the conclusion that axonal ER releases calcium under ischemic conditions. Inhibiting calcium release from the ER through RyR with ryanodine, as well as depleting ER calcium stores prior to ischemia with thapsigargin, resulted in a protection of axons. The same effect was accomplished when blocking L-Type  $\text{Ca}^{2+}$ -channels with nimodipine and diltiazem (Ouardouz et al. 2003). Further studies concluded that the activation of GluR6 leads to a membrane depolarization via a small calcium entry, activating L-Type- $\text{Ca}^{2+}$ -channels, which finally facilitate a calcium release from the ER through RyRs. Moreover, AMPA receptors prompt a calcium-induced calcium release via RyRs and GluR5 activate an ER calcium release by synthesizing  $\text{IP}_3$  through phospholipase C, which is coupled to this type of glutamate receptor. The calcium release via RyRs and  $\text{IP}_3$ Rs is enhanced by NO,

which is produced by the neuronal NO-Synthase that also gets activated by GluR5 and GluR6. These findings highlight the relevance of glutamate excitotoxicity and NO for axonal injury, damage mechanisms that have both been implicated in a number of neurological diseases including in MS (Ouardouz et al. 2009a; Ouardouz et al. 2009b).

In models of optic nerve ischemia ER calcium release has been linked to sodium influx. Elevated intra-axonal sodium levels can directly modulate RyRs to increase the release of ER calcium. There is no direct link between sodium and IP<sub>3</sub>Rs, but sodium influx might cause neurotransmitter release such as glutamate which then interacts with ER calcium stores via the already described mechanism (Nikolaeva et al. 2005).

Experiments of laser-induced spinal cord injury in ex vivo spinal cords could demonstrate that axons were immediately transected at the radiation site followed by a delayed axonal degeneration. Interestingly, axons close to the lesion site, that did not undergo initial transection, experienced a secondary bystander degeneration. As expected, elevated intra-axonal calcium levels could be found in degenerating axons. However, in conditions of low or zero extracellular calcium, axonal dieback could not be ameliorated. This suggests intra-axonal calcium stores to be responsible for increasing axoplasmic calcium levels. Blocking ER calcium release with ryanodine and 2-APB results in a reduced axonal dieback, whereas mobilizing ER calcium stores with thapsigargin or caffeine aggravated axonal degeneration (Stirling et al. 2014).

Another study also implicated the relevance of ER calcium stores for axon degeneration, as it could show that calcium release via RyRs and IP<sub>3</sub>Rs at MAMs induced the opening of the MPTP and mitochondrial dysfunction. This process then leads to an elevation of mitochondrial ROS and a further increase in intra-axonal calcium by a mitochondrial calcium leak and a reverse function of the NCX due to the reduced ATP synthesis in disrupted mitochondria (Villegas et al. 2014).

### **1.5. In vivo imaging of neuronal calcium levels**

Calcium acts as a universal second messenger in every mammalian cell and is involved in many cellular events. In neurons calcium influx occurs during action potentials as well as synaptic transmission and as reviewed before also during neuronal pathology. Therefore, imaging calcium in the nervous system has long been of particular interest. This was eventually achieved by the development of two processes: the invention and further improvement of calcium indicators and the development of applicable imaging instrumentation.

Bioluminescent proteins such as aequorin from the jellyfish were the first calcium indicators used to image intracellular calcium events (Shimomura et al. 1962). These were followed by the development of fluorescent calcium indicators (quin-2, fura-2, fluo-4) consisting of a calcium chelator like EGTA or BAPTA and a chromophore (Tsien 1980). Although they are widely used for calcium imaging, they have several drawbacks including the difficulty to target specific cells or cellular organelles and the invasiveness when loading these dyes into the tissue. In 1997 Roger Tsien developed the next generation of calcium indicators, genetically encoded calcium indicators (GECIs), which represented a major breakthrough in the field of calcium imaging (Miyawaki et al. 1997).

### 1.5.1. Genetically encoded calcium indicators

While all GECIs consist of a calcium binding domain (calmodulin, troponin C) and fluorescent proteins (FPs), there are two classes of GECIs, namely, non-ratiometric single FP ones and ratiometric Förster resonance energy transfer (FRET)-based two FPs sensors. The single-FP-type GECIs are constructed out of a circularly permuted FP, the calcium-binding protein calmodulin and a calmodulin-binding protein M13 with the two latter components inducing a conformational change of the FP upon binding of calcium (Akerboom et al. 2009). This results in an increase of fluorescence proportional to the amount of bound calcium which is why these GECIs are known as intensimetric sensors. Important examples are the green GCamPs (Nakai et al. 2001), red RCamPs (Akerboom et al. 2013) and GECOs (Zhao et al. 2011) which can be efficiently used for the measurement of temporal calcium dynamics in neurons. While also having a larger dynamic range, a value that indicates how much brighter the calcium-bound state is compared to the calcium-free state, these sensors do have disadvantages compared to FRET-based GECIs. They are less suitable for imaging steady-state calcium levels, suffer from a lower brightness and are not very convenient for recording calcium changes in moving structures (Thestrup et al. 2014).

FRET-based sensors consist of two fluorophores, mostly a CFP variant acting as the donor and a YFP variant serving as the acceptor. While in the calcium-free state fluorescent light is mainly emitted by the donor, upon calcium binding a conformational change brings the two FPs into close proximity of less than 10 nm. This facilitates the non-radiative transfer of energy (FRET) from the donor to the acceptor, so that the emission is now dominated by the acceptor's fluorescence (Jares-Erijman und Jovin

2003). Hence, the ratio between acceptor and donor increases when calcium is bound to the sensor. When choosing a sensor for an experiment, different aspects of an indicator have to be kept in mind. First, the affinity of a calcium indicator reflected by its dissociation constant ( $K_d$ ), the calcium concentration at which half of the sensors are in the calcium-bound state, is important when considering which amounts of calcium resting levels and transients are supposed to be measured. Low-affinity sensors are useful for large calcium changes, whereas high-affinity indicators respond well to small calcium transients. However, the affinity can be significantly influenced by environmental factors such as pH, temperature and the existence of other ions (e.g.  $Mg^{2+}$ ) competing for the calcium binding site. Second, the kinetics of a sensor should be respected depending on the time scale of the calcium event of interest. Finally, calmodulin is an abundant cellular protein interacting with other cellular targets which leads to high background noise and dysfunctional sensors (Tian et al. 2012). These sensor properties were responsible for the development of improved FRET-based GECIs. The first sensor, cameleon 1 consisting of a blue FP and a green FP got quickly replaced with other sensors using the FRET pairs CFP and YFP (Miyawaki et al. 1997). Further improvements were made by introducing variants of circularly permuted FPs with higher pH stability, photostability and less sensitivity for chloride (Griesbeck et al. 2001). The first troponin C (TnC)-based sensor was the TN-L15, which had a higher calcium sensitivity compared to calmodulin-based calcium indicators due to the absence of intracellular interactions. Swapping the donor CFP with Cerulean and introducing a mutation into the donor fluorophore Citrine lead to the creation of CerTN-L15, the sensor which is used in this project to monitor cytoplasmic calcium changes (Heim et al. 2007). Simplifying the TnC binding domain by reducing the amount of calcium binding sites and the introduction of a TnC variant from the toadfish resulted in a new class of GECIs called Twitch sensors. These improvements enhanced the properties of ratiometric sensors so that they are now reaching sensitivities comparable to calcium dyes or intensimetric calcium indicators (Thestrup et al. 2014). With neuronal ER containing calcium concentrations at around 150 – 170  $\mu M$  compared to the 10 – 100 nM in the cytoplasm, calcium indicators in this cellular compartment would require low affinities for calcium, favourably a  $K_d$  ranging at the baseline calcium concentration within the ER. The first measurement of ER calcium dynamics was achieved in DRG neurons with the low-affinity calcium dye Mag-Fura-2. However, these synthetic dyes also accumulate in the cytosol and other organelles,

thus, cell dialysis or membrane permeabilization needs to be performed to wash out unnecessary cytosolic dye (Gerasimenko et al. 2014). Direct targeting to the ER in GECIs was accomplished by adding an ER signalling and the KDEL ER retention sequence to yellow cameleon FRET sensors. Yet, their  $K_d$  was not well suited for imaging ER calcium so that further improvements were made yielding a sensor, D1ER, with enhanced sensitivity and kinetics (Palmer et al. 2004). Single-wavelength ER calcium sensors have also been designed, one of them being CatchER, an excitatory ratiometric calcium indicator. It consists of a GFP with an integrated calcium binding site that causes a change in absorption maxima when calcium is bound to the fluorophore. Compared to D1ER CatchER has a higher dynamic range, faster kinetics and less calcium buffering capacity (Tang et al. 2011). Another excitatory-ratiometric ER calcium sensor is the erGAP1, which is a fusion protein of GFP and apoaequorin. This sensor with a large dynamic range, thermal stability and insensitivity to  $Mg^{2+}$  and pH, has already successfully been used to measure ER calcium transients in hippocampal neurons, DRGs and in the spinal cord (Rodriguez-Garcia et al. 2014). In 2014, a new class of ER calcium indicators, namely CEPIAs, was created based on the properties of GECO sensors. Several colour variants of CEPIAs exist such as green or red CEPIAs and even a ratiometric variant (GEM-CEPIA), allowing the simultaneous usage of more sensors to image multiple calcium signals (Suzuki et al. 2014).

In our lab we decided to use the low-affinity Twitch sensor Twitch2B 54S+ with a  $K_d$  of 174  $\mu$ M and a dynamic range of 320% (Thestrup et al. 2014) to generate the transgenic mice used in my thesis work. This decision was based on the previously measured calcium concentrations in the ER (Juan-Sanz et al. 2017) and the preference of a FRET-base sensor that allows ratiometric imaging.

### 1.5.2. In vivo microscopy of the nervous system

In order to use GECIs to study calcium dynamics in neurons and their subcellular organelles, experimental animals must be created that stably express these sensors. The first transgenic mice expressing FPs in the nervous system were the Thy1-XFP mice. Each transgenic mouse expressed one of four FPs, yet, the labelling of subsets of neurons, the colour pattern and the signal intensity was unique in each mouse (Feng et al. 2000). The murine Thy1 protein is expressed at high levels in neurons and several other organs. Altering an intron in the Thy1 gene made a pan neuronal XFP

expression possible with eliminating their expression in non-neuronal tissues. Using different techniques such as varying the chromosomal position of the Thy1 reporter construct or conditioned expression, distinct subset-labelling of neurons in transgenic mice could be achieved (Misgeld und Kerschensteiner 2006). Over time a large number of different transgenic lines have been designed enabling researchers to study basic neuronal morphology, synapses, axonal transport, mitochondria and redox signals (Marinković et al. 2015). For neuronal calcium imaging previously described GECIs can be coupled to the Thy1-promoter, which for example was done to generate Thy1-CerTN-L15 transgenic mice (Heim et al. 2007).

The first devices used for calcium imaging were wide-field microscopy setups that consisted of a light source (usually xenon or mercury lamps), a dichroic mirror separating excitation and emission wavelength and a signal detecting device such as photodiode arrays or charged coupled detector-based video cameras. However, light scattering appears to be a main issue for these devices, especially when imaging deep areas in the CNS in an in vivo setting (Denk und Svoboda 1997). This concern was addressed when developing laser scanning microscopy setups. In confocal microscopy a single photon excites the area of interest in the focal plane, however, FPs above and below this plane can also be stimulated leading to photobleaching of fluorophores and photodamage. Using a pinhole, only photons that have been emitted in the focal plane will be recorded by photomultiplier tubes, whereas out-of-focus light will be blocked. Yet, photons out of the focal plane that get scattered on their path will not be recorded leading to lower signal intensities and the need for a higher excitation power and therefore again more photodamage. Thus, confocal microscopy is nowadays preferably used for in vitro setups rather than in in vivo settings (Grienberger und Konnerth 2012; Denk und Svoboda 1997). An important step, to overcome named issues, was made by the introduction of the multiphoton microscopy technique. The principle of exciting one fluorophore with multiple photons was first predicted in 1931 (Goeppert-Mayer 1931), then observed in 1961 and finally, in 1990, two photon microscopy was achieved by Winfried Denk and colleagues (Denk et al. 1990). In this technique two longer wavelength photons, generated by a pulsed laser, reach the fluorophore at almost the same time, adding up their energy leading to the excitation of the fluorophore. This has several advantages as on the one hand excitation only occurs at a focal point resulting in hardly any photobleaching in out-of-focus areas. On the other hand, the used near-infrared wavelengths are less absorbed and scattered

in most biological tissues, which extends the penetration depth. One further advantage is, since excitation only occurs at the focal point, that there is no need of a pinhole, as all photons, even the scattered ones, origin from this focal spot (Denk und Svoboda 1997).

In summary, using all these techniques together, namely two photon microscopy and GECIs expressed under the Thy1 promoter, calcium signals reaching from single action potentials or synaptic transmissions to long-term increases in axon degeneration can be imaged today. Moreover, this is not only limited to cytoplasmic events anymore as even calcium sensors targeted to the ER or mitochondria have been generated.

## 2. Materials and Methods

### 2.1. Reagents

#### 2.1.1. Surgery and in vivo imaging

4-Chloro-3-ethylphenol (4-CEP)	Sigma-Aldrich® Chemie GmbH, 82024 Taufkirchen, Germany
Adenosine 5'-triphosphate disodium salt (ATP)	Sigma-Aldrich® Chemie GmbH, 82024 Taufkirchen, Germany
Agarose	Sigma-Aldrich® Chemie GmbH, 82024 Taufkirchen, Germany
Bepanthen Augen- und Nasensalbe 5 g (eye ointment)	Bayer Vital GmbH, Leverkusen, Deutschland
Caffeine powder	Sigma-Aldrich® Chemie GmbH, 82024 Taufkirchen, Germany
Cutasept F Lösung 250 ml (disinfectant spray)	Bayer Vital GmbH, Leverkusen, Deutschland
Dimethylsulfoxid (DMSO)	Sigma-Aldrich® Chemie GmbH, 82024 Taufkirchen, Germany
Ethanol 70%	CLN GmbH, 85416 Niederhummel, Germany
Fentanyl B. Braun 0,1 mg	B. Braun Melsungen AG, Melsungen, Germany
Forene (Isoflurane)	Abbott AG, Baar, Switzerland
Histamine	Sigma-Aldrich® Chemie GmbH, 82024 Taufkirchen, Germany
Ketamine hydrochloride 10% (Ketamine)	Bremer Pharma GmbH, Warburg, Deutschland
Midazolam B. Braun 5 mg/ml	B. Braun Melsungen AG, Melsungen, Germany
Ringerlösung Fresenius KabiPac (Ringer's solution)	Fresenius KaBI Dtl., Bad Homburg, Deutschland
Sterile artificial mouse cerebrospinal fluid (aCSF)	Solution A: 8.66 g NaCl (Merck) 0.224 g KCl (Merck) 0.206 g CaCl <sub>2</sub> · 2H <sub>2</sub> O (Sigma-Aldrich) 0.163 g MgCl <sub>2</sub> · 6H <sub>2</sub> O (Sigma-Aldrich)  Solution B: 0.214 g Na <sub>2</sub> HPO <sub>4</sub> · 7H <sub>2</sub> O (Merck) 0.027 g NaH <sub>2</sub> PO <sub>4</sub> · H <sub>2</sub> O (Merck) dH <sub>2</sub> O ad 500 ml

	Mixture of solutions A and B in a 1:1 ratio
Thapsigargin	Merck KGaA, 64293 Darmstadt, Germany
Xylarium 20 mg (Xylazine)	Riemser Arzneimittel AG, Greifswald-Insel Riems, Germany

### 2.1.2. Immunization

Incomplete Freund Adjuvans (IFA)	Sigma-Aldrich® Chemie GmbH, 82024 Taufkirchen, Germany
M. tuberculosis H37 RA	Sigma-Aldrich® Chemie GmbH, 82024 Taufkirchen, Germany
Myelin Oligodendrocyte Glycoprotein (MOG)	Stock solution, produced by laboratory of Martin Kerschensteiner, 82152 Planegg, Germany
Pertussistoxin (Ptx) from B. pertussis, inactivated	Sigma-Aldrich® Chemie GmbH, 82024 Taufkirchen, Germany
Sodium acetate (3 mM, pH 3)	Merck KGaA, 64293 Darmstadt, Germany

### 2.1.3. Tissue processing / immunohistochemistry

Alexa Fluor® 647 Goat Anti-Rabbit IgG (H+L) Antibody	Life Technologies GmbH, 64293 Darmstadt, Germany
Gibco Goat Serum	Invitrogen GmbH, Darmstadt, Germany
PFA (paraformaldehyde) 4%	8% PFA (Sigma-Aldrich) in dH <sub>2</sub> O, heated up to 55 °C and stirred additional 10 min, filtrated and mixed in a 1:1 ratio with 0.2 M PB (Phosphate buffer), pH adjusted to 7,2 - 7,8
Phosphate Buffer (PB) 0,2 M	27.598 g NaH <sub>2</sub> PO <sub>4</sub> · H <sub>2</sub> O, 35.598 g Na <sub>2</sub> HPO <sub>4</sub> · 2H <sub>2</sub> O dH <sub>2</sub> O ad 1 l
Phosphate Buffered Saline (PBS), 10x 103,23 mg Na <sub>2</sub> HPO <sub>4</sub> · H <sub>2</sub> O	103.23 mg Na <sub>2</sub> HPO <sub>4</sub> H <sub>2</sub> O 26.52 g Na <sub>2</sub> HPO <sub>4</sub> · 2H <sub>2</sub> O 40 g NaCl H <sub>2</sub> O bidest. added to 1 l Prepared in house.
Rabbit polyclonal to GRP78 BiP antibody (ab21685)	Abcam, Cambridge, MA 02139-1517, USA
Sucrose	Sigma-Aldrich® Chemie GmbH, 82024 Taufkirchen, Germany
TBS 10x (Tris buffered saline), pH = 7,6	61 g Tris base (121.14 g/mol), (Sigma-Aldrich)

	90 g NaCl dH <sub>2</sub> O ad 1 l
Tissue Tek optimal cutting temperature (O.C.T.)	akura Finetek Europe B.V., Alphen aan den Rijn, The Netherlands
Triton X-100	Sigma-Aldrich® Chemie GmbH, 82024 Taufkirchen, Germany
Vectashield Mounting Medium, Fluorescence H-1000	Vector Labs, Burlingame, CA 94010, USA

## 2.2. Materials

### 2.2.1. Surgery and in vivo imaging

BD Plastipak Hypodermic luer slip syringe 1 ml (syringe for Ketamine/Xylazine and Ptx injection)	Becton, Dickinson and Company, Franklin Lakes (New Jersey), USA
Cast Alnico Button Magnets	Eclipse Magnetics Ltd, Sheffield, UK
Dumont Mini Forceps – Inox Style 3 (Small forceps)	Fine Science Tools GmbH, Heidelberg, Germany
Dumont Mini Forceps – Inox Style 5 (Small forceps)	Fine Science Tools GmbH, Heidelberg, Germany
Feather stainless steel blade (surgical blade)	pfm medical ag, Cologne, Germany
Hypodermic Needles BD Microlance 3 23 Gauge (0,6 mm, blue) for subcutaneous emulsion immunization	Becton, Dickinson and Company, Franklin Lakes (New Jersey), USA
Hypodermic Needles BD Microlance 3 30 Gauge (0,3 mm, yellow) for subcutaneous injection of Ptx and anesthesia	Becton, Dickinson and Company, Franklin Lakes (New Jersey), USA
Infinite Horizons Impactor	Precision Systems and Instrumentation, Fairfax Station, VA 22039, USA
Metal plate	Custom made
Noyes Spring Scissors (Large spring scissors)	Fine Science Tools GmbH, Heidelberg, Germany
Rubber bands	
Spongostan special (hemostatic gelatin sponge)	Ethicon Inc. Somerville, New Jersey, USA
Sugi (absorbent triangles)	Kettenbach GmbH & Co. KG, Eschenburg, Germany
Support cushion	Custom made
Vannas-Tübingen Spring Scissors (Small angled spring scissors)	Fine Science Tools GmbH, Heidelberg, Germany

Venofix® A, 0,40 x 10 mm, 30 cm Schlauchlänge, G 27 grau	B. Braun Melsungen AG, Melsungen, Germany
Wella contura W7807 (Hair clipper)	Wella, Darmstadt, Germany

### 2.2.2. Tissue processing / immunohistochemistry

15 ml and 50 ml Falcon tubes	Greiner Bio-One GmbH, Frickenhausen, Germany
24-Well microtiter plates	Becton, Dickinson and Company, Franklin Lakes, New Jersey, USA
Microscope cover slips 24 x 60 mm	Gerhard Menzel Glasbearbeitungswerk, GmbH & Co. KG, Braunschweig, Germany
Microscope slides 76 x 26 mm	Gerhard Menzel Glasbearbeitungswerk, GmbH & Co. KG, Braunschweig, Germany
Parafilm	Brand GmbH & Co. KG, Wertheim Germany
Pipettes, pipette tips and tubes (2 ml and 1,5 ml)	Eppendorf AG, Hamburg, Germany
Tissue Tek Cryomold Biopsy, 10 x 10 x 5 mm	Sakura Finetek Europe B.V., Alphen aan den Rijn, The Netherlands
Tissue Tek Cryomold Biopsy, 25 x 20 x 5 mm	Sakura Finetek Europe B.V., Alphen aan den Rijn, The Netherlands
Tissue Tek optimal cutting temperature (O.C.T.)	Sakura Finetek Europe B.V., Alphen aan den Rijn, The Netherlands
Transparent nail varnish	

## 2.3. Technical devices

### 2.3.1. Surgery and in vivo imaging

100W infrared lamp	Beurer GmbH, Ulm, Germany
FST 250 Hot Bead Sterilizer (sterilizer for surgical instruments)	Fine Science Tools GmbH, Heidelberg, Germany
MiniVent Ventilator for Mice (Model 845), single animal, volume controlled	Harvard Apparatus, Holliston (Massachusetts), USA
Olympus KL 1500 LCD (cold light source for stereomicroscopy)	Olympus Deutschland GmbH, Hamburg, Germany
Olympus Stereo Microscope SZ51	Olympus Deutschland GmbH, Hamburg, Germany
Spinal Cord Clamps	NARISHIGE INTERNATIONAL LIMITED, London, U.K.

T/Pump (Heating pad)	Gaymar Industries, Orchard Park (New York), USA
----------------------	---

### 2.3.2. Microscopy

Leica TCS SP8 confocal microscope equipped with 20x / 0.75 objective and 63x / 1.40 oil immersion objective	Leica Microsystems GmbH, Wetzlar, Germany
MaiTai Deep See® Titanium:sapphire Laser	Newport/ Spectraphysics, Irvine, California, USA
Manual XY translation stage	Luigs & Neumann Feinmechanik und Elektrotechnik GmbH, Ratingen, Deutschland parts by Thorlabs Inc Newton (New Jersey), USA
Olympus FV1200 MPE multiphoton Microscope x 25 / 1.05 water immersion objective	Olympus GmbH, Hamburg, Germany

### 2.3.3. Tissue processing / immunohistochemistry

HISTO LEICA Vibratome VT1200S	Leica Microsystems GmbH, Wetzlar, Germany
KERN EW 150-3M (Scale)	Kern & Sohn GmbH, Balingen-Frommern, Germany
Laboratory pH-meter inoLAB	WTW Wissenschaftliche-Technische Werkstätten, Weilheim, Germany
Leica CM1850 Cryostat	Leica Microsystems GmbH, Wetzlar, Germany
Magnetic stirring hotplate MR 3001K and stirring bars	Heidolph Instruments GmbH & Co. KG, Schwabach, Germany
Olympus IX71 inverse fluorescence micro-scope (initial assessment of stainings and expression)	Olympus GmbH, Hamburg, Germany
Vortex-Genie 2	Scientific Industries, Inc., Bohemia, New York, USA

### 2.4. Data analysis / software

Adobe Creative Suite 6 (Photoshop, Illustrator)	Adobe Systems, Inc., San Jose, California, USA
Graphpad Prism	GraphPad Software, La Jolla, California, USA

ImageJ / FIJI	General Public License <a href="http://rsbweb.nih.gov/ij/download.html">http://rsbweb.nih.gov/ij/download.html</a>
Microsoft Office (Powerpoint, Excel, Word)	Microsoft Corporation, Redmond, Washington, USA

## 2.5. Experimental animals

All experimental mice were bred on a C57/BL6 background. For the illustration of intra-axonal calcium levels Thy1-CerTN-L15 mice and for the imaging of ER calcium concentrations Thy1-TwitchER (Witte et al. 2019) mice were used. These experimental animals express the GECI CerTN-L15 (Heim et al. 2007) or Twitch2B 54S+ ER (Thestrup et al. 2014) controlled under the Thy1 promoter. All mice were kept and bred in our animal facilities under specific pathogen free standard conditions. They were held in Eurostandard Type II long cages 365 x 207 x 140 mm (Tecniplast, Hohenpeißenberg, Germany) stored in an IVC rack system. A maximum amount of five mice per cage was accepted and the animals were housed on 12 h light / dark cycles. Mice were fed autoclaved food (regular food ‘Maus’ from Ssniff, Soest, Germany) and water ad libitum. All animal experiments were approved by the Regierung von Oberbayern.

## 2.6. Methods

### 2.6.1. Tissue processing and immunohistochemistry

Following lethal anaesthesia using isoflurane mice were first transcardially perfused with 1 x PBS/Heparin, then with 4% paraformaldehyde (PFA) diluted in 0.1 M phosphate buffered saline (PBS). After macro-dissection, that is cutting away everything but the skull and spine, the residual tissue was post-fixed in 4% PFA in PBS for 24 hours. This was followed by a micro-dissection where the spinal cord and its attached DRGs were carefully removed from the rest of the tissue. Afterwards, spinal cords were put into 30% sucrose in 1 x PBS for one to three days for cryoprotection. Parts of the tissue were then embedded in O.C.T. and immediately frozen using an ethanol-dry-ice bath. Next, 30 to 40 µm thick transverse sections were cut in a Leica CM1850 cryostat and then washed three times for ten minutes with 1 x PBS at room temperature. After blocking the sections in 10% goat serum (g.s.) / 0.5% Triton X-100 (T) / 1 x PBS for one hour, they were incubated for two days at 4°C in a 1:100 dilution of the primary antibody GRP78/BiP prepared in 1% g.s. / 0.5% T / 1 x PBS. Following a second washing step with 0.5% T / 1 x PBS the sections were put into a 1:500 dilution

of the secondary antibody AF 647 goat anti rabbit, prepared with the same solution as the primary antibody, for three hours. Finally, after washing the stained tissue three times for 30 minutes in 1 x PBS, spinal cord and attached DRG sections were carefully mounted with Vectashield onto microscope slides and then covered with cover slips, with the edges being sealed with nail varnish. Spinal cord and DRG overview images were scanned with the Leica TCS SP8 confocal microscope, equipped with a 20x / 0.75 objective, using a 514 nm laser for excitation and a bandpass filter of 520 – 550 nm for the hybrid-PMT (HyD) detector. For colocalization of Twitch2B 54S+ ER and GRP78 BiP single DRG and spinal cord neurons were imaged with a 63x / 1.40 oil immersion objective, a 514 nm laser line for the YFP of Twitch2B 54S+ ER and a 633 nm laser for the AF 647 secondary antibody. Emission light from Twitch2B 54S+ ER was collected as described before, whereas the AF 647 infrared-emission was detected by another HyD detector and a bandpass filter of 645 – 715 nm.

### 2.6.2. In vivo microscopy

Mice used for 2 photon microscopy of the spinal cord underwent surgical procedures as described in an established protocol (Kerschensteiner et al. 2005; Nikić et al. 2011). Anaesthesia was performed by an intraperitoneal injection of MMF (a combination of medetomidine, midazolam and fentanyl) with an amount of 15 times the weight of the mouse. Afterwards, they were put into a heating pad for around 30 minutes until anaesthesia was deep enough to start the surgery. Next, the fur above the spinal cord was shaven and the skin cleared of residual hair. After being fixed on a metal plate with magnets and rubber bands entangling all limbs, the skin was opened, and the spine exposed by removing muscles and connective tissue. A bilateral dorsal laminectomy of two lumbar vertebrae was done to uncover the spinal cord. From then on, the spinal cord was constantly rinsed with artificial cerebrospinal fluid (aCSF) to avoid exsiccation. Followed by the careful removal of the dura mater the vertebral column was fixed with clamps from a Narishige clamping device. Finally, a well was built around the laminectomy site using 2% agarose / aCSF so that a fluid reservoir of aCSF could be obtained for the immersion of the microscope's objective and the application of pharmacological agents. A waiting time of at least 1.5 hours before imaging was established for Thy1-TwitchER mice.

The clamping device with the prepared mice was then fixed to a manual XY translation stage attached to the Olympus FV1200 MPE multiphoton microscope geared with a

MaiTai Deep See titanium-sapphire laser. A 25x / 1.05 N.A. water immersion objective was used to acquire the images. The laser's wavelength was tuned to 840 nm for the excitation of the CFP from the FRET pair of CerTN-L15 and Twitch2B 54S+ ER and the intensity was adjusted to the brightness of fluorescence of each mouse. Emitted photons were then separately detected using a 455 – 490 nm bandpass filter for CFP and 526 – 557 nm for YFP. The gallium arsenide phosphide (GaAsP) detectors were set to 640 V for the CFP channel and 500 V for the YFP channel. Depending on the experiment volume stacks of different depth and repetition frequency were imaged. Depth of anaesthesia was continuously monitored and reobtained with injections of small amounts of MMF in case of a decreasing level of anaesthesia. Euthanasia was performed with isoflurane after in vivo imaging was finished.

### 2.6.3. Pharmacological experiments

Pharmacological experiments with caffeine were done in Thy1-TwitchER and Thy1-CerTN-L15 mice. Surgical procedures were performed as described above with the addition of a tracheotomy for the insertion of a tracheal tube of the MiniVent Ventilator in order to reach controlled breathing and therefore image stability. An adjusted Venofix butterfly with its needle removed was inserted into the agarose well for drug application during the process of imaging. Prior to caffeine application at least four volume stacks were acquired, as well as a 15 minutes time series with images taken every 30 seconds. Next, another time series of ten minutes with images taken every ten seconds was started during which the same amount of a 100 mM caffeine stock solution diluted in aCSF as aCSF in the agarose well was injected to reach an effective caffeine concentration of 50 mM. Afterwards volume stacks at the same locations as prior to caffeine application were acquired.

For the thapsigargin application two image stacks with a time interval of ten minutes were taken in Thy1-TwitchER mice before administering 100  $\mu$ M thapsigargin diluted in 1% DMSO and aCSF to the spinal cord. Immediately afterwards and subsequently in ten minutes intervals images were acquired.

For the application of 4-chloro-3-ethylphenol (4-CEP) one image stack was generated before administering either 3 mM 4-CEP (one mouse) diluted in 3.3% DMSO or 5 mM 4-CEP (one mouse) in 0.5% DMSO and aCSF to the spinal cord. Afterwards images were taken every five minutes for a maximum duration of 35 minutes.

#### 2.6.4. EAE induction and in vivo imaging

Thy1-TwitchER and Thy1-CerTN-L15 mice were induced with active EAE according to an established protocol (Abdul-Majid et al., 2000; Nikić et al., 2011). In brief, animals were immunized with 250 µl of an emulsion containing 400 µg of purified recombinant myelin oligodendrocyte glycoprotein (MOG, N1-125, expressed in *E. coli*) and incomplete Freund's adjuvant with 5 mg/ml mycobacterium tuberculosis H37 Ra. First, they received a short anaesthesia with KX (mixture of 87 µg/g body weight Ketamine and 13 µg/g body weight Xylazin) followed by injections of the defined emulsion into the tail and both flanks. Afterwards and 48 hours later, 250 ng of pertussis toxin was injected intraperitoneally. On a daily basis, immunized mice were then weighed and scored for neurological deficits according to the following EAE scoring scale:

Score	Clinical signs
0	No detectable clinical signs
0.5	Partial tail weakness
1	Tail paralysis
1.5	Gait instability or impaired righting ability
2	Hind limb paresis
2.5	Hind limb paresis with partial dragging
3	Hind limb paralysis
3.5	Hind limb paralysis and fore limb paresis
4	Hind limb and fore limb paralysis
5	Death

**Table 1: EAE clinical scoring scale**

Imaging was performed two or three days after the onset of clinical symptoms only when the EAE score was equal or higher than 2.5. Eight to ten regions were imaged based on the visual infiltration of immune cells. After a 15 minutes time series with images taken every 30 seconds, a solution of 50 mM caffeine was applied to the spinal cord and ten minutes later four volume stacks of previously recorded regions were acquired. For Thy1-CerTN-L15 EAE mice a caffeine time series was imaged as described above.

### 2.6.5. Spinal cord contusion model

Spinal cord contusion experiments were done adapted from a previous protocol (Williams et al. 2014). Surgical procedures were performed as described, however, without the removal of the dura mater. After the established 1.5 hours waiting time two pre-lesion image stacks were taken and their x/y-positions were saved. The contusion injury was then induced with the Infinite Horizons impactor using a force of 40 kDyne resulting in an actual force of 40 to 45 kDynes. In case of no significant subdural bleeding mice were then quickly re-installed below the microscope and a first post-lesion image of the previously saved regions was taken within less than 10 minutes. Then a time series was acquired for two hours in intervals of 15 minutes.

### 2.6.6. Image processing and data analysis

Acquired images were analysed using the open-source image-analysis software Image J / Fiji. In Fiji, images were separated into their respective channels and displayed in a grey-scale look-up table, with the YFP channel being used for the selection of regions of interest (ROIs) due to its better signal-to-noise ratio. Time series were also split into single timepoints for analysis and only axons that could be tracked at every timepoint were evaluated. Longitudinal ROIs were then drawn freehand into the axons, along with equally sized ROIs in adjacent non-axonal areas. Then, the mean intensity of all ROIs in the CFP and YFP channel was measured in Fiji and copied into Microsoft Excel sheets. After background correction, calculated by subtracting the intensity of non-axonal ROIs from the corresponding axonal ROIs, a YFP/CFP ratio, expressing the calcium concentration of either the ER (Thy1-TwitchER mice) or the axoplasm (Thy1-CerTN-L15 mice), was calculated. These ratios were then normalized to the mean ratio of all control mice or to the mean ratio of the first time point of a time series. For the analysis of cytoplasmic calcium concentrations axons were regarded as high calcium if the YFP/CFP ratio was above the mean plus three standard deviations (SD) of the ratios of axons in healthy control mice. ER was considered depleted of calcium if the YFP/CFP ratio was below the mean minus three SD of the ratios of axons in healthy control mice. In EAE mice axons were morphologically classified into the previously described stages: normal appearing stage 0, swollen stage 1 and fragmented stage 2 axons (Nikić et al. 2011). Axons of Thy1-Twitch-ER mice in spinal cord contusion experiments were visually classified into

fragmented or non-fragmented ER according to the existence of continuity or fragments of the ER.

The ratiometric images that are shown in this work were processed as follows: maximum-intensity projections of the CFP and YFP channels were generated and a binary thresholded mask of axonal structures was created from the brighter YFP channel. After multiplying each channel with the binary mask, the resulting YFP image was divided by the new CFP image. Then, a pseudocoloured look-up table, with high ratios depicted in yellow and low ratios in purple, was applied with ratio boundaries set differently for Thy1-TwitchER and Thy1-CerTN-L15 mice. RGB images were then exported to Adobe Photoshop, despeckled and by using the “overlay” function overlaid with the greyscale maximum-intensity projection of the YFP channel.

Analysed data was visualized in GraphPad Prism version 7.01 and modified in Adobe Illustrator. Statistical analysis was done in Prism with (un)paired t-tests when normality of distribution was confirmed with the Shapiro-Wilk test. Mann-Whitney U or Wilcoxon signed-rank tests were used when normal distribution could not be proved. Data was regarded as statistically significant when p values were below 0.05.

### **3. Contributions of other lab members to the thesis project**

Experiments in this thesis are based on preceding findings of my colleague Alexander Scheiter, who generated the transgenic mouse line for measuring intra-axonal ER calcium changes and performed preliminary experiments in experimental models of neuroinflammation and spinal cord injury. These experiments are detailed in the thesis work of Alexander Scheiter (Scheiter 2020) and will be summarized in the following paragraphs.

After showing that the ER can be labelled in axons using the green FP mEmeraldER, Alexander Scheiter carefully assessed different ER GECIs and finally chose the low affinity sensor Twitch2B 54S+ ER for the generation of a transgenic reporter mouse line. This ER calcium indicator was selected due to its  $K_d$  being close to reported axonal ER calcium concentrations, its high dynamic range, FRET-based ratiometric properties and quasi-linear response kinetics. Pharmacological depletion of ER calcium contents with the SERCA inhibitor thapsigargin and refilling it with ionomycin in Hek-293 cells showed expected results in ratio changes of Twitch2B 54S+ ER. Furthermore, he could show that mutating the calcium binding EF hand of this sensor, rendering it insensitive to calcium, lead to no FRET changes upon administering thapsigargin, confirming that Twitch2B 54S+ ER actually measures ER calcium levels.

Next, Alexander Scheiter generated Thy1-TwitchER transgenic mice and screened the yielded lines for proper expression of the sensor in the CNS and PNS. Thy1-TwitchER 481 and 509 were the two mouse lines that featured an appropriate labelling in the spinal cord and DRG neurons and these lines were selected for further characterization. Thy1-TwitchER 509 mice showed a larger amount of Twitch2B 54S+ ER expressing DRG neurons and thus a denser labelling of axons in the dorsal column of the spinal cord, however, with a lower signal-to-noise ratio when compared to Thy1-TwitchER 481 mice, so that the Thy1-TwitchER 481 mouse line was selected for all subsequent experimental analysis. In vivo two photon microscopy of the chosen transgenic mouse line showed an adequate labelling of dorsal column axons for further experiments but a large spread of baseline YFP/CFP ratios. In initial proof-of-concept experiments ER calcium depletions in axons of two mice, induced by applying thapsigargin to the spinal cord, could again be well measured by the ER calcium indicator and resulted in a reduction of the ratio spread. Hence, it could be concluded that Thy1-TwitchER mice reliably detect ER calcium levels and therefore can be used

to study the role of ER calcium in experimental models of axon degeneration. Here Alexander Scheiter also performed initial experiments that yielded results that were consistent with my subsequent experiments and the extended analyses presented in my thesis.

## 4. Objectives

Previous work in our lab could show that axon degeneration in neuroinflammatory lesions and after traumatic spinal cord injury can still be reversible in early stages of the degeneration process (Nikić et al. 2011; Williams et al. 2014). Further experiments did reveal that prolonged elevated intra-axonal calcium levels predict the axonal fate (Schumacher 2016; Williams et al. 2014). Calcium release from the ER, a major intra-axonal calcium store, has been implicated in ex vivo studies as a major contributor to cytoplasmic calcium increases and thus a potential trigger of axonal degeneration processes (Ouardouz et al. 2003; Stirling et al. 2014). Thus, my colleague Alexander Scheiter developed the transgenic Thy1-TwitchER mouse line that allowed us to investigate ER calcium dynamics in vivo. The overall aim of this present thesis was to further validate this in vivo imaging approach and to investigate the spatial and temporal dynamics of ER calcium and morphology in models of neuroinflammation and mechanical trauma. The following specific questions were addresses in this thesis:

- Is the low-affinity calcium sensor Twitch2B 54S+ ER reliably expressed in those neurons of Thy1-TwitchER mice whose axons are subject to in vivo spinal cord imaging?
- Can baseline intra-ER calcium levels and their response to pharmacological manipulations be detected in vivo in spinal cord axons of the Thy1-TwitchER mouse line?
- What is the response of the ER, in terms of calcium levels and morphology, to traumatic spinal cord injury?
- Are there changes in ER calcium concentrations in neuroinflammatory lesions induced in a multiple sclerosis model?
- If calcium is released from the ER, how does this affect intra-axonal calcium levels and potentially influence the axon degeneration process?

## 5. Results

### 5.1. Imaging ER calcium in spinal cord axons of Thy1-TwitchER mice

#### 5.1.1. Evaluation of Twitch2B 54S+ ER expression pattern and intracellular localization

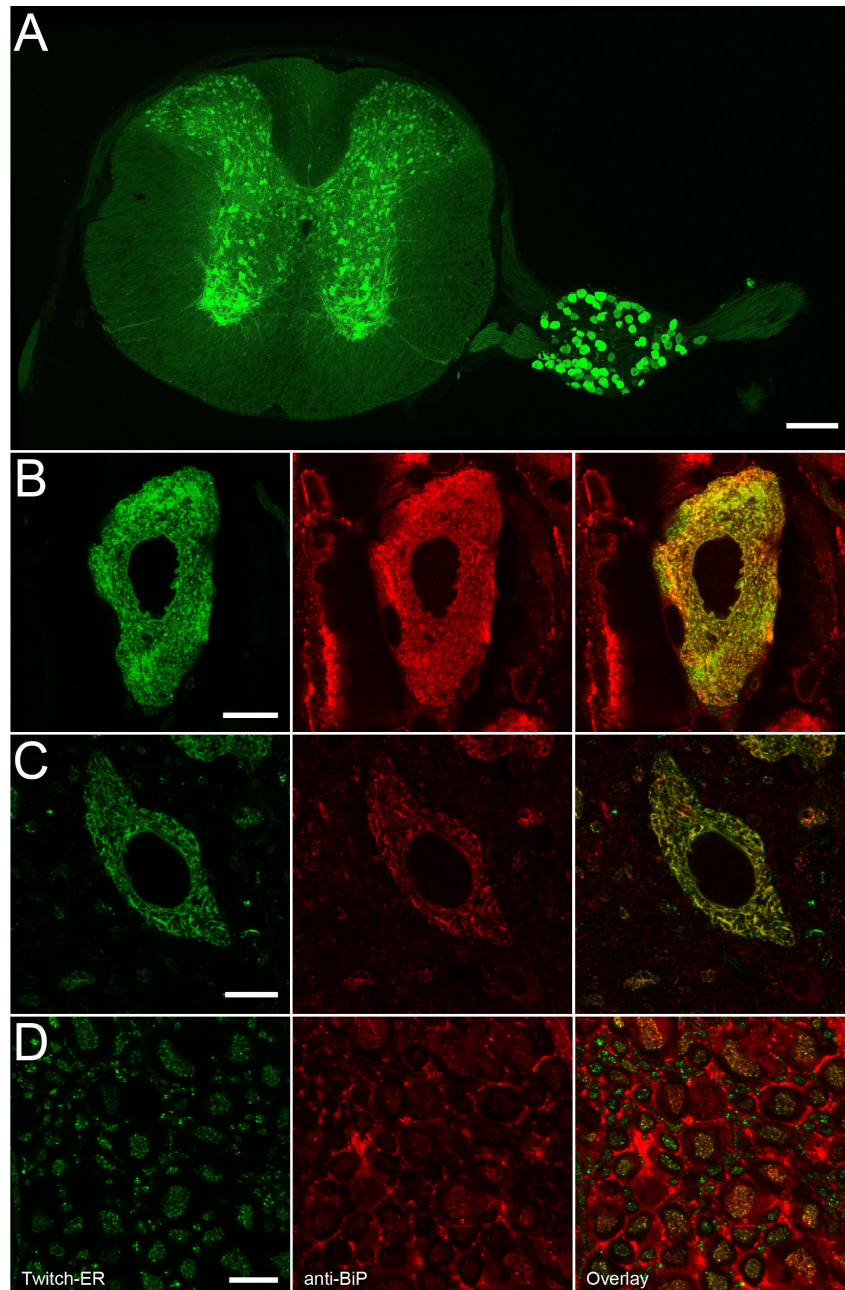


**Figure 7: Twitch2B 54 S+ ER expression pattern and colocalization with GRP78/BiP**

(A) Confocal overview image of a thoracic spinal cord transverse section with an attached DRG of a Thy1-TwitchER mouse. (B-D) Colocalization images of Thy1-TwitchER (green, left) and the ER marker GRP78/BiP (red, middle) and an overlay of both channels (right) of (B) a DRG neuron, (C) a spinal neuron, (D) cross-sectioned axons. Scale bars in A, 200  $\mu$ m and in B-D 10  $\mu$ m. Figure and caption adapted from (Witte et al. 2019)

First, the Thy1-TwitchER mouse line generated by Alexander Scheiter needed a more extended evaluation. For further validation of the expression pattern and localization of the ER calcium indicator I used a careful method of microdissection to yield a higher amount of DRGs that are attached to the spinal cord. Thereby, a full overview of a cross-section of the thoracic spinal cord with a connected DRG could be created by merging z-projections of every image of a confocal tile-scan (Figure 7 A). Due to dorsal column axons being imaged for in vivo microscopy, correct localization of Twitch2B 54S+ ER in the ER needed to be confirmed in the corresponding DRG neurons. Analysis of the anatomy of the spinal cord has indicated that the dorsal column consists of different types of fibres. A large group of the axons are short and only pass some segments before entering the dorsal horn. The other axons either originate from large DRG neurons or are part of the so-called postsynaptic dorsal column pathway arising from dorsal horn neurons and form the gracile and cuneate fasciculi (Watson et al. 2009). In his work Alexander Scheiter could confirm colocalization of Twitch2B 54S+ ER and the established ER marker GRP78/BiP for spinal interneurons, so that the immunostaining protocol was adapted to reach bright enough GRP78/BiP stainings. This was achieved by using higher amounts of the respective primary antibody, as well as an increased incubation time of two days. The resulting images can be seen in Figure 7 B-D, with the green colour showing the expression of Twitch2B 54S+ ER and the red image illustrating the GRP78/BiP immunostaining visualized by the fluorescent secondary antibody AF 647. Colocalization, which is well visible in the right image generated by overlaying both other images, could be confirmed for DRG and spinal neurons. Interestingly, not only the known nuclear envelope and the reticular pattern of the ER were apparent but also regions of stacked or clumped ER especially in the subplasmalemmal areas of DRG neurons. As expected, GRP78/BiP staining was also existent in other cells than neurons. Previously, the same antibody has been used to stain ER in dorsal root axons (Stirling et al. 2014). Confocal images of cross-sectioned axons could also show a putative colocalization between GRP78/BiP and Twitch2B 54S+ ER but the results were not as clear as in neurons likely due to the weak GRP78/BiP antibody staining in axons and the fact that the ER appeared to have a punctuated pattern which is most likely caused by ER fragmentation post fixation. In summary, these findings, however, demonstrate that in Thy1-TwitchER mice the sensor protein is expressed in DRG neurons and localized to the ER.

### 5.1.2. Optimization of in vivo imaging conditions for ER calcium measurements

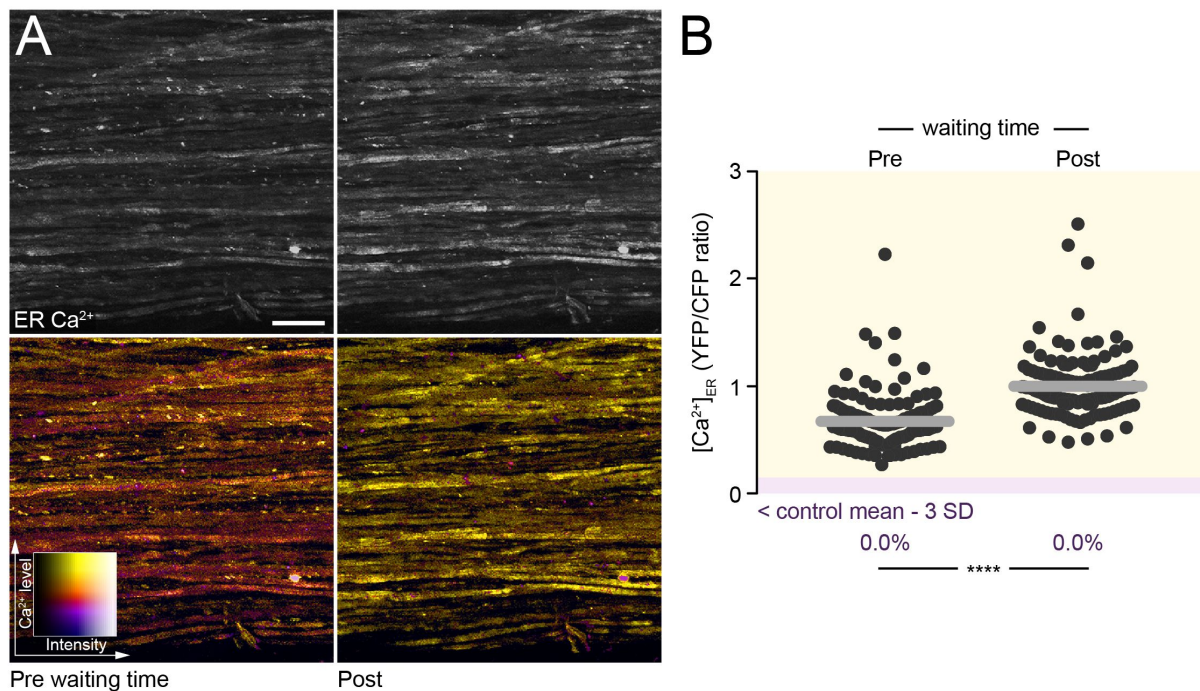


**Figure 8: Introducing a 1:30 h waiting time post-surgery increases ER calcium levels in Thy1-TwitchER mice**

(A) In vivo projection images of the spinal cord of healthy control Thy1-TwitchER mice directly after surgery (left) and post a 1:30 h waiting time (right). Upper row greyscale YFP channels for axon morphology, pseudocoloured YFP/CFP ratiometric images in lower row. (B)  $[Ca^{2+}]_{ER}$  (YFP/CFP ratio) of single axons pre and post 1:30 h waiting time ( $n = 5$  mice, Wilcoxon signed-rank test). Percentages below represent the fraction of axons with a  $[Ca^{2+}]_{ER}$  below control mean  $- 3$  SD. Scale bar in (A)  $25 \mu m$ . \*\*\*\* $P < 0.0001$ . Figure and caption adapted from (Witte et al. 2019)

After confirming the correct localization of Twitch2B 54S+ ER experiments were from then on performed in an in vivo setting. Initial in vivo microscopy using Thy1-TwitchER mice by Alexander Scheiter reported a large spread of baseline YFP/CFP ratios in healthy control mice. This was also observed in my initial experiments, where an internal spread of ratios within each mouse and a spread between the mean ratios of each mouse could be seen. The properties of GECIs might contribute to this finding as its functioning can be influenced by temperature, pH and magnesium (Grienberger und Konnerth 2012). While not being able to completely rule out the latter ones, the usage of the same sterile artificial mouse cerebrospinal fluid with controlled concentrations of ions and pH for each mouse diminishes the possible involvement of magnesium and pH to the baseline ratio spread. Furthermore, Twitch sensors have been designed in a way that the chance for magnesium binding to the EF hand has been minimized (Thestrup et al. 2014). When imaging one mouse over time changing the temperature

of the aCSF, surrounding the spinal cord, in a controlled manner, no correlation between temperature and YFP/CFP ratio changes could be detected (data not shown). Another explanation might be the physical spinal cord disturbance caused by the surgery since contusion experiments have shown reversible drops in ER calcium concentrations after mechanical trauma. Damaging single axons during surgery might result in partial depletion of the ER calcium store in some axons leading to the observed spread. Therefore, images of five Thy1-TwitchER mice were directly taken after surgery and repeated after a waiting time of one and a half hours. Interestingly, ER calcium levels significantly increased over that time, however, the spread in YFP/CFP ratios did not seem to be reduced (Figure 8). Taken together, the spread in baseline ER calcium concentrations still displayed an unsolved issue. Yet, an improved protocol for in vivo microscopy of Thy1-TwitchER mice could be implemented that included a waiting time of at least one and a half hours after spinal cord surgery enabling ER calcium pools to replenish.

### 5.1.3. Pharmacological characterization of Thy1-TwitchER mice

Next, I continued the pharmacological characterization of Thy1-TwitchER mice that was initiated by Alexander Scheiter. First, I complemented his preceding two ER depletion experiments using 10  $\mu$ M thapsigargin with a dataset of four mice where two images were taken before the bath application of 100  $\mu$ M thapsigargin dissolved in 1% DMSO in aCSF. In vivo imaging was then continued for another 80 minutes with images generated every ten minutes. As previously reported, the agent blocking the SERCA resulted in a continuous calcium leak from the ER which, however, took a long time of at least 60 minutes until the maximum observed effect (Figure 9 A, B). Therefore, I investigated other pharmacological agents that interact with the ER calcium pools to obtain a drug for a reliable and quick depletion of ER calcium. ATP and histamine have been shown to be capable of releasing calcium from the ER via the phospholipase C – IP3 pathway (Salter und Hicks 1995; Di Giuro et al. 2017), but did not have the same expected effect on axoplasmic ER in the spinal cord (data not shown). 4-Chloro-3-ethylphenol (4-CEP), which displays an agent that has been used for studying store-operated calcium entry, acts as an agonist at ryanodine receptors (Zeng et al. 2014). Upon application of 3 mM 4-CEP in one mouse the YFP/CFP ratio showed a quicker but less pronounced decline compared to thapsigargin, so that a

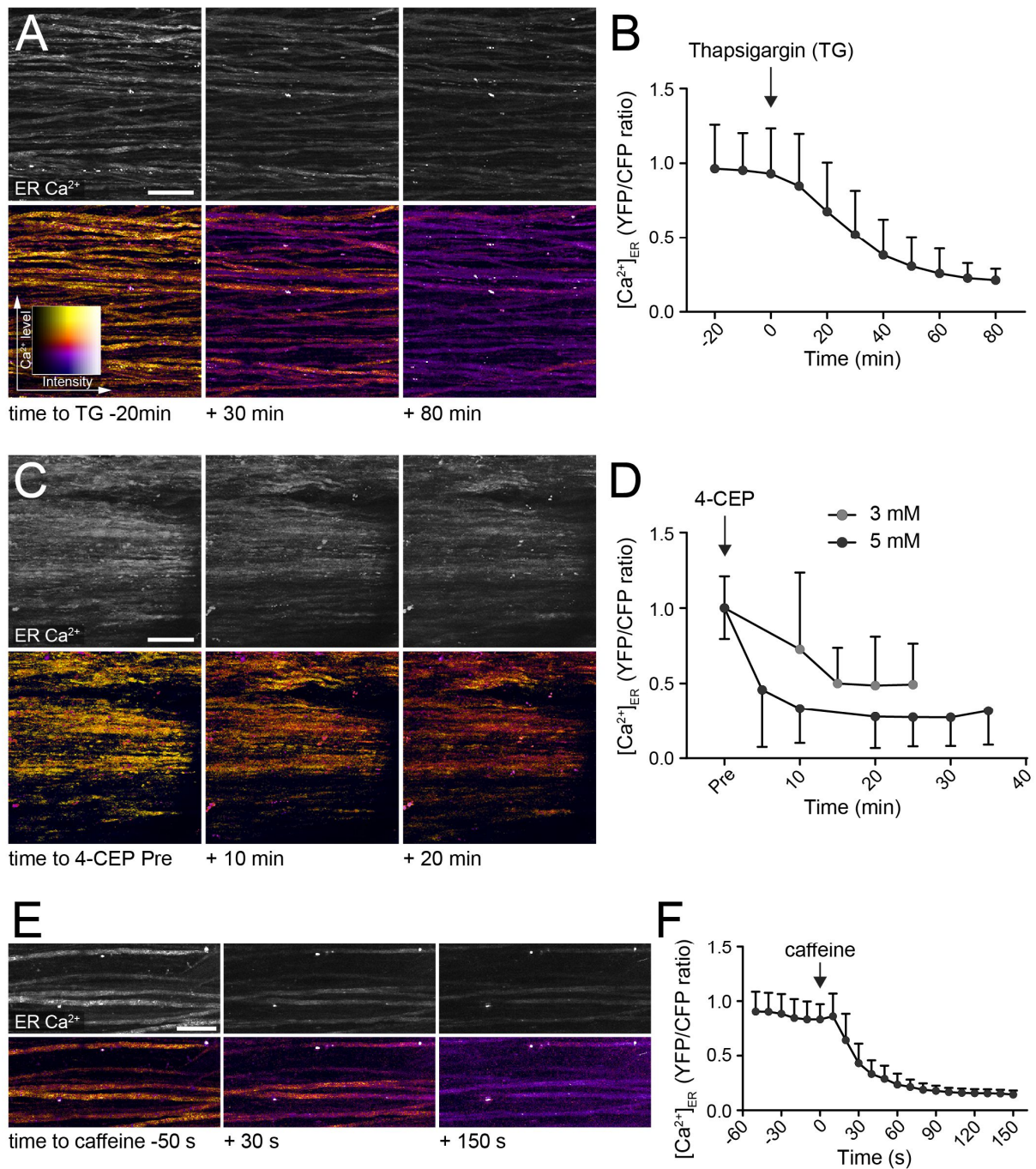


### Figure 9: Response of Thy1-TwitchER mice to ER calcium depleting agents

(A, C, E) Time-lapse projection images of Thy1-TwitchER axons before and after application of 100  $\mu$ M thapsigargin (TG) (A), 3 mM 4-CEP (C) and 50 mM caffeine (E). Greyscale YFP images in upper row, [Ca<sup>2+</sup>]<sub>ER</sub> colour coded in lower row. (B, D, F) Time course graphs of [Ca<sup>2+</sup>]<sub>ER</sub> pre and post application of TG measured every 10 min (n = 4 mice) (B), 3 mM (grey circles) and 5 mM (black circles) 4-CEP measured every 5 to 10 min (n = 1 mouse each) (D), 50 mM caffeine measured every 10 s (n = 5 mice) (F). Presented as mean  $\pm$  SD. Scale bars in (A), (C), (E) 25  $\mu$ m. Figure and caption adapted from (Witte et al. 2019)

second experiment with 5 mM of the same agent was performed. In that, in vivo imaging over 35 minutes in five minutes steps revealed a release of ER calcium within ten minutes (Figure 9 C, D). In these experiments, axons localized further from the

spinal cord surface depleted slower than superficial axons most likely due to a slow diffusion of the drug into the tissue. Finally, I performed experiments with caffeine as this agent is widely used for ER calcium depletion through ryanodine receptors (Fill und Copello 2002). Pilot studies with caffeine revealed that this drug acts very quickly so that a special setup for an ER calcium depletion time series was established. The bath above the mouse spinal cord was partially filled with aCSF and time-lapse imaging of small volume stacks was started with images being created every ten seconds. After one minute 100 mM caffeine in aCSF of the same amount of volume as already in the bath was applied through a butterfly system during the scan to reach a final concentration of 50 mM which had been tested before. The result can be seen in Figure 9 E and F, showing that caffeine rapidly depletes the ER calcium pool. In addition, the baseline spread also appeared to get reduced by caffeine. This set of experiments lead to the two following conclusions: Twitch2B 54S+ ER in Thy1-TwitchER mice can reliably be used for monitoring ER calcium concentrations at fast and slow time scales. Moreover, caffeine is well suited to serve as a positive control for complete ER calcium depletion.

## **5.2. Imaging structural and calcium dynamics of the ER in models of axon degeneration**

After validating sensor expression and function and optimizing the imaging conditons I subsequently studied axonal ER calcium levels in experimental models of axon degeneration. The results obtained in a contusion spinal cord injury model and in acute EAE will be presented in the following paragraphs.

### **5.2.1. ER calcium release and fragmentation after contusion injury**

As already described in chapter 1.4.2 an ER calcium release has been discussed to play a major role in axon degeneration. Given these studies, Alexander Scheiter performed initial experiments with laser-induced and contusion spinal cord injury models, in which a significant depletion of ER calcium and ER fragmentation could be detected in transected axons several minutes after injury. In light of these findings, I was interested to not only investigate the immediate effects of spinal cord injury on ER calcium and fragmentation but also to investigate the temporal dynamics of these processes over time. Therefore, I performed contusion injuries in five Thy1-TwitchER mice following an established protocol (Williams et al. 2014). When no significant bleeding occurred, that could filter emitted light from the YFP, the positions of the

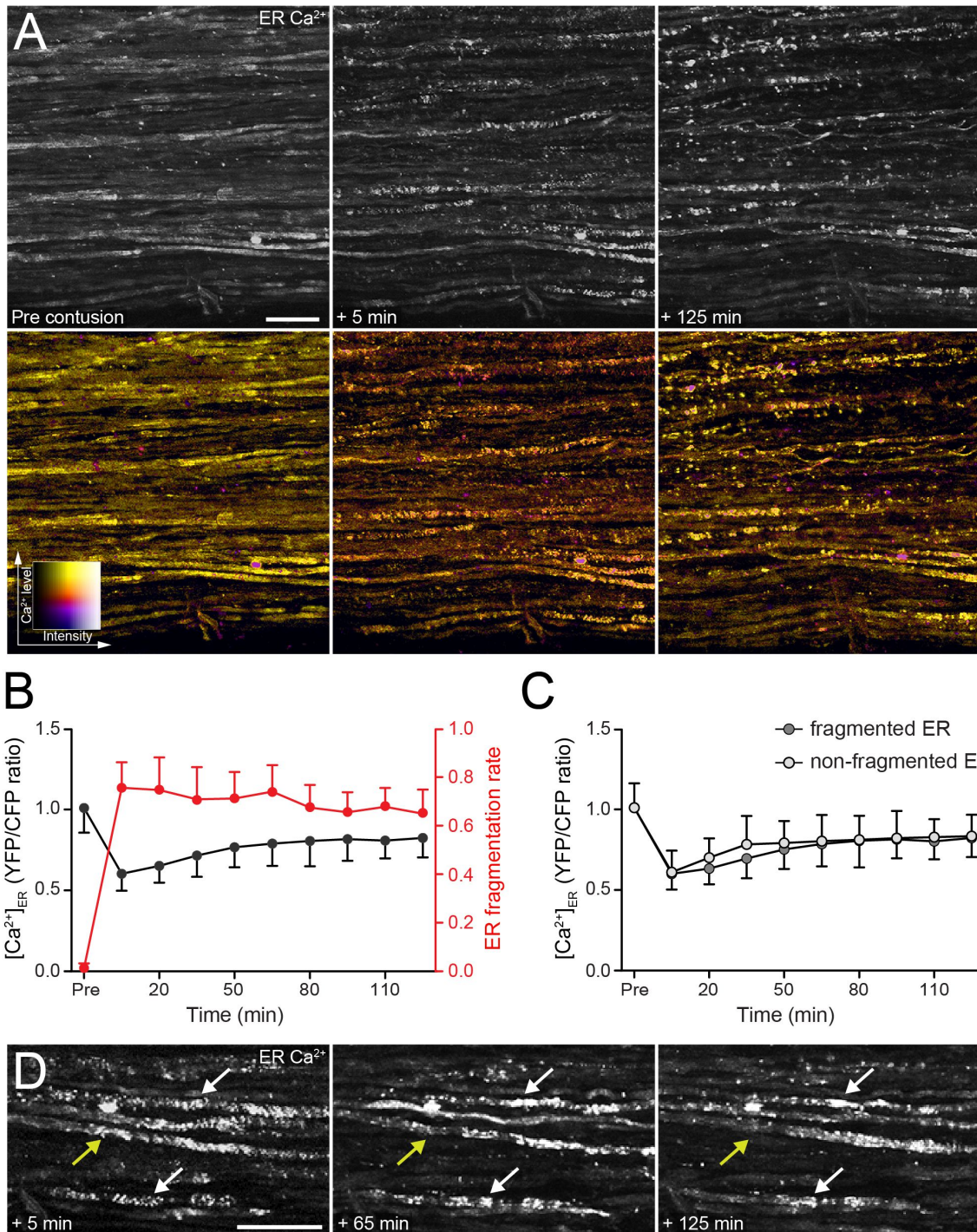


**Figure 10: Temporal dynamics of ER calcium and structure after contusion injury**

(A) In vivo microscopy maximum intensity projections of spinal cord axons in Thy1-TwitchER mice pre-contusion (left), 5 min (middle) and 125 min (right) post spinal cord contusion injury. Top row: greyscale image of the YFP channel, bottom row: colour-coded images for  $[Ca^{2+}]_{ER}$ . (B) Time course graph of  $[Ca^{2+}]_{ER}$  (black) and ER fragmentation rate (red) of single axons measured every 15 min for 125 min before and after contusion. (C) Time course graph of  $[Ca^{2+}]_{ER}$  in axons with fragmented (dark grey) and non-fragmented ER (light grey). N = 5 Thy1-TwitchER mice. (D) Exemplary greyscale images of Thy1-TwitchER spinal cord axons 5 min (left), 65 min (middle) and 125 min (right) post contusion injury with clustering of ER fragments (white arrows) and recovery of normal ER morphology (yellow arrows). Presented as mean  $\pm$  SD. Scale bars in (A, D) 25  $\mu$ m. Figure and caption adapted from (Witte et al. 2019)

images taken before the injury were relocated and a time series of two hours with volume stacks every 15 minutes was started. Analysis of ER calcium did reveal a rapid uniform drop of ER calcium levels directly after contusion injury, which, however, was not in the range of what could be induced by caffeine. When tracking axons over time ER calcium levels seemed to gradually increase again, yet, not to the initial levels before the injury (Figure 10 B).

At the same time a fragmentation of the ER could be observed after injury, which, however, was dynamic over time. When following the structural dynamics of single axons, as far as it was resolvable in the generated overview images, an interesting behaviour of the ER fragments could be discovered. Initially many small mobile fragments did occur, which then started to cluster over time forming large vesicular bodies (Figure 10 D, white arrows). Fluorescence in these clusters was very high which on the one hand suggests that the ER seems to concentrate from long tubules to bulky structures and on the other hand indicates the ER membrane integrity is still intact. Strikingly, these ER clusters were often located close to the plasma membrane. However, this did not appear to be a terminal state since the ER could recover its normal morphology again (Figure 10 D, yellow arrows). Still, these findings must be regarded with caution because the resolution of the images is probably not adequate to make precise assertions about ER morphology. Nonetheless, comparable processes were seen in laser transections of explanted intercostal nerve axons where a better resolution could be achieved (data not shown).

Finally, I separately analysed ER calcium concentrations in axons with fragmented or non-fragmented ER in order to see whether there would be a correlation between these two aspects of ER pathology. However, there was no detectable difference in ER calcium levels between the two observed morphological patterns neither immediately after contusion injury nor over time (Figure 10 C).

Taken together, these data present a consistent behaviour of the ER to mechanical injury. Structural and calcium alterations of the ER do occur post injury, are independent from each other and capable of recovery. This newly discovered ER calcium release in the in vivo model of traumatic axon injury supports the findings that were made in previous in vitro studies (Stirling et al. 2014; Villegas et al. 2014). However, since cytoplasmic calcium increases and axon fragmentation did only occur in a substantially smaller fraction of axons in the exact same experimental setup

(Williams et al. 2014), it seems unlikely that the here observed homogenous ER calcium depletions are causative for the elevated cytosolic calcium levels. Still a relevant contribution to axon degeneration cannot be ruled out.

### 5.2.2. Absence of ER calcium release in early stages of FAD

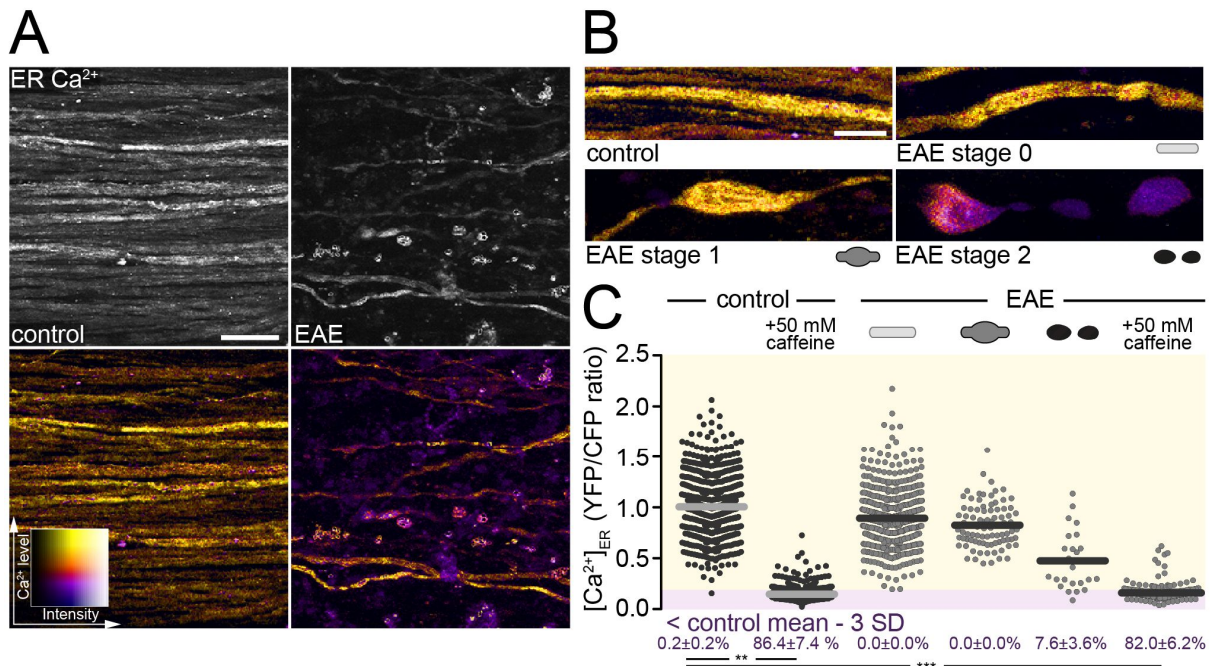


**Figure 11: ER calcium release only occurs late in FAD**

(A) Representative in vivo microscopy maximum intensity projections of axons in the healthy (left) and EAE afflicted (right) spinal cord of Thy1-TwitchER mice. Top row: greyscale image of the YFP channel, bottom row: colour-coded images for  $[Ca^{2+}]_{ER}$ . (B) Exemplary ratiometric (YFP/CFP) images of healthy control axons (upper left), normal-appearing stage 0 (upper right), swollen stage 1 (lower left) and fragmented stage 2 (lower right) axons in acute EAE lesions. (C) Axonal  $[Ca^{2+}]_{ER}$  (YFP/CFP ratio normalized to the mean of control axons) in healthy control mice and the different stages of FAD in EAE (pre and post application of 50 mM caffeine). Bars indicate means, percentages (below) display fraction of axons with depleted  $[Ca^{2+}]_{ER} < \text{control mean} - 3 \text{ SD}$ . Paired t-test for control pre and post caffeine, Mann-Whitney U test for control vs. EAE stages 0, 1, 2  $\pm$  caffeine. N = 7 control mice, n = 7 EAE mice. Scale bars in (A) 25  $\mu\text{m}$  and in (B) 10  $\mu\text{m}$ . \*\*P < 0.01; \*\*\*P < 0.001. Figure and caption adapted from (Witte et al. 2019)

Focal axonal degeneration represents a pattern of axon degeneration first described in the inflammatory lesions of FAD with distinct morphological axon stages. There are normal-appearing stage 0 axons, swollen stage 1 axons in a meta-state capable of both recovery and subsequent progression to fragmented stage 2 axons whose fate has already been determined (Nikić et al. 2011). Previous work in our lab could identify increases in cytoplasmic calcium levels as the driving force for the progression of axon

degeneration (Witte et al. 2019). With the ER being a major intracellular calcium storage site, possible changes of the axonal ER calcium content, as already detected after spinal cord contusion injury, were investigated in the neuroinflammatory setting. ER calcium was first measured in healthy control axons, which showed no relevant ER calcium depletion – defined by a calcium concentration below the control mean minus three standard deviations – and a normal morphology of axons. Application of 50 mM caffeine in healthy control mice lead to a large calcium release from the ER with 86.4% of all the axons' ER calcium being below the established cut-off. Next, I induced acute EAE in seven mice and imaged them with an EAE score of at least 2.5 two or three days after onset of neurological symptoms. Lesions were determined by the amount of infiltrating immune cells in the spinal cord and the YFP/CFP ratio was calculated. Normal-appearing stage 0 axons showed a comparable distribution of ER calcium levels as healthy control axons. The same assertion can be made for swollen stage 1 axons, which did not display ER calcium depletion although the mean calcium concentration of all axons appeared to be a bit lower than in the controls. Only in a proportion of already fragmented stage 2 axons depleted ER could be observed (Figure 11 C). These data indicate that the intra-axonal ER calcium stores just release calcium in the irreversible fragmented stage of FAD. In stage 0 axons and swollen stage 1 axons, whose fate is still undecided, there is no relevant change of ER calcium levels leading to the conclusion that calcium release from the ER is not causative for the increase in cytoplasmic calcium and thus the progression of FAD. When I administered 50 mM caffeine to the spinal cord of EAE mice a calcium release from the ER could again reliably be seen. This supports the notion that a high amount of calcium is stored in the ER in inflamed axons and can still be released upon pharmacological manipulation. Moreover, it confirms that the Twitch2B 54S+ ER sensor is not perturbed by the altered conditions in inflammatory lesions and therefore real ER calcium changes are being measured.

### 5.2.3. Spatial regulation of ER calcium levels along stage 1 axons

Spatially regulated RyR-mediated calcium release from the ER has been reported in the neuronal soma, proximal dendrites and in axons (Miyazaki et al. 2012; Vierra et al. 2019). At contact sites between the ER and other cellular organelles such as mitochondria and lysosomes localized calcium fluxes are also supposed to occur (La

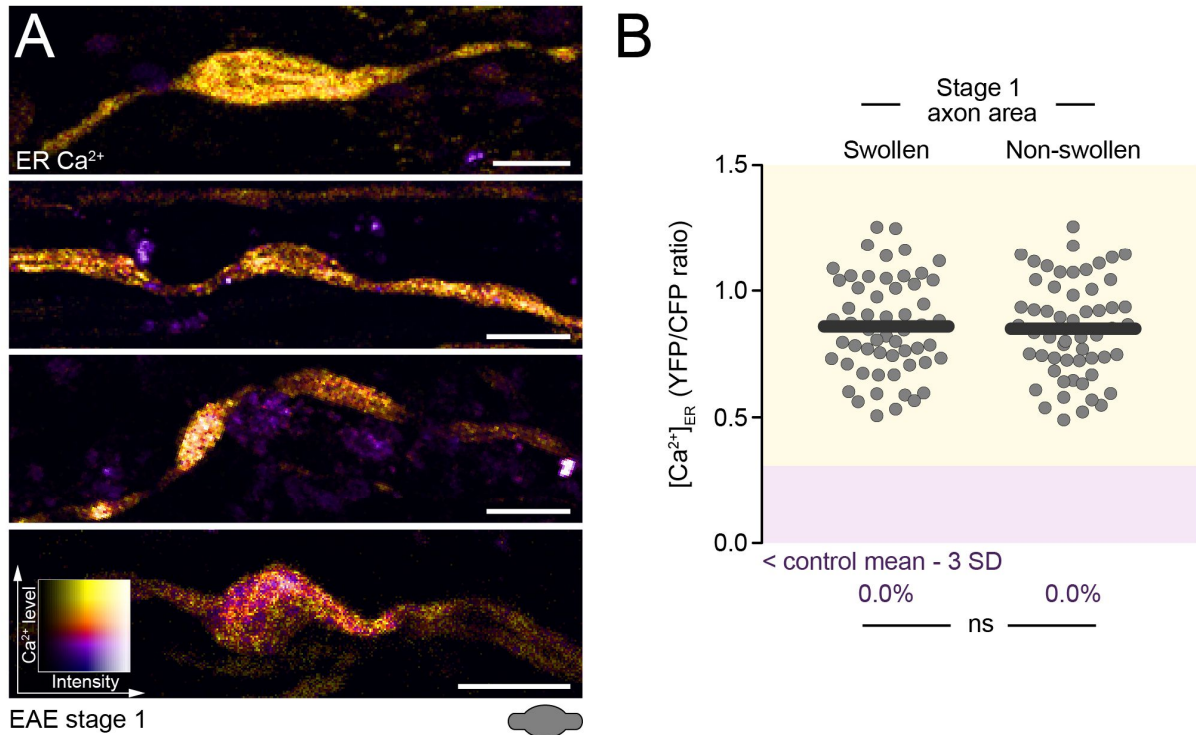


**Figure 12: ER calcium levels are similar in swollen and non-swollen sections of stage 1 axons**

(A) Exemplary ratiometric images displaying  $[Ca^{2+}]_{ER}$  in swollen stage 1 axons in EAE of Thy1-TwitchER mice. (B)  $[Ca^{2+}]_{ER}$  (YFP/CFP ratio) of single stage 1 axons measured in swollen and non-swollen axon areas ( $n = 4$  mice, paired t-test). Percentages below represent the fraction of axons with a  $[Ca^{2+}]_{ER}$  below control mean  $- 3$  SD. Scale bars in (A)  $10 \mu m$ . ns  $P > 0.05$ . Figure and caption adapted from (Witte et al. 2019)

Rovere et al. 2016). Therefore, it can be speculated that ER calcium releases, even if not as large as the ones induced by caffeine, might potentially happen in swollen areas of stage 1 axons where intra-axonal homeostasis is disturbed the most. This might account for the group of axons with lower ER calcium levels of all stage 1 axons. Thus, I analysed ER calcium concentrations in all stage 1 axons of four EAE mice at two different regions of interest: directly in the swollen area and in another remote non-swollen area. This analysis showed no significant difference of YFP/CFP ratios between the measured areas with the distribution of ER calcium of all axons being very similar (Figure 12 B). This result can also be seen in the shown exemplary images of different stage 1 axons. Visually there is no detectable alteration of colour along the displayed sections of the axons. However, the already observed large spread of ER calcium concentrations can be noticed in the representative images (Figure 12 A). In summary, these data indicate that there are no localized events of ER calcium release in swollen stage 1 axons that might contribute to predicting the axons' fate.

## 5.2.4. Absence of temporal ER calcium fluctuations in FAD

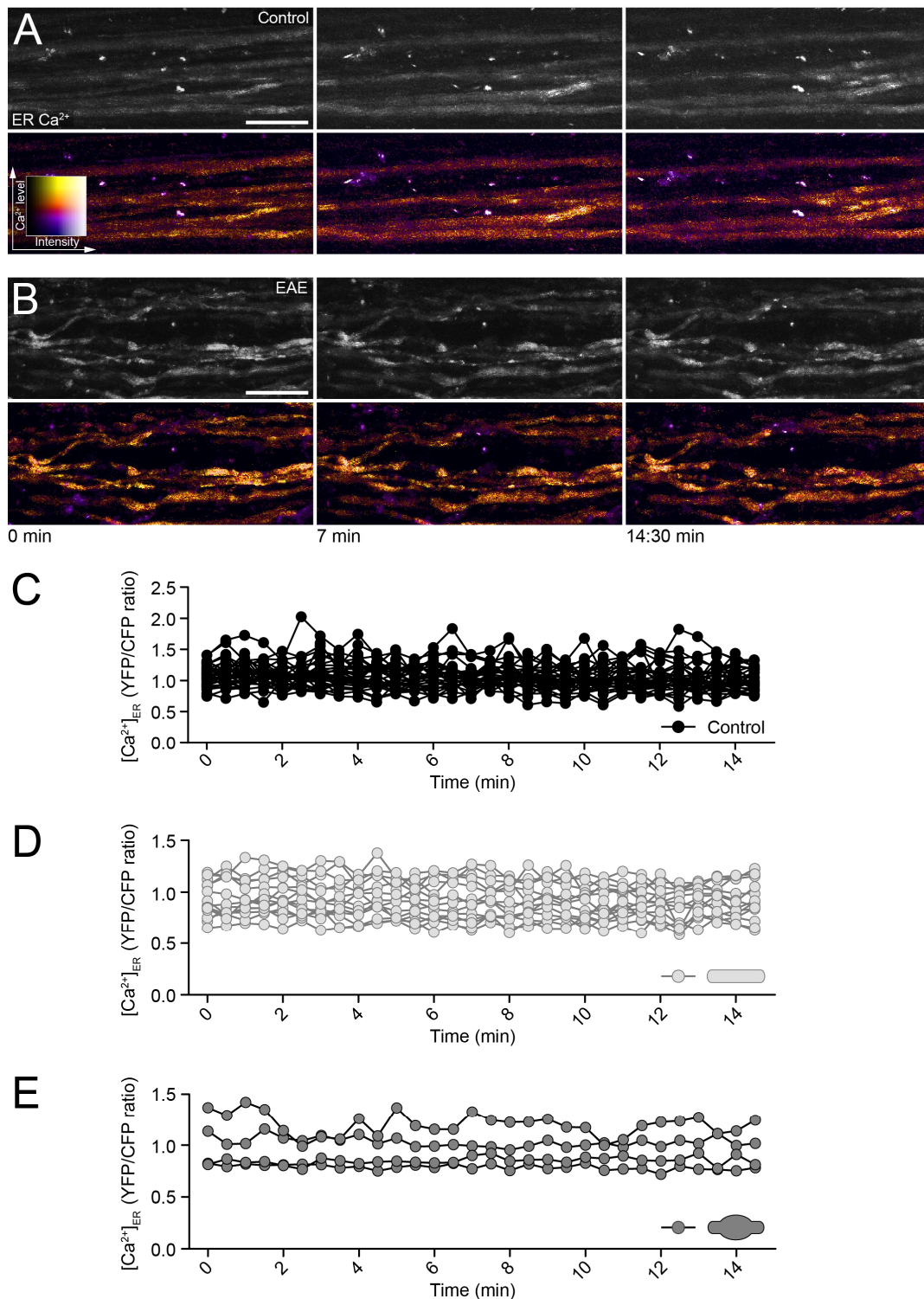


**Figure 13: No temporal ER calcium release events occur in healthy control and EAE mice**

(A, B) Time-lapse projection images of Thy1-TwitchER axons of healthy control (A) and EAE (B) mice at 0, 7 and 14:30 minutes under standard conditions. Top row: greyscale image of the YFP channel, bottom row: colour-coded images for  $[Ca^{2+}]_{ER}$ . (C, D, E) Time course graphs of  $[Ca^{2+}]_{ER}$  imaged every 30 s for 14:30 minutes. Healthy control axons depicted in black (n = 4 control mice) (C), stage 0 axons in light grey (n = 3 EAE mice) (D) and stage 1 axons in dark grey (n = 3 EAE mice) (E). Presented as mean  $\pm$  SD. Scale bars in (A) and (B) 25  $\mu$ m. Figure and caption adapted from (Witte et al. 2019)

ER calcium release events cannot only occur spatially but also temporary, followed by the refilling of the internal calcium stores mainly by SOCE (Vierra et al. 2019; Wegierski und Kuznicki 2018). Previous experiments with Thy1-TwitchER mice have shown that Twitch2B 54S+ ER can resolve immediate and delayed ER calcium changes. The images taken in control and EAE mice in Figure 11 A for the analysis of a large population of axons only represent several snapshots in time. Hence, for the attempt of visualizing short events of ER calcium release I performed the following experiments. First, time-lapse imaging was done in four healthy control mice under standard conditions for fourteen and a half minutes with image stacks being taken every 30 seconds (Figure 13 A). ER calcium concentration of axons that could be tracked at every single time point were then measured which revealed that there were no relevant fluctuations in ER calcium over the observed time course (Figure 13 C). This was hypothesized to be potentially different in acute EAE due to perturbed axonal homeostasis in inflammatory lesions. Thus, I repeated the same experiment in EAE mice two or three days after onset of neurological symptoms. Imaged areas were chosen in acute lesions where stage 0 and stage 1 axons could be found. The gathered data did not show any evidence for temporary depletions of ER calcium in both normal-appearing and swollen axons within the intervals that were imaged (Figure 13 B, D, E). In addition, there were again no differences in ER calcium concentrations between healthy control, stage 0 and stage 1 axons. Calcium sparks at even shorter intervals are unlikely given the fact that depleting the ER with caffeine took over a minute. Even if they would occur, they would then have most likely been caught in at least one of the generated images.

#### 5.2.5. Relation of ER and cytoplasmic calcium levels in spinal cord axons

After having ruled out ER calcium as a potent source of the cytoplasmic calcium increase in neuroinflammatory lesions, I carried out another set of experiments to investigate the effect of a complete ER calcium depletion on axoplasmic calcium levels. The response of ER calcium stores upon application of caffeine has already been described in the paragraphs above and was here used as a positive control for calcium release from the ER. In line with the experiments performed in the Thy1-TwitchER mice the same procedure was conducted in healthy control Thy1-CerTN-L15 mice, which record cytoplasmic calcium levels. However, surprisingly directly after the

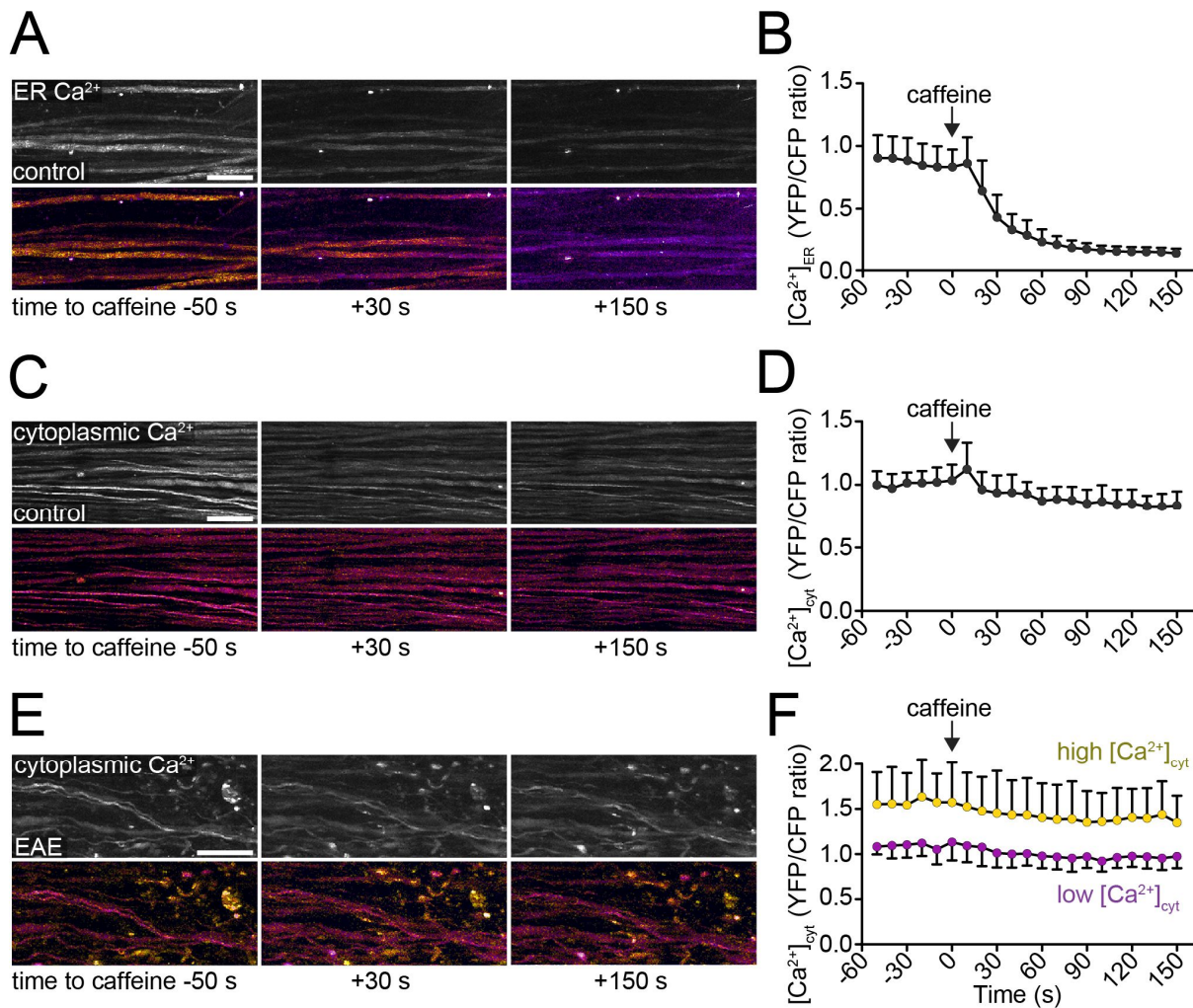


**Figure 14: Caffeine-mediated ER calcium depletion does not cause measurably increases of cytoplasmic calcium**

(A, C, E) Time-lapse projection images of Thy1-TwitchER axons (A) and Thy1-CerTN-L15 mice (C, E) before and after application of 50 mM caffeine in healthy control (A, C) and EAE (E) mice. Top row: greyscale image of the YFP channel, bottom row: colour-coded images for  $[\text{Ca}^{2+}]_{\text{ER}}$ . (B, D, F) Time course graphs of  $[\text{Ca}^{2+}]_{\text{ER}}$  (B) and  $[\text{Ca}^{2+}]_{\text{cyt}}$  (D, F) pre and post application of 50 mM caffeine. Yellow circles in (F) display high and purple circles low  $[\text{Ca}^{2+}]_{\text{cyt}}$  axons at -50 s. N = 5 control Thy1-TwitchER mice, n = 5 control Thy1-CerTN-L15 mice, n = 5 EAE Thy1-CerTN-L15 mice. Presented as mean  $\pm$  SD. Scale bars in (A), (C) and (E) 25  $\mu\text{m}$ . Figure and caption adapted from (Witte et al. 2019)

application of caffeine no increase in cytoplasmic calcium could be observed (Figure 14 C, D). This finding might be explained by the existence of calcium buffering capacities in the cytoplasm. On the one hand, calcium influx from the extracellular or intracellular stores can be buffered by cytosolic calcium binding proteins such as parvalbumins, calbindin and calretinin. These are responsible for the rapid buffering of short-lived calcium increases. On the other hand, there are slow buffers including several pumps and calcium exchangers which either release calcium through the plasma membrane (NCX, plasma membrane calcium ATPase) or sequester large

amounts of the ion into the ER (SERCA) or mitochondria (Murchison und Griffith 2007; Schwaller 2010). All these mechanisms are completely functional under healthy conditions, yet, in EAE they may be disturbed. For example, reactive oxygen and nitrogen species mediated damage to mitochondria, as reportedly occurring in EAE, potentially renders them incapable of buffering calcium and more importantly ineffective in producing enough ATP for neuronal homeostasis. This might cause the cytosolic slow buffering system, which uses ATP, to not be fully functional for expelling calcium. For this reason, I induced EAE in five Thy1-CerTN-L15 mice and imaged them two or three days after neurological symptoms occurred. Another time lapse imaging experiment with application of 50 mM caffeine was performed in putative inflammatory lesions. Yet again, like in healthy control mice, the depletion of ER calcium stores did not have any marked effect on intra-axonal calcium levels in normal-appearing and swollen axons (Figure 14 E, F). These data indicate that, even if a calcium release from the ER would take place in the neuroinflammatory environment, it would not be sufficient to increase cytoplasmic calcium concentrations to the levels which were observed in FAD (Witte et al. 2019). Additionally, they also indicate that the ER calcium depletion in the traumatic axon injury model, which was even less than the caffeine-induced effect, is unlikely to explain the cytoplasmic calcium increases which are detected in axons after spinal cord injury (Williams et al. 2014). More general, these results question the critical contribution of ER calcium release to axon degeneration processes in the central nervous system that has previously been predicted (Stirling et al. 2014; Villegas et al. 2014).

## 6. Discussion

Axon degeneration is a detrimental process and important contributor to the long-term disabilities in multiple sclerosis and spinal cord injury. In the previous years, studies in our laboratory have not only generated tools to investigate the underlying axon degeneration processes but also found a responsible mechanism for determining the axonal fate in models of neuroinflammation and traumatic axon injury, namely elevated intra-axonal calcium levels (Williams et al. 2014; Witte et al. 2019). In this thesis after an in-depth analysis of the newly generated Thy1-TwitchER mouse line, the contribution of ER calcium and the alterations of ER structure in the two disease models were studied.

### 6.1. In vivo imaging of ER calcium signals in axons

#### 6.1.1. Evaluation of Twitch2B 54S+ ER

The endeavour of imaging calcium dynamics in living cells has undergone a vast progress since the first experiments of monitoring calcium dynamics with the bioluminescent aequorin. However, most of the research was initially focused on measuring cytoplasmic calcium dynamics. With alterations of organellar calcium levels, including the ER, being implicated in pathological conditions appropriate calcium sensors needed to be generated. Hence, in the last years different types of ER GECIs, including single FP intensimetric as well as excitation and emission ratiometric calcium indicators, have been developed, enabling researchers to study calcium in the ER (Suzuki et al. 2014; Rodriguez-Garcia et al. 2014). In this thesis an ER-targeted form of the low-affinity sensor Twitch2B 54S+ was used to measure ER calcium due to the following reasons.

First, the used GECI represents a ratiometric sensor which is indispensable for the experiments performed in this thesis. This is since fluorescence brightness of a sensor might vary between all axons or might be affected by infiltrating immune cells. Here, an intensimetric sensor would cause wrong assumptions about ER calcium concentrations given the fact that mainly one time-point measurements, in which baseline values are unknown, are being conducted when studying FAD in EAE (Palmer et al. 2011).

The ideal GECI should have a calcium affinity which is suitable for detecting ER calcium dynamics. To achieve this, the sensor's dissociation constant  $K_d$  should be in

close range of the baseline calcium levels in the ER. In a recent study ER calcium levels were measured in primary dissociated hippocampal neurons using a low-affinity ER calcium indicator (ER-GCaMP6). Here, somatic ER calcium concentrations were estimated to be around  $164 \pm 7 \mu\text{M}$  with no significant difference to axonal ER calcium concentrations of  $156 \pm 15 \mu\text{M}$  given the continuity of the ER in neurons (Juan-Sanz et al. 2017). Yet, the exact calcium levels of the ER in DRG or spinal neurons are unknown. Still, with Twitch2B 54S+ ER having a  $K_d$  of  $174 \mu\text{M}$ , which is very close to the estimated axonal ER calcium concentrations, the decision to use this sensor was reached. Furthermore, Twitch2B 54S+ ER also features a favourable dynamic range of 320% and a short decay time of 70 ms which enables this sensor to detect small and short lasting calcium dynamics (Thestrup et al. 2014).

Changes in FRET ratios should be generated by alterations of real calcium concentrations and not be perturbed by other ions such as magnesium or chloride. Due to the improved properties of the used fluorophores and the calcium-binding domain in Twitch sensors such perturbations can be assumed to be minimal (Thestrup et al. 2014). In addition, decreased pH values, which have been reported in neuroinflammatory lesions (Friese et al. 2007), could influence the measured FRET ratios of Twitch2B 54S+ ER. However, experiments in our laboratory could show that YFP/CFP ratios in EAE mice expressing both fluorophores without a calcium-binding unit were the same as in healthy control mice (Schumacher 2016). Furthermore, Twitch2B 54S+ ER consists of a Venus fluorophore which is supposed to have a lower pH sensitivity than the original YFP (Hsu et al. 2010). Thus, acidosis to the extent of which is seen in neuroinflammatory lesions should not influence the used sensor's function. Moreover, the depletion of ER calcium stores with thapsigargin in Hek-293 cells did not affect YFP/CFP ratios in a mutated calcium-insensitive version of Twitch2B 54S+ ER (Scheiter 2020). This finding suggests that ratio changes in the functional sensor are caused by real ER calcium changes.

In summary, Twitch2B 54S+ ER fulfils the necessary requirements to be used for the generation of a transgenic mouse line for the measurement of neuronal calcium dynamics.

### 6.1.2. Morphological characterization of Thy1-TwitchER mice

The generated Thy1-TwitchER mouse line, expressing Twitch2B 54S+ ER in the CNS and PNS needed a full characterization before any experiments could be conducted in disease models.

In previous experiments colocalization of Twitch2B 54S+ ER and the well-known ER-resident protein GRP78/BiP was only demonstrated in interneurons. For arguing that calcium dynamics measured in dorsal column axons are really formed in the ER and not in another intra-axonal sub-compartment, this was not enough. Therefore, I investigated the localization of the sensor in the ER of dorsal horn spinal neurons and DRG neurons, where the investigated axons originate from. For this purpose, first, the immunostaining protocol was improved with higher concentrations of GRP78/BiP antibodies and longer incubation times so that the colocalization requirement could be adequately addressed. By these means Twitch2B 54S+ ER and the immunostaining showed a colocalizing fine reticular network suggesting the correct localization of the sensor. The expression pattern of Twitch2B 54S+ ER also looked comparable to the one of ER-targeted GCaMP6 (Juan-Sanz et al. 2017). However, the appearance of clumped ER structures, specifically in DRG neurons, seemed troubling since it has been shown that some fluorescent proteins possess dimerizing properties. These would result in low affinity interactions between nearby proteins, especially when highly expressed, leading to the stacking of the ER, a process also known as formation of organized smooth ER (OSER) (Snapp et al. 2003). If this would be the case it might indicate that the amount of the expressed sensor could be toxic to the cells. Yet, pilot experiments, in which C57/BL6 mice were perfused and immunostained with GRP78/BiP did reveal the same morphological phenomenon so that a toxic overexpression of Twitch2B 54S+ ER could be presumably ruled out (data not shown). Moreover, in electron microscopy images of DRG neurons of mice not expressing the sensor, areas with numerous parallel ER tubules or cisternae could be seen suggesting the presence of stacked ER (data not shown). Stacks of cisternal ER have also been described in cerebral, hippocampal and Purkinje neurons during hypoxia which occurs when perfusing mice. Here, the length of perfusion correlated with the amount of ER stacking. Intriguingly, this process was mostly found in Purkinje neurons in which a very large amount of IP<sub>3</sub>R are existent. This ER calcium release channel has been made responsible for the formation of ER stacks leading to the hypothesis that IP<sub>3</sub>R interaction in stacked ER reduces the accessibility for IP<sub>3</sub> to its receptor and

thereby limits ER calcium release. Glutamate excitation and high potassium levels have also been demonstrated to induce ER stacking (Tao-Cheng 2018). These findings thus provide a likely explanation for the structural anomalies of the ER found in neurons of Thy1-TwitchER mice.

Furthermore, in this thesis colocalization between Twitch2B 54S+ ER in Thy1-TwitchER mice and GRP78/BiP could also be found in immunostained cross-sectioned axons, however, not as convincingly as in neuronal somata. This was most likely due to the reduced immunostaining intensity and the fragmented appearance of the ER in the axon. In line with the observed ER stacks, this ER fragmentation is presumably also caused by hypoxia during the process of mouse perfusion (Kucharz et al. 2011b).

In summary, in my thesis I could confirm the correct localization of Twitch2B 54S+ ER in the ER lumen and with a highly probability rule out toxic effects of the sensor on the ER structure.

### 6.1.3. Functional characterization of Thy1-TwitchER mice

In vivo two photon microscopy of the spinal cord revealed a sufficiently bright labelling of dorsal column axons in Thy1-TwitchER mice. Compared to cytoplasmic calcium concentrations which appear to be tightly regulated in spinal axons (Witte et al. 2019) we observed a large baseline spread of ER calcium concentrations when analysing YFP/CFP ratios in several Thy1-TwitchER mice. This variation of ratios was apparent within each mouse but importantly the mean ratios between individual mice seemed to vary as well. Further experiments with altering the bath temperature around the exposed spinal cord lead to no conclusive explanation that these variations might have been caused by different temperatures which is supposed to affect the fluorophores. Proton, magnesium and chloride sensitivities of the sensor might give a reason for the spread in baseline ratios, however, Twitch2B 54S+ ER represents an over the years refined version of a GECl with low perturbation by stated ions (Thestrup et al. 2014). In addition, mice that were imaged on the same day after another with the same aCSF did show different FRET ratios. Another theory, namely varying damage to axons caused by the surgery, could again not explain the baseline spread. However, the slow increase of ER calcium concentrations over time after surgery lead to the adaption of the imaging protocol of Thy1-TwitchER mice. As most likely a mechanical trauma during spinal cord surgery causes a small reversible ER calcium release, a post-

surgery waiting time of at least one and a half hours was implemented in every further experiment to enable replenishment of ER calcium pools. Besides differences in axonal activity levels as a result of a varying depth of anaesthesia, which was not further investigated in this work, the ER calcium baseline spread can be explained by a simple biological heterogeneity of axonal intra-ER calcium concentrations. The idea that calcium levels in the ER are not as tightly controlled as in the cytosol, has been supported by Juan-Sanz et al. 2017 who described inter-neuronal variations of ER calcium concentrations.

The functionality, meaning that the sensor responds to a pharmacological depletion of ER calcium stores, was confirmed by using thapsigargin that prevents ER refilling. However, the constant calcium leak from the ER is very slow in vivo taking up to more than an hour for maximum depletion after drug application. One explanation for that finding could be that the diffusion of the drug through the tissue and fluids might be slow. Moreover, since smooth axonal ER consists of no translocon pores, which partially facilitate the calcium leak, ER calcium depletion might take a longer time. A slow ER calcium release can most likely be buffered quickly enough by cytosolic calcium buffering mechanisms, namely fast chelating of the ions or a slow energy-dependent calcium release into the extracellular space. Given the intention of also monitoring cytosolic calcium levels after ER depletion, a drug enabling a faster ER calcium release was required. Here I identified caffeine as the most suitable drug for this purpose, as other drugs, such as ATP, histamine or 4-CEP were either not causing ER calcium depletion or were not as effective as caffeine. The duration of a complete calcium release from the ER after caffeine application was around 90 seconds which is about 40 times faster than the one observed after thapsigargin application. Proper functioning of Twitch2B 54S+ ER in vivo could have also been confirmed by inducing an increase in ER calcium, for example with a substance that activates the SERCA (Tadini-Buoninsegni et al. 2018). Pilot experiments with CDN1163 could however, not show an increase of baseline ER calcium concentrations. This might be due to ER calcium levels already being at their maximum or the sensor not being capable of binding more calcium which can be assumed because the CFP channel intensity was very low at baseline compared to the YFP channel.

Summarizing the characterization experiments, I conclude, that Thy1-TwitchER transgenic mice, with a bright labelling of single neurons and their axons as well as a correct functionality of the sensor, are well suited for detecting calcium dynamics in the

ER on different time scales with two photon microscopy. With this validation the mouse line could now be implemented for studying the role of ER calcium in different models of neurological diseases.

## **6.2. Structural and calcium dynamics of the ER in axon degeneration**

### 6.2.1. Evaluation of the used animal models

#### 6.2.1.1 Acute EAE model

For studying the pathomechanism of inflammation and neurodegeneration in multiple sclerosis many different experimental models in different animal species exist, from which each model only represents some aspects of MS pathology. In the present study ER calcium dynamics were studied in MOG-induced acute EAE in transgenic C57/BL6 mice. This model is characterized by a rapid development of clinical symptoms after only 10 to 14 days which remain for a couple of days followed by a more or less marked recovery with no further progression or relapses. Immunization with the CNS antigen triggers antigen-presenting cells to interact with circulating lymphocytes forming a mainly CD4<sup>+</sup> Th1 and Th17 cell dominated immune response that induces focal inflammatory lesions in the CNS. Affected areas are the spinal cord, the cerebellum and the optic nerve, whereas the forebrain is vastly spared from the immune response. Histopathologically, in inflammatory lesions large-scale axon degeneration via FAD can be seen with a less dominant demyelination (Kipp et al. 2017).

When looking at the clinical course of the acute EAE model, major differences to MS can already be identified. Evidently, the relapse-remitting feature of RRMS and the disease progression in PPMS and SPMS cannot be captured by a monophasic model. In addition, the underlying pathology of continuous disease progression is not focal inflammation but rather a diffuse inflammation as well as chronic axon and neuron degeneration leading to brain and spinal cord atrophy in MS patients (Mahad et al. 2015). Furthermore, brain lesions and atrophy, CD8<sup>+</sup> T cell mediated inflammation and B cells are important facets of MS, all features which are not entirely reproduced by the used murine model (Gold et al. 2006). These discrepancies between EAE and MS are also reflected in the failure of translating many drugs, including anti-inflammatory and immunosuppressive substances, that were successful for ameliorating EAE, into the treatment of MS patients.

During a MS relapse focal inflammation causes clinical deficits by demyelination, compression of axons due to an inflammatory edema and, very importantly, axonal damage (Kipp et al. 2017). Recovery of symptoms can happen spontaneously over time or be accelerated by the treatment with systemic corticosteroids, which most likely act via a reduction of the focal CNS inflammation. Thus, studying inflammatory axon damage is essential to further understand the pathomechanism behind acute relapses. Experiments in our laboratory did reveal transected and temporarily damaged axons in inflammatory CNS lesions with the latter being capable of recovery, especially when inflammatory mediators were reduced. Comparative axon morphologies could be found in biopsies of active MS lesions in humans (Nikić et al. 2011). Hence, transient axonal damage might be the driving contributor for causing clinical symptoms during acute MS relapses. Altogether, even if acute EAE does not fully mimic MS it resembles one important aspect of the disease, namely acute inflammatory axon damage. This argues for using the acute murine EAE model in this thesis.

#### 6.2.1.2 Spinal cord contusion model

In order to study the pathomechanism of spinal cord injury many different experimental models have been introduced. These models vary in the used animal species, as well as in the region and the pattern of the induced injury. Therefore, the selection of the ideal animal model depends on which aspects of spinal cord injury are being studied. In this work, an Infinite Horizons impactor induced contusion model of the lumbar spinal cord in mice was used to investigate ER dynamics in vivo in traumatic axon degeneration.

Larger animals and non-human primates are the models that resemble humans the most, so that they are used to test promising therapeutics prior to clinical trials on humans. However, higher costs, special housing and animal welfare aspects are responsible for their rare usage. Therefore, most preclinical SCI experiments are performed in rodents with rats being used in more than 70% of all studies. Yet, mice are more and more implemented as experimental animals due to their even lower cost, easier handling and reproductive capacities. On the downside, histopathology after SCI in mice is different to humans as the lesion site is densely filled with cells and the inflammatory response shows other temporal dynamics. Furthermore, the size of the

injury site decreases over time as mice do not develop cysts which is common in human SCI (Sharif-Alhoseini et al. 2017).

Although in most cases SCIs in humans occur on the cervical level, most animal experiments are performed on the thoracic spinal cord. This is partly due to the reliability and easy reproducibility of injuries to this region. However, there are anatomical differences between the different regions of the spinal cord such as the diameter, vascularization, allocation between grey and white matter or the distance of the injured axons to their distinct cell body. This translates to observed clinical symptoms as for example cervical injuries cause spastic paralysis, neuropathic pain and autonomic and cardiac dysfunctions which are not comparatively found in lower SCIs (Lujan et al. 2018).

Finally, experimental SCI can be induced by transection, dislocation, distraction, contusion and compression. As a matter of fact, most SCIs in humans are caused by compression of the spinal cord due to dislocated fractures or constant spinal canal occlusion as well as by contusion injuries such as in car accidents, sports or suicide attempts (Sharif-Alhoseini et al. 2017). This common mechanism of injury is represented in the used contusion model by the utilization of the Infinite Horizon Impactor, a device which grants good reproducibility, sufficient control over the impact force and force-adapted measurements (Cheriyian et al. 2014).

The aim in this thesis was to study the contribution of the ER to axonal damage in the first hours of the primary injury phase in order to potentially find targets for acute neuropreservative treatments. Thus, the altered histopathology of the murine SCI model, which mainly affects the later injury phases, should not be of major importance. Previous experiments in our laboratory revealed that axons are in a metastable state after injury capable of spontaneous recovery or further fragmentation (Williams et al. 2014). Hence, for studying the temporal dynamics of axonal behaviour in the crucial phase, single time point analysis is not plausible, whereas in vivo imaging allows us to follow degeneration and recovery processes live (Misgeld und Kerschensteiner 2006). In order to achieve good image and readout quality we opted for the lumbar region of the spinal cord as it provides fewer breathing artefacts and easier surgical handling. Furthermore, the feasibility of easily generating transgenic models, in which even subcellular structures, like the ER, can be visualized, argues for the usage of a mouse

model. In sum, using the present contusion model in mice seems reasonable to study the fundamental pathophysiology of traumatic axon injury.

### 6.2.2. ER dynamics in traumatic axon injury

In this thesis the acute post contusion injury dynamics of ER calcium and ER morphology were described for the first time in the spinal cord of living mice. While we could detect ER fragmentation and alterations in ER calcium concentrations immediately after traumatic axon injury, it was of interest to investigate the ensuing behaviour of this organelle. Two-hour time-lapse imaging again confirmed the initial ER calcium release and furthermore revealed the reversibility of this process. This resembles the effect, which can be seen after performing spinal cord surgery on Thy1-TwitchER mice. Here, an increase in ER calcium levels, the reason for introducing a post-surgery waiting time, was also described. Taking these findings together it can be suggested that any kind of mechanical trauma or pressure onto axons causes an immediate reversible release of parts of the stored ER calcium pools. This is in line with several previous studies where an ER calcium release in models of traumatic axon injury was described (Stirling et al. 2014; Villegas et al. 2014). However, in contrary to the claimed major contribution of an ER calcium depletion to axon degeneration in these studies, our present work could not confirm this claim at least for in vivo spinal cord injury models. As demonstrated with the experiments of caffeine application in Thy1-CerTN-L15 mice, the observed liberation of ER calcium after spinal cord contusion would not be enough to increase cytoplasmic calcium concentrations to cause axon degeneration. The possible reasons for the negligible effect of an ER calcium release on cytoplasmic calcium levels will be discussed in chapter 6.2.3 where the ER calcium dynamics in EAE are reviewed. Yet, the detected ER calcium release after traumatic injury proves that pathological ER calcium alterations can in principal be measured with Thy1-TwitchER mice and thus affirm that this mouse line can reliably be used for the investigation of ER calcium dynamics in other models of axon degeneration. Furthermore, even if the partial ER calcium depletion does not cause large cytoplasmic calcium rises, a relevant contribution of this event to axonal homeostasis cannot be ruled out.

In addition to the ER calcium release marked alterations in ER morphology could be found in most axons after traumatic axon injury. This ER fragmentation, like the calcium

dynamics, was reversible over the course of time. Given the findings that ER fragmentation appeared in a large majority of axons and that the ER calcium release was homogenous it can be stipulated that both events are not directly responsible for determining axonal fate after contusion injury. This is because in previous experiments cytoplasmic calcium increases and axon degeneration did only appear in a proportion of axons and not extensively (Williams et al. 2014). When tracking the temporal dynamics of ER fragments over two hours, interesting behaviours could be observed. ER fragments did not appear to be static, to the contrary, they were mobile, potentially indicating that they were detached from the cytoskeleton, and showed subsequent clustering and the formation of larger vesicular bodies often located close to the borders of the axon. Only in a small proportion of axons (10 – 20%) the initial pre-injury structure of the ER could be regained. In light of these differences in the morphological behaviour of the ER one can speculate that some structural dynamics might occur in degenerating axons and others only in axons which are spared from degeneration after contusion injury. When analysing ER calcium and structural changes together, there was no difference in ER calcium concentrations in axons with fragmented or non-fragmented ER. This finding suggests that both events are distinct and happen independent from each other, also when considering that ER fragmentation does hardly take place after a normal spinal cord surgery where mechanical trauma is tried to be minimized. Therefore, it is likely that ER fragmentation is a force-dependent process, which could be further studied in experiments, in which the applied force onto the spinal cord is increased step-by-step.

ER fragmentation and its reversibility have been described before in *in vitro* and *in vivo* experiments. Glutamate stimulation of hippocampal neurons or potassium-induced depolarisation lead to a rapid fission of dendritic ER, which could recover over time and was partially prevented by treatment with a NMDA-receptor antagonist (Kucharz et al. 2009; Kucharz et al. 2011a). The same behaviour was observed after cardiac arrest in mice where the lack of energy supply leads to increased cytosolic calcium levels, which has been deemed to be causative for ER fission (Kucharz et al. 2011b). However, the fact that at least in our observations axonal cytoplasmic calcium increase only occurs in a small proportion of axons after traumatic axon injury indicates that other mechanisms are likely to be involved in causing ER fragmentation in the contusion model. The observed temporal dynamics of ER morphology were comparable to the ones described in this work with the advantage of a better resolution

in the used widefield setup. In laser transection or contusion spinal cord injury models major damage to the plasma membrane is induced. Previous studies in cell cultures with saponin, a cell membrane permeabilization compound, and mechanical damage did reveal a quick ER vesiculation as a consequence to the caused plasma membrane injury. This process was independent of a cytoplasmic calcium increase, as it also appeared under calcium-free conditions. In addition, if saponin exposure was not too long, the ER could regain its structure after 75 minutes. Given these findings, the authors came up with the theory that the structural changes of the ER would result in a decreased luminal calcium concentration in the ER as an ER vesicle is supposed to have a higher volume for the same membrane area compared to a tubule. Although this might also account for the lower ER calcium levels found after spinal cord contusion, a real ER calcium release still seems very likely as such decreased ER calcium concentrations were also found in axons with visually non-fragmented ER and after spinal cord surgery where no ER fragmentation was visible (Raeymaekers und Larivière 2011). In summary, it remains unclear which exact mechanism – calcium influx, depolarisation, membrane damage or possibly a common executive pathway with several triggers – drives ER fragmentation.

### 6.2.3. ER calcium release in EAE

Besides grey-matter pathology, axon degeneration is a major contributor to the long-term development of disability in multiple sclerosis. Given that and the fact that all current treatment options focus on the immunological aspects of the disease, it is of great importance to understand and potentially target the molecular pathomechanisms behind axon degeneration. Here, the sequence of events, meaning which event happens at what stage of the degeneration cascade, is crucial as upstream events are of particular therapeutic interest. One of such has been discovered to be an intra-axonal calcium increase that is initiated during the early stages of the axon degeneration process. Time-lapse studies of axons in EAE have shown that elevated cytoplasmic calcium promotes FAD progression. However, if axonal calcium homeostasis could be resumed, even in already swollen stage 1 axons, axonal recovery became more likely. These findings indicate that there is a window of opportunity for a therapeutic intervention to rescue injured axons, which are otherwise prone to complete FAD (Schumacher 2016). Calcium increases can be claimed to be

an upstream event due to following reasons: First, it can activate intra-axonal proteases like calpain which degrades cytoskeletal proteins that are responsible for regulating the axonal diameter (Costa et al. 2018). Furthermore, the cytoskeleton is used as a route for axonal transport so that its degradation leads to the accumulation of transport products which causes axonal swelling. Second, elevated cytoplasmic calcium results in mitochondrial calcium sequestration, which can cause the production of reactive oxygen species that further harm the axon. Besides that, high cytosolic calcium generates the formation of the mitochondrial permeability transition pore that allows the efflux of apoptotic proteins which initiates cell-death programs (Fрати et al. 2017). Thus, finding the origin of the increased intra-axonal calcium in neuroinflammatory lesion was of great interest to our laboratory. As already reviewed in chapter 1.4.2, ER calcium depletion has been implicated to contribute to axon degeneration and was detected after contusion injury in this work. Hence, I investigated the possible existence of this event in acute EAE using a novel in vivo imaging approach.

As in healthy control mice, fluorescence in axonal ER of Thy1-TwitchER mice was bright enough under EAE conditions making it possible for the first time to analyse ER calcium concentrations in vivo in neuroinflammatory lesions. However, the results did not show any biologically relevant differences in ER calcium levels between stage 0 and 1 axons of FAD compared to healthy control axons, meaning that there is no detectable ER calcium release occurring in the early stages of FAD. Only in already fragmented stage 2 axons the ER seemed to be depleted of calcium, which can be explained by the lack of fuel for the SERCA due to mitochondrial impairment in irreversibly damaged axons. This would resemble the pharmacological effect of thapsigargin, where the constant ER calcium leak cannot be compensated. This is an interesting but expected finding and of no big importance because stage 2 axons cannot be rescued anymore by any therapeutic intervention. In addition, caffeine was applied to both healthy and EAE mice resulting in a robust decrease of ER calcium concentrations. On the one hand, this experiment proves that the ER calcium sensor is still functioning in an inflamed environment. On the other hand, it supports the prior findings that there is still a readily accessible pool of calcium left in the ER in stage 0 and stage 1 axons of FAD.

Arguments could be made that ER calcium releases could happen in spatially localized areas within the axons and limited in time. The former was ruled out when I

comparatively analysed swollen and non-swollen areas of stage 1 axons where no difference in ER calcium concentrations could be found. Temporarily restricted events were investigated with time-lapse imaging because the single time-point population-based analysis, given the large inter-axonal ratio spread, would fail to detect such events. Yet again, ER calcium fluctuations could not be observed in either healthy control or stage 0 and stage 1 axons in inflammatory lesions. It would be possible that ER calcium releases occur in even shorter time periods, but such events seem unlikely because, firstly, there would be a high chance of catching at least one release spark in the performed time lapse imaging. Secondly, experiments in healthy mice have revealed that ER calcium refilling after caffeine application, which even takes about 90 seconds, lasts for several tens of minutes.

Another claim for the negligible role of ER calcium in neuroinflammatory lesions was made with the experiments of caffeine-induced ER calcium depletion in both Thy1-TwitchER and Thy1-CerTN-L15 mice. Robust and quick decreases of ER calcium did not lead to any detectable changes in cytoplasmic calcium, measured by the CerTN-L15 sensor, or any signs of axon degeneration. This was not only the case in healthy control mice but also when ER calcium depletion was induced in diseased Thy1-CerTN-L15 mice. Thus, even under conditions of axonal dyshomeostasis and energy production impairment, where calcium buffering mechanisms are most likely diminished, a complete ER calcium release cannot raise cytoplasmic calcium levels to the extent which can be observed in EAE and after spinal cord injury. These findings are in accordance with *in vitro* measurements of the interplay between ER and cytoplasmic calcium concentrations. Juan-Sanz et al. (2017) used a GCaMP6f with a  $K_d$  of 375 nM for assessing cytoplasmic calcium transients given a resting cytosolic calcium concentration of around 120 nM in axons and dendrites. When applying the reversible SERCA-inhibitor cyclopiazonic acid (CPA) to hippocampal neurons cytoplasmic calcium elevations of 11.8 nM, which is comparable to the amount of a single action potential (9.6 nM), could be observed in dendrites. However, in the axonal compartment no increase of baseline cytosolic calcium levels could be measured after CPA application so that they concluded that axonal ER takes up less volume-percent of the axon compared to dendrites (Juan-Sanz et al. 2017). Ultrastructural analysis by electron microscopy support this theory as they revealed that ER in axons form a system of anastomosed tubules or even only a single tubule in thin axons with a very narrow diameter of 20 to 30 nm. These narrow tubules also exist in the cell body but

only make up a small fraction of the whole ER. In dendrites the ER mostly consists of interconnected tubules and intermittent cisternae, especially in large spines, suggesting a higher volume fraction of the ER in comparison to axons (Wu et al. 2017; Terasaki 2018). Although in vivo two photon microscopy was not fit to resolve such structural differences, confocal scans of Thy1-TwitchER mice revealed that fluorescence intensity of Twitch2B 54S+ ER was a lot brighter in the neuronal soma and proximal dendrites than in axons, indicating that axonal ER occupies only a small proportion of the axonal volume. Combining these results with the fact that CerTN-L15 has a  $K_d$  of 1.2  $\mu$ M, which is far away from baseline cytosolic calcium levels in neurons and therefore only capable to detect large calcium alterations, it is understandable why a depletion of ER calcium stores does not trigger axon degeneration. Based on these findings, an ER calcium release as a relevant cause for the increased cytoplasmic calcium concentrations observed in FAD and after traumatic axon injury can be ruled out. Still, the ER might play an important role to axon degeneration via other means such as ER stress and the unfolded protein response, which were not studied in this work.

#### 6.2.4. Sources of elevated intra-axonal calcium in EAE

After having ruled out an ER calcium release in FAD, other potential sources for the detrimental elevated intra-axonal calcium levels had to be studied. The extracellular space with a calcium concentration of around ten-thousand-fold higher than in the cytoplasm represents such a source. Experiments performed by my colleague Christoph Mahler with EGTA, a calcium chelator that only scavenges extracellular calcium without affecting intracellular calcium pools, could reveal that the removal of extracellular calcium can on the one hand effectively prevent a cytoplasmic calcium increase and on the other hand decrease already pathologically high calcium levels in spinal axons (Figure 15 B). Another important finding was that this calcium decrease did have an advantageous effect on the axon fate as stage 0 axons showed a diminished degeneration progression when treated with EGTA. Moreover, swollen stage 1 axons were protected from undergoing fragmentation and could even recover to their healthy state (Figure 15 C). EGTA-mediated buffering of extracellular calcium in healthy Thy1-CerTN-L15 mice did not influence the observed YFP/CFP ratios so that a calcium sensor modulation by EGTA could be precluded. In conclusion, these

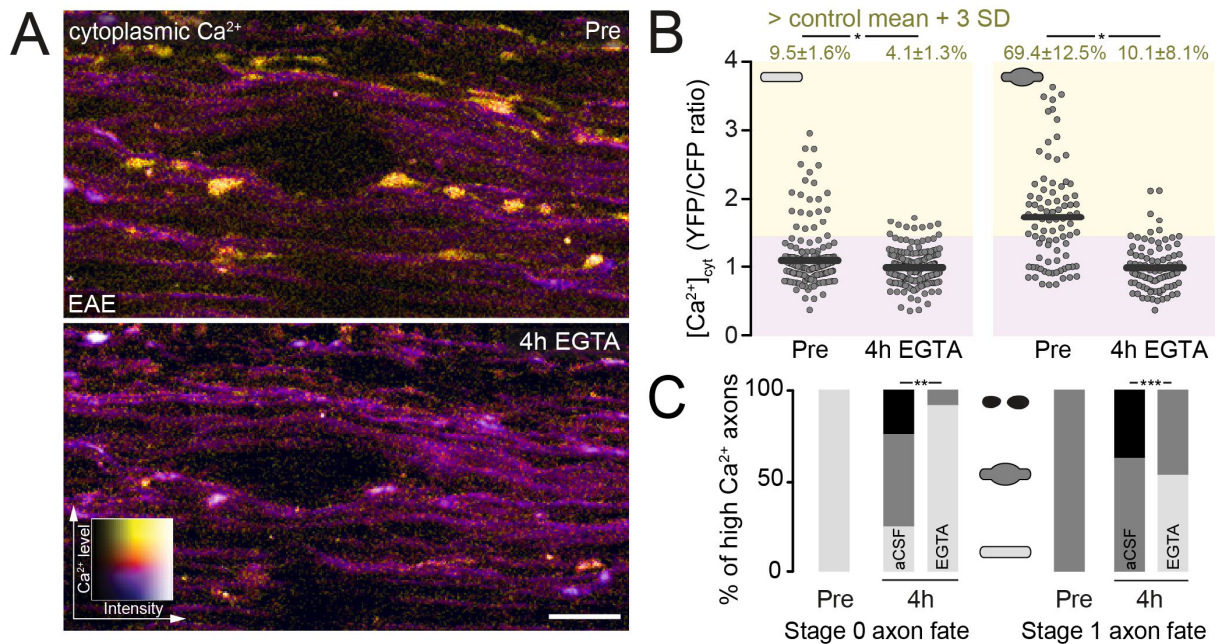


**Figure 15: Extracellular calcium is responsible for elevated cytoplasmic calcium levels and axon degeneration**

(A) Representative in-vivo microscopy maximum intensity projections of axons in the EAE afflicted spinal cord of Thy1-CerTN-L15 mice. Colour-coded images for  $[Ca^{2+}]_{cyt}$  before (top) and after (bottom) the removal of extracellular  $Ca^{2+}$  with EGTA. (B) Cytoplasmic  $Ca^{2+}$  levels of stage 0 (left) and stage 1 (right) axons before and after the removal of extracellular  $Ca^{2+}$  with a 4h incubation of EGTA. Bars indicate means, percentages (above) display fraction of axons with increased  $[Ca^{2+}]_{cyt} > \text{control mean} + 3 \text{ SD}$ . Paired t-test for 'Pre' vs. '4 h EGTA'.  $N = 5$  EAE mice for stage 0 axons,  $n = 5$  EAE mice for stage 1 axons. (C) Fate of single stage 0 axons (left, 31 axons, 8 mice) and stage 1 axons (right, 66 axons, 8 mice) with initially elevated  $[Ca^{2+}]_{cyt}$  over 4 h with ('EGTA') and without ('aCSF') chelating of extracellular  $Ca^{2+}$  (chi-square test). Scale bar in (A) 25  $\mu\text{m}$ . \* $P < 0.05$ , \*\* $P < 0.01$ , \*\*\* $P < 0.001$ . Figure and caption adapted from (Witte et al. 2019). Experimenter: Christoph Mahler

findings indicate that a calcium influx from the extracellular space is responsible for triggering and advancing axon degeneration under neuroinflammatory conditions (Witte et al. 2019).

This opens up the question of how the influx of extracellular calcium into the axon is mediated. Various preceding studies of axon degeneration have investigated several mechanisms for calcium entry, for example voltage-gated calcium channels (VGCCs) (Knöferle et al. 2010), pH-sensitive ion channels (ASICs) (Friese et al. 2007), glutamate receptors (AMPA, Kainat and NMDA) (Ouardouz et al. 2009a; Ouardouz et al. 2009b) and the NCX (Stys et al. 1992). VGCCs have been shown to be involved in acute axon degeneration in spinal cord injury and optic nerve crush as blocking these channels resulted in a reduction of the degeneration process (Knöferle et al. 2010). There are ten different types of VGCCs, of which nearly all are expressed in neurons. Blockade of L-type-VGCCs with nimodipine, a drug that is normally used for the

treatment of hypertension and vasospasms after subarachnoid haemorrhage, in EAE mice lead to an attenuation of the disease course and enhanced remyelination (Schampel et al. 2017). Furthermore, treating EAE mice with pregabalin, an antagonist to P/Q-, N- and L-type-VGCCs, could also ameliorate the EAE course by reducing neuronal calcium increases. Therefore, the authors concluded that this drug should be re-purposed as a therapeutic for early stages of MS, in addition to its current admission for the treatment of neuropathic pain in the late stages of the disease (Hundehege et al. 2018). However, pharmacological inhibition of L- and T-type calcium channels with lomerizine could not reduce the elevated cytoplasmic calcium concentrations or improve axon fate in FAD when tracking single stage 0 and 1 axons over four hours (Witte et al. 2019).

During CNS inflammation mitochondrial failure leads to a disturbed energy metabolism resulting in an increase of lactate levels which causes tissue acidosis. Under these acidic conditions (pH of around 6.5) the abundant proton-gated cation channels ASIC1a gets activated allowing the influx of sodium and calcium. A protective effect on axons in EAE could be observed for the blockade of this receptor with amiloride or in *Asic1*-knockout mice (Friese et al. 2007). Therefore, my colleague Christoph Mahler performed *in vivo* calcium imaging experiments with acidic aCSF (pH of 6.5) in healthy control and EAE mice in which no cytoplasmic calcium increase or morphological signs of axon degeneration could be demonstrated. As artificially induced acidic conditions might affect the functionality of the CerTN-L15 calcium sensor, EAE was also induced in *Asic1*-KO mice. Yet again, no effect on cytoplasmic calcium levels or the distribution of the different stages of FAD could be seen for the acute phase of inflammation-mediated axon degeneration (Mahler 2019). These findings are in line with the results of the phase 2b clinical trial MS-SMART which unfortunately secondary progressive multiple sclerosis (Chataway et al. 2020).

Glutamate is an excitatory neurotransmitter that leads to an influx of calcium into the cytoplasm via the binding to ionotropic glutamate receptors during synaptic transmission. NMDA receptors, which are important for synaptic plasticity and learning, have a dichotomous influence on neurons depending on their localization. Activation of synaptic NMDA receptors is necessary for neuroprotection and neuronal survival, whereas increased levels of extrasynaptic NMDA receptor activity are responsible for the glutamate excitotoxicity mediated neurodegeneration processes (Hardingham und Bading 2010). Several studies in MS patients could show that glutamate levels were

elevated in blood and cerebrospinal fluid samples leading to oligodendroglial and neuronal damage (Pampliega et al. 2008; Sarchielli et al. 2003). Moreover, treatment of EAE mice with antagonists of NMDA receptors induced a decreased glutamate release and thus an amelioration of the clinical EAE scores (Sulkowski et al. 2014). However, in our in vivo imaging experiments the application of high doses of glutamate or glutamate receptor agonists to the healthy or EAE spinal cord did not cause cytoplasmic calcium increases or morphological alterations in axons. On the contrary, in neurons and dendrites a large calcium influx was observed, as well as the fragmentation of dendrites. These findings might be explained by the different expression levels of glutamate receptors in the soma and the axon. Hence, it can be concluded that high levels of glutamate do not trigger the observed increased intra-axonal calcium concentrations in acute EAE. However, long-term harming effects on neurons and oligodendrocytes could not be ruled out with these experiments (Witte et al. 2019).

The NCX is a protein that can exchange sodium and calcium over the plasma membrane in both directions depending on the ions' electrochemical membrane gradient. Studies have shown that nitric oxide (NO), one of the ROS/RNS molecules which are supposed to be released by inflammatory cells in EAE, can directly influence the NCX to mediate a calcium influx (Kitao et al. 2010). Furthermore, the lack of ATP after axon injury leads to a decreased activity of the Na<sup>+</sup>/K<sup>+</sup>-ATPase and thus to increased intracellular sodium levels which results in a reverse functioning of the NCX and an intra-axonal calcium accumulation (Wolf et al. 2001). Additionally, inhibition of the NCX by bepiridil has been demonstrated to alleviate the disease course in EAE (Brand-Schieber und Werner 2004). When my colleague Christoph Mahler used this drug after the application of NO to healthy control mice, a reduction in NO-mediated axon injury could be detected. However, elevated calcium levels and FAD could not be ameliorated by a four-hour treatment with bepiridil in vivo. In addition, an intrathecal application of the NCX inhibitor via osmotic minipumps, started at the day of onset of symptoms, did again not improve FAD or the clinical course of EAE mice (Witte et al. 2019).

With calcium release from internal stores and an influx via calcium channels being ruled out in the context of EAE, the existence of nanoruptures in the plasma membrane in FAD was investigated. Prior experiments of acute axon degeneration in spinal cord contusion injury models have shown that after mechanical injury such ruptures are

formed which then mediate the influx and accumulation of high levels of calcium in the cytoplasm which predicts the axons' fate (Williams et al. 2014). Therefore, fluorescent dyes of increasing sizes (0.8 kDa cadaverine and 3, 10 and 70 kDa dextran) were subdurally injected onto the spinal cord of healthy and EAE mice. Analysis of fixed tissue did reveal that there was no dye uptake into healthy axons of the control animals. However, in correlation with inflammatory cell infiltration, about 20% of stage 0 axons and an even higher proportion of stage 1 axons showed cadaverine dye labelling in EAE mice. The percentages of axonal dye uptake decreased with the size of the applied dyes as for example merely any uptake of 70 kDa dextrans could be found. Furthermore, analysis at different time points after clinical EAE onset did show that nanoruptures are induced at disease onset and last for several weeks. Hence, we concluded that membrane ruptures with a diameter of less than 10 nm do exist in the acute and chronic phase of EAE in the different stages of FAD. In order to explore the hypothesis whether these membrane disruptions provide the way of calcium influx into the axon, cadaverine was applied to EAE Thy1-CerTN-L15 mice *in vivo*. Here, a strong correlation between increased cytoplasmic calcium levels in normal-appearing and swollen axons and dye uptake could be seen, whereas only very few high calcium axons did not take up dye. In summary, these experiments clearly suggest that the plasma membrane integrity is harmed in axons traversing through neuroinflammatory lesions and that this membrane disturbance is responsible for the fate-predicting intra-axonal calcium increases (Witte et al. 2019).

Consequently, the question arises how the membrane disruptions are formed in the context of neuroinflammation. One possible explanation might be the existence of mechanical forces as they are seen in traumatic axon injury. Intra-axonal edema due to osmotic imbalances, as well as the sheer stress that might be induced by the large amount of infiltrating immune cells, could result in the formation of membrane nanoruptures. Yet, this event seems unlikely because mechanoporation and calcium influx is already initiated in a large proportion of normal-appearing axons. Hence, other possible scenarios of membrane disruptions, involving secreted products of inflammatory cells, should be taken into consideration. First, toxic mediators such as reactive oxygen and nitrogen species can be found in high concentrations in neuroinflammatory lesions and have been shown to be capable of oxidizing lipids, especially cholesterol and unsaturated fatty acid chains of phospholipids, of neuronal membranes. As a result, membrane rigidity and permeability are supposed to increase

(Di Domenico et al. 2017). Second, secreted phospholipases, which are expressed in high levels by infiltrating immune cells, astrocytes and some oligodendrocytes in EAE, could harm the plasma membrane by hydrolysing its phospholipids and thus form small holes into the membrane (Kalyvas et al. 2009). Finally, studies could demonstrate that the complement system gets activated in EAE resulting in the formation of the membrane attack complex (MAC), a transmembrane channel that might allow a calcium influx. Inhibition of the MAC formation could protect from axonal and synaptic damage and mitigated the progression of neurological disability (Michailidou et al. 2018). In summary, irrespective to the exact mechanism of mechanoporation, targeting the formation or facilitating the resealing process of these nanopores seems to be a promising approach in the development of new therapies in the treatment of multiple sclerosis.

### **6.3. Concluding remarks and outlook**

In this thesis the Thy1-TwitchER mouse line, generated by my colleague Alexander Scheiter, was extensively validated for the correct localization of the genetically encoded low-affinity calcium indicator Twitch2B 54 S+ ER in the ER of spinal cord and DRG neurons. Detectable ER calcium releases in healthy spinal cord axons could be induced by thapsigargin, 4-CEP and caffeine and proved the functionality of the ER calcium sensor in the in vivo imaging setting. By means of this new transgenic mouse line, I then investigated the role of ER calcium stores in traumatic axon injury and in acute EAE. While reversible partial ER calcium releases could be detected after spinal cord contusion injury, ER calcium dysregulations did only occur late in the process of focal axon degeneration. Studying cytoplasmic calcium levels after a caffeine-induced complete ER calcium depletion in Thy1-CerTN-L15 mice, in which the effects of intra-axonal calcium on axon degeneration were described, revealed that axons do not comprise large enough ER calcium pools to cause such detrimental increases in intra-axonal calcium. Hence, a relevant contribution of an ER calcium release to axon degeneration could be excluded, which stands in direct contrast to assumptions of preceding ex vivo studies. That being said, the influx of extracellular calcium through plasma membrane disruptions under both traumatic and neuroinflammatory conditions presents a target that should be further addressed in order to find an approach to attenuate axon degeneration and thus halt progressive neurological disability.

In the context of spinal cord contusion injury, I detected ER fragmentation immediately after injury and could follow its temporal dynamics over time. As far as resolvable in the given setup, the ER seemed to be capable of recovering to normal morphology or form consolidations of small vesicles into large vacuoles. Due to this ER fragmentation affecting most axons it seems unlikely that initial fragmentation is fate-determining for axons, however, the different subsequent dynamics might contribute to axon degeneration or display a result of the degeneration process. Besides its existence under pathological conditions, ER fragmentation could also be detected after a physiological stimulus like whisker stimulation (Kucharz und Lauritzen 2018). Cytoplasmic calcium increases and plasma membrane damage have been described as potential mechanistic causes for fragmentation (Kucharz et al. 2011b; Raeymaekers und Larivière 2011), which are both existent after spinal cord injury, but also in EAE, where no alteration of ER morphology was seen in this thesis. Hence, not only is there a need to further uncover the physiology of the fragmentation process, but also to reveal its consequences for neuronal homeostasis. Regarding this, it is speculated that ER fragmentation limits the amount of releasable calcium from the ER lumen, as under normal conditions calcium can flow freely through the continuous ER network. This is supposed to be beneficial since ER calcium depletions have been implicated as contributors to neuronal damage. Besides calcium sequestration in single ER fragments, damaged proteins can also be segregated so that the induction of the unfolded protein response and thus ER stress can be limited to a small area of the axon (Kucharz et al. 2009). Other researchers have suggested that the decreased ER calcium concentration due to the larger volume of each fragment might enable the ER to store more calcium and therefore counteract increased cytoplasmic calcium concentrations (Raeymaekers und Larivière 2011). With the ER being involved in the biosynthesis of plasma membrane lipids and lipid transfer at ER-PM contact sites, combined with the finding that ER fragments seemed to frequently cluster close to the axonal margin, it can be hypothesized that the ER might participate in the sealing of plasma membrane disruptions. However, despite all potential advantageous effects of ER fragmentation, continuous fragmentation of the ER is most likely deadly for the neuron as, generally, neuronal homeostasis depends on ER continuity (Öztürk et al. 2020).

For a long time, axonal ER has not been in the focus of many researchers, even though the ER has first been described in 1902. However, we are now starting to understand

the importance of the ER for the physiology and pathology of axons. With the development of the Thy1-TwitchER mouse line new insights into the basic biology of ER calcium and structural dynamics in axons can be gained. As a result, it might be possible to better define the role of the ER in the process of axon degeneration and find potential therapeutic targets to affect neurodegenerative diseases.

## 7. References

- Agarwal, N. K.; Mathur, N. (2009): Deep vein thrombosis in acute spinal cord injury. In: *Spinal cord* 47 (10), S. 769. DOI: 10.1038/sc.2009.37.
- Agrawal, S. K.; Nashmi, R.; Fehlings, M. G. (2000): Role of L- and N-type calcium channels in the pathophysiology of traumatic spinal cord white matter injury. In: *Neuroscience* 99 (1), S. 179–188. DOI: 10.1016/s0306-4522(00)00165-2.
- Akerboom, Jasper; Carreras Calderón, Nicole; Tian, Lin; Wabnig, Sebastian; Prigge, Matthias; Tolö, Johan et al. (2013): Genetically encoded calcium indicators for multi-color neural activity imaging and combination with optogenetics. In: *Frontiers in molecular neuroscience* 6, S. 2. DOI: 10.3389/fnmol.2013.00002.
- Akerboom, Jasper; Rivera, Jonathan D. Vélez; Guilbe, María M. Rodríguez; Malavé, Elisa C. Alfaro; Hernandez, Hector H.; Tian, Lin et al. (2009): Crystal structures of the GCaMP calcium sensor reveal the mechanism of fluorescence signal change and aid rational design. In: *The Journal of biological chemistry* 284 (10), S. 6455–6464. DOI: 10.1074/jbc.M807657200.
- Baker, David; Gerritsen, Wouter; Rundle, Jon; Amor, Sandra (2011): Critical appraisal of animal models of multiple sclerosis. In: *Multiple sclerosis (Houndmills, Basingstoke, England)* 17 (6), S. 647–657. DOI: 10.1177/1352458511398885.
- Berridge, M. J. (1997): Elementary and global aspects of calcium signalling. In: *The Journal of physiology* 499 (Pt 2), S. 291–306.
- Bjartmar, C.; Kidd, G.; Mörk, S.; Rudick, R.; Trapp, B. D. (2000): Neurological disability correlates with spinal cord axonal loss and reduced N-acetyl aspartate in chronic multiple sclerosis patients. In: *Annals of neurology* 48 (6), S. 893–901.
- Bjelobaba, Ivana; Begovic-Kupresanin, Vesna; Pekovic, Sanja; Lavrnja, Irena (2018): Animal models of multiple sclerosis: Focus on experimental autoimmune encephalomyelitis. In: *Journal of neuroscience research* 96 (6), S. 1021–1042. DOI: 10.1002/jnr.24224.
- Blamire, Andrew M.; Cader, Sarah; Lee, Martin; Palace, Jackie; Matthews, Paul M. (2007): Axonal damage in the spinal cord of multiple sclerosis patients detected by magnetic resonance spectroscopy. In: *Magnetic resonance in medicine* 58 (5), S. 880–885. DOI: 10.1002/mrm.21382.
- Bolender, R. P. (1974): Stereological analysis of the guinea pig pancreas. I. Analytical model and quantitative description of nonstimulated pancreatic exocrine cells. In: *The Journal of cell biology* 61 (2), S. 269–287.
- Bramham, Clive R.; Wells, David G. (2007): Dendritic mRNA: transport, translation and function. In: *Nature reviews. Neuroscience* 8 (10), S. 776–789. DOI: 10.1038/nrn2150.
- Brandman, Onn; Liou, Jen; Park, Wei Sun; Meyer, Tobias (2007): STIM2 is a feedback regulator that stabilizes basal cytosolic and endoplasmic reticulum Ca<sup>2+</sup> levels. In: *Cell* 131 (7), S. 1327–1339. DOI: 10.1016/j.cell.2007.11.039.

- Brand-Schieber, Elimor; Werner, Peter (2004): Calcium channel blockers ameliorate disease in a mouse model of multiple sclerosis. In: *Experimental neurology* 189 (1), S. 5–9. DOI: 10.1016/j.expneurol.2004.05.023.
- Bridgman, P. C. (1999): Myosin VA Movements in Normal and Dilute-Lethal Axons Provide Support for a Dual Filament Motor Complex. In: *The Journal of cell biology* 146 (5), S. 1045–1060.
- Browne, Paul; Chandraratna, Dhia; Angood, Ceri; Tremlett, Helen; Baker, Chris; Taylor, Bruce V.; Thompson, Alan J. (2014): Atlas of Multiple Sclerosis 2013: A growing global problem with widespread inequity. In: *Neurology* 83 (11), S. 1022–1024. DOI: 10.1212/WNL.0000000000000768.
- Cabral-Costa, J. V.; Kowaltowski, A. J. (2019): Neurological disorders and mitochondria. In: *Molecular aspects of medicine*, S. 100826. DOI: 10.1016/j.mam.2019.10.003.
- Casley, C. S.; Canevari, L.; Land, J. M.; Clark, J. B.; Sharpe, M. A. (2002): Beta-amyloid inhibits integrated mitochondrial respiration and key enzyme activities. In: *Journal of neurochemistry* 80 (1), S. 91–100. DOI: 10.1046/j.0022-3042.2001.00681.x.
- Chataway, Jeremy; Angelis, Floriana de; Connick, Peter; Parker, Richard A.; Plantone, Domenico; Doshi, Anisha et al. (2020): Efficacy of three neuroprotective drugs in secondary progressive multiple sclerosis (MS-SMART): a phase 2b, multiarm, double-blind, randomised placebo-controlled trial. In: *The Lancet. Neurology* 19 (3), S. 214–225. DOI: 10.1016/S1474-4422(19)30485-5.
- Chen, Peiwen; Piao, Xianhua; Bonaldo, Paolo (2015): Role of macrophages in Wallerian degeneration and axonal regeneration after peripheral nerve injury. In: *Acta neuropathologica* 130 (5), S. 605–618. DOI: 10.1007/s00401-015-1482-4.
- Cheriyian, T.; Ryan, D. J.; Weinreb, J. H.; Cheriyian, J.; Paul, J. C.; Lafage, V. et al. (2014): Spinal cord injury models: a review. In: *Spinal cord* 52 (8), S. 588–595. DOI: 10.1038/sc.2014.91.
- Christodoulou, Andri; Santarella-Mellwig, Rachel; Santama, Niovi; Mattaj, Iain W. (2016): Transmembrane protein TMEM170A is a newly discovered regulator of ER and nuclear envelope morphogenesis in human cells. In: *Journal of cell science* 129 (8), S. 1552–1565. DOI: 10.1242/jcs.175273.
- Chung, Jeeyun; Torta, Federico; Masai, Kaori; Lucast, Louise; Czapla, Heather; Tanner, Lukas B. et al. (2015): INTRACELLULAR TRANSPORT. PI4P/phosphatidylserine countertransport at ORP5- and ORP8-mediated ER-plasma membrane contacts. In: *Science (New York, N.Y.)* 349 (6246), S. 428–432. DOI: 10.1126/science.aab1370.
- Comi, G.; Martinelli, V.; Rodegher, M.; Moiola, L.; Bajenaru, O.; Carra, A. et al. (2009): Effect of glatiramer acetate on conversion to clinically definite multiple sclerosis in patients with clinically isolated syndrome (PreCISe study): a randomised, double-blind, placebo-controlled trial. In: *Lancet (London, England)* 374 (9700), S. 1503–1511. DOI: 10.1016/S0140-6736(09)61259-9.

- Confavreux, Christian; Vukusic, Sandra (2006): Age at disability milestones in multiple sclerosis. In: *Brain : a journal of neurology* 129 (Pt 3), S. 595–605. DOI: 10.1093/brain/awh714.
- Correale, Jorge; Marrodan, Mariano; Ysraelit, María Cécica (2019): Mechanisms of Neurodegeneration and Axonal Dysfunction in Progressive Multiple Sclerosis. In: *Biomedicines* 7 (1). DOI: 10.3390/biomedicines7010014.
- Costa, Ana Rita; Pinto-Costa, Rita; Sousa, Sara Castro; Sousa, Mónica Mendes (2018): The Regulation of Axon Diameter: From Axonal Circumferential Contractility to Activity-Dependent Axon Swelling. In: *Frontiers in molecular neuroscience* 11, S. 319. DOI: 10.3389/fnmol.2018.00319.
- Crawford, Michael P.; Yan, Shirley X.; Ortega, Sterling B.; Mehta, Riyaz S.; Hewitt, Rachel E.; Price, David A. et al. (2004): High prevalence of autoreactive, neuroantigen-specific CD8+ T cells in multiple sclerosis revealed by novel flow cytometric assay. In: *Blood* 103 (11), S. 4222–4231. DOI: 10.1182/blood-2003-11-4025.
- Cummins, Nadia; Tweedie, Andrea; Zuryn, Steven; Bertran-Gonzalez, Jesus; Götz, Jürgen (2019): Disease-associated tau impairs mitophagy by inhibiting Parkin translocation to mitochondria. In: *The EMBO journal* 38 (3). DOI: 10.15252/embj.201899360.
- Dahlberg, A.; Kotila, M.; Leppänen, P.; Kautiainen, H.; Alaranta, H. (2005): Prevalence of spinal cord injury in Helsinki. In: *Spinal cord* 43 (1), S. 47–50. DOI: 10.1038/sj.sc.3101616.
- Davis, R. J. (2000): Signal transduction by the JNK group of MAP kinases. In: *Cell* 103 (2), S. 239–252. DOI: 10.1016/s0092-8674(00)00116-1.
- Denk, W.; Strickler, J. H.; Webb, W. W. (1990): Two-photon laser scanning fluorescence microscopy. In: *Science (New York, N. Y.)* 248 (4951), S. 73–76. DOI: 10.1126/science.2321027.
- Denk, W.; Svoboda, K. (1997): Photon upmanship: why multiphoton imaging is more than a gimmick. In: *Neuron* 18 (3), S. 351–357. DOI: 10.1016/s0896-6273(00)81237-4.
- DeVivo, M. J.; Fine, P. R.; Maetz, H. M.; Stover, S. L. (1980): Prevalence of spinal cord injury: a reestimation employing life table techniques. In: *Archives of neurology* 37 (11), S. 707–708. DOI: 10.1001/archneur.1980.00500600055011.
- Di Domenico, Fabio; Tramutola, Antonella; Butterfield, D. Allan (2017): Role of 4-hydroxy-2-nonenal (HNE) in the pathogenesis of alzheimer disease and other selected age-related neurodegenerative disorders. In: *Free radical biology & medicine* 111, S. 253–261. DOI: 10.1016/j.freeradbiomed.2016.10.490.
- Di Giuro, Cristiana M. L.; Shrestha, Niroj; Malli, Roland; Groschner, Klaus; van Breemen, Cornelis; Fameli, Nicola (2017): Na<sup>+</sup>/Ca<sup>2+</sup> exchangers and Orai channels jointly refill endoplasmic reticulum (ER) Ca<sup>2+</sup> via ER nanojunctions in vascular endothelial cells. In: *Pflugers Archiv : European journal of physiology* 469 (10), S. 1287–1299. DOI: 10.1007/s00424-017-1989-8.

- Ditunno, J. F.; Little, J. W.; Tessler, A.; Burns, A. S. (2004): Spinal shock revisited: a four-phase model. In: *Spinal cord* 42 (7), S. 383–395. DOI: 10.1038/sj.sc.3101603.
- Donnelly, Dustin J.; Popovich, Phillip G. (2008): Inflammation and its role in neuroprotection, axonal regeneration and functional recovery after spinal cord injury. In: *Experimental neurology* 209 (2), S. 378–388. DOI: 10.1016/j.expneurol.2007.06.009.
- Dudley-Javoroski, Shauna; Shields, Richard K. (2008): Muscle and bone plasticity after spinal cord injury: Review of adaptations to disuse and to electrical muscle stimulation. In: *Journal of rehabilitation research and development* 45 (2), S. 283–296.
- Fehlings, Michael G.; Tetreault, Lindsay A.; Wilson, Jefferson R.; Skelly, Andrea C. (2013): Cervical spondylotic myelopathy: current state of the art and future directions. In: *Spine* 38 (22 Suppl 1), S1-8. DOI: 10.1097/BRS.0b013e3182a7e9e0.
- Feng, G.; Mellor, R. H.; Bernstein, M.; Keller-Peck, C.; Nguyen, Q. T.; Wallace, M. et al. (2000): Imaging neuronal subsets in transgenic mice expressing multiple spectral variants of GFP. In: *Neuron* 28 (1), S. 41–51. DOI: 10.1016/s0896-6273(00)00084-2.
- Ferguson, B.; Matyszak, M. K.; Esiri, M. M.; Perry, V. H. (1997): Axonal damage in acute multiple sclerosis lesions. In: *Brain : a journal of neurology* 120 (Pt 3), S. 393–399. DOI: 10.1093/brain/120.3.393.
- Fill, Michael; Copello, Julio A. (2002): Ryanodine receptor calcium release channels. In: *Physiological reviews* 82 (4), S. 893–922. DOI: 10.1152/physrev.00013.2002.
- Fisniku, L. K.; Brex, P. A.; Altmann, D. R.; Miszkiel, K. A.; Benton, C. E.; Lanyon, R. et al. (2008): Disability and T2 MRI lesions: a 20-year follow-up of patients with relapse onset of multiple sclerosis. In: *Brain : a journal of neurology* 131 (Pt 3), S. 808–817. DOI: 10.1093/brain/awm329.
- Flachenecker, Peter; Kobelt, Gisela; Berg, Jenny; Capsa, Daniela; Gannedahl, Mia (2017): New insights into the burden and costs of multiple sclerosis in Europe: Results for Germany. In: *Multiple sclerosis (Houndmills, Basingstoke, England)* 23 (2\_suppl), S. 78–90. DOI: 10.1177/1352458517708141.
- Flourakis, Matthieu; van Coppenolle, Fabien; Lehen'kyi, V'yacheslav; Beck, Benjamin; Skryma, Roman; Prevarskaya, Natalia (2006): Passive calcium leak via translocon is a first step for iPLA2-pathway regulated store operated channels activation. In: *FASEB journal : official publication of the Federation of American Societies for Experimental Biology* 20 (8), S. 1215–1217. DOI: 10.1096/fj.05-5254fje.
- Fрати, Alessandro; Cerretani, Daniela; Fiaschi, Anna Ida; Frati, Paola; Gatto, Vittorio; La Russa, Raffaele et al. (2017): Diffuse Axonal Injury and Oxidative Stress: A Comprehensive Review. In: *International journal of molecular sciences* 18 (12). DOI: 10.3390/ijms18122600.

- Freund, Patrick; Curt, Armin; Friston, Karl; Thompson, Alan (2013): Tracking Changes following Spinal Cord Injury: Insights from Neuroimaging. In: *The Neuroscientist* 19 (2), S. 116–128. DOI: 10.1177/1073858412449192.
- Friedman, Jonathan R.; Lackner, Laura L.; West, Matthew; DiBenedetto, Jared R.; Nunnari, Jodi; Voeltz, Gia K. (2011): ER tubules mark sites of mitochondrial division. In: *Science (New York, N.Y.)* 334 (6054), S. 358–362. DOI: 10.1126/science.1207385.
- Friedman, Jonathan R.; Webster, Brant M.; Mastronarde, David N.; Verhey, Kristen J.; Voeltz, Gia K. (2010): ER sliding dynamics and ER-mitochondrial contacts occur on acetylated microtubules. In: *The Journal of cell biology* 190 (3), S. 363–375. DOI: 10.1083/jcb.200911024.
- Friese, Manuel A.; Craner, Matthew J.; Etzensperger, Ruth; Vergo, Sandra; Wemmie, John A.; Welsh, Michael J. et al. (2007): Acid-sensing ion channel-1 contributes to axonal degeneration in autoimmune inflammation of the central nervous system. In: *Nature medicine* 13 (12), S. 1483–1489. DOI: 10.1038/nm1668.
- Fujino, I.; Yamada, N.; Miyawaki, A.; Hasegawa, M.; Furuichi, T.; Mikoshiba, K. (1995): Differential expression of type 2 and type 3 inositol 1,4,5-trisphosphate receptor mRNAs in various mouse tissues: in situ hybridization study. In: *Cell and tissue research* 280 (2), S. 201–210.
- Garcia-Arguello, L. Y.; O'Horo, J. C.; Farrell, A.; Blakney, R.; Sohail, M. R.; Evans, C. T.; Safdar, N. (2017): Infections in the spinal cord-injured population: a systematic review. In: *Spinal cord* 55 (6), S. 526. DOI: 10.1038/sc.2016.173.
- Gentleman, S. M.; Nash, M. J.; Sweeting, C. J.; Graham, D. I.; Roberts, G. W. (1993): Beta-amyloid precursor protein (beta APP) as a marker for axonal injury after head injury. In: *Neuroscience letters* 160 (2), S. 139–144. DOI: 10.1016/0304-3940(93)90398-5.
- Gerasimenko, Julia V.; Petersen, Ole H.; Gerasimenko, Oleg V. (2014): Monitoring of intra-ER free Ca<sup>2+</sup>. In: *WIREs Membr Transp Signal* 3 (3), S. 63–71. DOI: 10.1002/wmts.106.
- Goeppert-Mayer, Maria (1931): Über Elementarakte mit zwei Quantensprüngen. Göttingen. Math.-naturwiss. Diss., 1930. Leipzig: J. A. Barth.
- Gold, Ralf; Lington, Christopher; Lassmann, Hans (2006): Understanding pathogenesis and therapy of multiple sclerosis via animal models: 70 years of merits and culprits in experimental autoimmune encephalomyelitis research. In: *Brain : a journal of neurology* 129 (Pt 8), S. 1953–1971. DOI: 10.1093/brain/awl075.
- Goverman, J.; Woods, A.; Larson, L.; Weiner, L. P.; Hood, L.; Zaller, D. M. (1993): Transgenic mice that express a myelin basic protein-specific T cell receptor develop spontaneous autoimmunity. In: *Cell* 72 (4), S. 551–560. DOI: 10.1016/0092-8674(93)90074-z.

- Grienberger, Christine; Konnerth, Arthur (2012): Imaging calcium in neurons. In: *Neuron* 73 (5), S. 862–885. DOI: 10.1016/j.neuron.2012.02.011.
- Griesbeck, O.; Baird, G. S.; Campbell, R. E.; Zacharias, D. A.; Tsien, R. Y. (2001): Reducing the environmental sensitivity of yellow fluorescent protein. Mechanism and applications. In: *The Journal of biological chemistry* 276 (31), S. 29188–29194. DOI: 10.1074/jbc.M102815200.
- Hagen, Ellen Merete (2015): Acute complications of spinal cord injuries. In: *World Journal of Orthopedics* 6 (1), S. 17–23. DOI: 10.5312/wjo.v6.i1.17.
- Haile, Yohannes; Deng, Xiaodan; Ortiz-Sandoval, Carolina; Tahbaz, Nasser; Janowicz, Aleksandra; Lu, Jian-Qiang et al. (2017): Rab32 connects ER stress to mitochondrial defects in multiple sclerosis. In: *Journal of neuroinflammation* 14 (1), S. 19. DOI: 10.1186/s12974-016-0788-z.
- Hains, Bryan C.; Klein, Joshua P.; Saab, Carl Y.; Craner, Matthew J.; Black, Joel A.; Waxman, Stephen G. (2003): Upregulation of sodium channel Nav1.3 and functional involvement in neuronal hyperexcitability associated with central neuropathic pain after spinal cord injury. In: *The Journal of neuroscience : the official journal of the Society for Neuroscience* 23 (26), S. 8881–8892.
- Hall, Edward D.; Wang, Juan A.; Bosken, Jeffrey M.; Singh, Indrapal N. (2016): Lipid peroxidation in brain or spinal cord mitochondria after injury. In: *Journal of Bioenergetics and Biomembranes* 48 (2), S. 169–174. DOI: 10.1007/s10863-015-9600-5.
- Hardingham, Giles E.; Bading, Hilmar (2010): Synaptic versus extrasynaptic NMDA receptor signalling: implications for neurodegenerative disorders. In: *Nature reviews. Neuroscience* 11 (10), S. 682–696. DOI: 10.1038/nrn2911.
- Harirchian, Mohammad Hossein; Fatehi, Farzad; Sarraf, Payam; Honarvar, Niyaz Mohammadzadeh; Bitarafan, Sama (2018): Worldwide prevalence of familial multiple sclerosis: A systematic review and meta-analysis. In: *Multiple sclerosis and related disorders* 20, S. 43–47. DOI: 10.1016/j.msard.2017.12.015.
- Hauser, Stephen L.; Bar-Or, Amit; Comi, Giancarlo; Giovannoni, Gavin; Hartung, Hans-Peter; Hemmer, Bernhard et al. (2017): Ocrelizumab versus Interferon Beta-1a in Relapsing Multiple Sclerosis. In: *The New England journal of medicine* 376 (3), S. 221–234. DOI: 10.1056/NEJMoa1601277.
- Heim, Nicola; Garaschuk, Olga; Friedrich, Michael W.; Mank, Marco; Milos, Ruxandra I.; Kovalchuk, Yury et al. (2007): Improved calcium imaging in transgenic mice expressing a troponin C-based biosensor. In: *Nature methods* 4 (2), S. 127–129. DOI: 10.1038/nmeth1009.
- Herrmann, Julia E.; Imura, Tetsuya; Song, Bingbing; Qi, Jingwei; Ao, Yan; Nguyen, Thu K. et al. (2008): STAT3 is a critical regulator of astrogliosis and scar formation after spinal cord injury. In: *The Journal of neuroscience : the official journal of the Society for Neuroscience* 28 (28), S. 7231–7243. DOI: 10.1523/JNEUROSCI.1709-08.2008.

- Hetz, Claudio; Saxena, Smita (2017): ER stress and the unfolded protein response in neurodegeneration. In: *Nature reviews. Neurology* 13 (8), S. 477–491. DOI: 10.1038/nrneurol.2017.99.
- Hirai, Takashi; Mulpuri, Yatendra; Cheng, Yanbing; Xia, Zheng; Li, Wei; Ruangsri, Supanigar et al. (2017): Aberrant plasticity of peripheral sensory axons in a painful neuropathy. In: *Scientific reports* 7 (1), S. 3407. DOI: 10.1038/s41598-017-03390-9.
- Hollenbach, Jill A.; Oksenberg, Jorge R. (2015): The immunogenetics of multiple sclerosis: A comprehensive review. In: *Journal of autoimmunity* 64, S. 13–25. DOI: 10.1016/j.jaut.2015.06.010.
- Hong, W.; Tang, B. L. (1993): Protein trafficking along the exocytotic pathway. In: *BioEssays : news and reviews in molecular, cellular and developmental biology* 15 (4), S. 231–238. DOI: 10.1002/bies.950150403.
- Howell, Owain W.; Reeves, Cheryl A.; Nicholas, Richard; Carassiti, Daniele; Radotra, Bishan; Gentleman, Steve M. et al. (2011): Meningeal inflammation is widespread and linked to cortical pathology in multiple sclerosis. In: *Brain : a journal of neurology* 134 (Pt 9), S. 2755–2771. DOI: 10.1093/brain/awr182.
- Hsu, Shang-Te Danny; Blaser, Georg; Behrens, Caroline; Cabrita, Lisa D.; Dobson, Christopher M.; Jackson, Sophie E. (2010): Folding study of Venus reveals a strong ion dependence of its yellow fluorescence under mildly acidic conditions. In: *The Journal of biological chemistry* 285 (7), S. 4859–4869. DOI: 10.1074/jbc.M109.000695.
- Hu, Junjie; Shibata, Yoko; Voss, Christiane; Shemesh, Tom; Li, Zongli; Coughlin, Margaret et al. (2008): Membrane proteins of the endoplasmic reticulum induce high-curvature tubules. In: *Science (New York, N.Y.)* 319 (5867), S. 1247–1250. DOI: 10.1126/science.1153634.
- Hundehege, Petra; Fernandez-Orth, Juncal; Römer, Pia; Ruck, Tobias; Müntefering, Thomas; Eichler, Susann et al. (2018): Targeting Voltage-Dependent Calcium Channels with Pregabalin Exerts a Direct Neuroprotective Effect in an Animal Model of Multiple Sclerosis. In: *Neuro-Signals* 26 (1), S. 77–93. DOI: 10.1159/000495425.
- International Multiple Sclerosis Genetics Consortium (2019a): A systems biology approach uncovers cell-specific gene regulatory effects of genetic associations in multiple sclerosis. In: *Nature communications* 10 (1), S. 2236. DOI: 10.1038/s41467-019-09773-y.
- International Multiple Sclerosis Genetics Consortium (2019b): Multiple sclerosis genomic map implicates peripheral immune cells and microglia in susceptibility. In: *Science (New York, N.Y.)* 365 (6460). DOI: 10.1126/science.aav7188.
- Ivannikov, Maxim V.; Macleod, Gregory T. (2013): Mitochondrial free Ca<sup>2+</sup> levels and their effects on energy metabolism in *Drosophila* motor nerve terminals. In: *Biophysical journal* 104 (11), S. 2353–2361. DOI: 10.1016/j.bpj.2013.03.064.

- Jager, Philip L. de; Jia, Xiaoming; Wang, Joanne; Bakker, Paul I. W. de; Ottoboni, Linda; Aggarwal, Neelum T. et al. (2009): Meta-analysis of genome scans and replication identify CD6, IRF8 and TNFRSF1A as new multiple sclerosis susceptibility loci. In: *Nature genetics* 41 (7), S. 776–782. DOI: 10.1038/ng.401.
- Jain, Nitin B.; Ayers, Gregory D.; Peterson, Emily N.; Harris, Mitchel B.; Morse, Leslie; O'Connor, Kevin C.; Garshick, Eric (2015): Traumatic spinal cord injury in the United States, 1993-2012. In: *JAMA* 313 (22), S. 2236–2243. DOI: 10.1001/jama.2015.6250.
- Jares-Erijman, Elizabeth A.; Jovin, Thomas M. (2003): FRET imaging. In: *Nature biotechnology* 21 (11), S. 1387–1395. DOI: 10.1038/nbt896.
- John, L. M.; Lechleiter, J. D.; Camacho, P. (1998): Differential modulation of SERCA2 isoforms by calreticulin. In: *The Journal of cell biology* 142 (4), S. 963–973.
- Juan-Sanz, Jaime de; Holt, Graham T.; Schreiter, Eric R.; Juan, Fernando de; Kim, Douglas S.; Ryan, Timothy A. (2017): Axonal Endoplasmic Reticulum Ca<sup>2+</sup> Content Controls Release Probability in CNS Nerve Terminals. In: *Neuron* 93 (4), 867-881.e6. DOI: 10.1016/j.neuron.2017.01.010.
- Julien, J. P. (1999): Neurofilament functions in health and disease. In: *Current opinion in neurobiology* 9 (5), S. 554–560. DOI: 10.1016/S0959-4388(99)00004-5.
- Kalyvas, Athena; Baskakis, Constantinos; Magrioti, Victoria; Constantinou-Kokotou, Violetta; Stephens, Daren; López-Vales, Rubèn et al. (2009): Differing roles for members of the phospholipase A2 superfamily in experimental autoimmune encephalomyelitis. In: *Brain : a journal of neurology* 132 (Pt 5), S. 1221–1235. DOI: 10.1093/brain/awp002.
- Kapoor, Raju; Ho, Pei-Ran; Campbell, Nolan; Chang, Ih; Deykin, Aaron; Forrestal, Fiona et al. (2018): Effect of natalizumab on disease progression in secondary progressive multiple sclerosis (ASCEND): a phase 3, randomised, double-blind, placebo-controlled trial with an open-label extension. In: *The Lancet. Neurology* 17 (5), S. 405–415. DOI: 10.1016/S1474-4422(18)30069-3.
- Karnezis, Tara; Mandemakers, Wim; McQualter, Jonathan L.; Zheng, Binhai; Ho, Peggy P.; Jordan, Kelly A. et al. (2004): The neurite outgrowth inhibitor Nogo A is involved in autoimmune-mediated demyelination. In: *Nature neuroscience* 7 (7), S. 736–744. DOI: 10.1038/nn1261.
- Kerschensteiner, Martin; Schwab, Martin E.; Lichtman, Jeff W.; Misgeld, Thomas (2005): In vivo imaging of axonal degeneration and regeneration in the injured spinal cord. In: *Nature medicine* 11 (5), S. 572–577. DOI: 10.1038/nm1229.
- Kipp, Markus; Nyamoya, Stella; Hochstrasser, Tanja; Amor, Sandra (2017): Multiple sclerosis animal models: a clinical and histopathological perspective. In: *Brain pathology (Zurich, Switzerland)* 27 (2), S. 123–137. DOI: 10.1111/bpa.12454.
- Kitao, Tatsuya; Takuma, Kazuhiro; Kawasaki, Toshiyuki; Inoue, Yuriko; Ikehara, Aki; Nashida, Tetsuaki et al. (2010): The Na<sup>+</sup>/Ca<sup>2+</sup> exchanger-mediated Ca<sup>2+</sup> influx

- triggers nitric oxide-induced cytotoxicity in cultured astrocytes. In: *Neurochemistry international* 57 (1), S. 58–66. DOI: 10.1016/j.neuint.2010.04.016.
- Knöferle, Johanna; Koch, Jan C.; Ostendorf, Thomas; Michel, Uwe; Planchamp, Véronique; Vutova, Poly et al. (2010): Mechanisms of acute axonal degeneration in the optic nerve in vivo. In: *Proceedings of the National Academy of Sciences of the United States of America* 107 (13), S. 6064–6069. DOI: 10.1073/pnas.0909794107.
- Krishnamoorthy, Gurumoorthy; Lassmann, Hans; Wekerle, Hartmut; Holz, Andreas (2006): Spontaneous optico-spinal encephalomyelitis in a double-transgenic mouse model of autoimmune T cell/B cell cooperation. In: *The Journal of clinical investigation* 116 (9), S. 2385–2392. DOI: 10.1172/JCI28330.
- Kucharz, Krzysztof; Krogh, Morten; Ng, Ai Na; Toresson, Håkan (2009): NMDA receptor stimulation induces reversible fission of the neuronal endoplasmic reticulum. In: *PloS one* 4 (4), e5250. DOI: 10.1371/journal.pone.0005250.
- Kucharz, Krzysztof; Lauritzen, Martin (2018): CaMKII-dependent endoplasmic reticulum fission by whisker stimulation and during cortical spreading depolarization. In: *Brain : a journal of neurology* 141 (4), S. 1049–1062. DOI: 10.1093/brain/awy036.
- Kucharz, Krzysztof; Wieloch, Tadeusz; Toresson, Håkan (2011a): Potassium-induced structural changes of the endoplasmic reticulum in pyramidal neurons in murine organotypic hippocampal slices. In: *Journal of neuroscience research* 89 (8), S. 1150–1159. DOI: 10.1002/jnr.22646.
- Kucharz, Krzysztof; Wieloch, Tadeusz; Toresson, Håkan (2011b): Rapid fragmentation of the endoplasmic reticulum in cortical neurons of the mouse brain in situ following cardiac arrest. In: *Journal of cerebral blood flow and metabolism : official journal of the International Society of Cerebral Blood Flow and Metabolism* 31 (8), S. 1663–1667. DOI: 10.1038/jcbfm.2011.37.
- La Rovere, Rita M. L.; Roest, Gemma; Bultynck, Geert; Parys, Jan B. (2016): Intracellular Ca<sup>2+</sup> signaling and Ca<sup>2+</sup> microdomains in the control of cell survival, apoptosis and autophagy. In: *Cell calcium* 60 (2), S. 74–87. DOI: 10.1016/j.ceca.2016.04.005.
- Lan, C.; Lai, J. S.; Chang, K. H.; Jean, Y. C.; Lien, I. N. (1993): Traumatic spinal cord injuries in the rural region of Taiwan: an epidemiological study in Hualien county, 1986-1990. In: *Paraplegia* 31 (6), S. 398–403. DOI: 10.1038/sc.1993.66.
- Lee, C.; Chen, L. B. (1988): Dynamic behavior of endoplasmic reticulum in living cells. In: *Cell* 54 (1), S. 37–46.
- Lee, Do-Hun; Lee, Jae K. (2013): Animal models of axon regeneration after spinal cord injury. In: *Neuroscience Bulletin* 29 (4), S. 436–444. DOI: 10.1007/s12264-013-1365-4.
- Levin, Lynn I.; Munger, Kassandra L.; Rubertone, Mark V.; Peck, Charles A.; Lennette, Evelyne T.; Spiegelman, Donna; Ascherio, Alberto (2005): Temporal relationship between elevation of epstein-barr virus antibody titers and initial onset

- of neurological symptoms in multiple sclerosis. In: *JAMA* 293 (20), S. 2496–2500. DOI: 10.1001/jama.293.20.2496.
- Li, Yu-Feng; Zhang, Sheng-Xiao; Ma, Xiao-Wen; Xue, Yu-Long; Gao, Chong; Li, Xin-Yi (2017): Levels of peripheral Th17 cells and serum Th17-related cytokines in patients with multiple sclerosis: A meta-analysis. In: *Multiple sclerosis and related disorders* 18, S. 20–25. DOI: 10.1016/j.msard.2017.09.003.
- Li, Yun; Camacho, Patricia (2004): Ca<sup>2+</sup>-dependent redox modulation of SERCA 2b by ERp57. In: *The Journal of cell biology* 164 (1), S. 35–46. DOI: 10.1083/jcb.200307010.
- Lin, Michael T.; Beal, M. Flint (2006): Mitochondrial dysfunction and oxidative stress in neurodegenerative diseases. In: *Nature* 443 (7113), S. 787–795. DOI: 10.1038/nature05292.
- Lingor, Paul; Koch, Jan C.; Tönges, Lars; Bähr, Mathias (2012): Axonal degeneration as a therapeutic target in the CNS. In: *Cell and tissue research* 349 (1), S. 289–311. DOI: 10.1007/s00441-012-1362-3.
- Liu, Jing; Gao, Hong-Yan; Wang, Xiao-Feng (2015): The role of the Rho/ROCK signaling pathway in inhibiting axonal regeneration in the central nervous system. In: *Neural Regeneration Research* 10 (11), S. 1892–1896. DOI: 10.4103/1673-5374.170325.
- Liu, Tina Y.; Bian, Xin; Sun, Sha; Hu, Xiaoyu; Klemm, Robin W.; Prinz, William A. et al. (2012): Lipid interaction of the C terminus and association of the transmembrane segments facilitate atlastin-mediated homotypic endoplasmic reticulum fusion. In: *Proceedings of the National Academy of Sciences of the United States of America* 109 (32), E2146-54. DOI: 10.1073/pnas.1208385109.
- Lublin, Fred; Miller, David H.; Freedman, Mark S.; Cree, Bruce A. C.; Wolinsky, Jerry S.; Weiner, Howard et al. (2016): Oral fingolimod in primary progressive multiple sclerosis (INFORMS): a phase 3, randomised, double-blind, placebo-controlled trial. In: *Lancet (London, England)* 387 (10023), S. 1075–1084. DOI: 10.1016/S0140-6736(15)01314-8.
- Lucchinetti, C.; Brück, W.; Parisi, J.; Scheithauer, B.; Rodriguez, M.; Lassmann, H. (2000): Heterogeneity of multiple sclerosis lesions: implications for the pathogenesis of demyelination. In: *Annals of neurology* 47 (6), S. 707–717.
- Lujan, Heidi L.; Tonson, Anne; Wiseman, Robert W.; DiCarlo, Stephen E. (2018): Chronic, complete cervical6-7 cord transection: distinct autonomic and cardiac deficits. In: *Journal of applied physiology (Bethesda, Md. : 1985)* 124 (6), S. 1471–1482. DOI: 10.1152/jappphysiol.01104.2017.
- Lunn, E. R.; Perry, V. H.; Brown, M. C.; Rosen, H.; Gordon, S. (1989): Absence of Wallerian Degeneration does not Hinder Regeneration in Peripheral Nerve. In: *The European journal of neuroscience* 1 (1), S. 27–33. DOI: 10.1111/j.1460-9568.1989.tb00771.x.

- Luo, Liqun; O'Leary, Dennis D. M. (2005): Axon retraction and degeneration in development and disease. In: *Annual review of neuroscience* 28, S. 127–156. DOI: 10.1146/annurev.neuro.28.061604.135632.
- Mahad, Don H.; Trapp, Bruce D.; Lassmann, Hans (2015): Pathological mechanisms in progressive multiple sclerosis. In: *The Lancet. Neurology* 14 (2), S. 183–193. DOI: 10.1016/S1474-4422(14)70256-X.
- Mahler, Christoph (2019): Mechanismen axonaler Kalziumdynamiken im Tiermodell der Multiplen Sklerose. Unter Mitarbeit von Martin Kerschensteiner. München: Universitätsbibliothek der Ludwig-Maximilians-Universität.
- Marinković, Petar; Godinho, Leanne; Misgeld, Thomas (2015): Generation and Screening of Transgenic Mice with Neuronal Labeling Controlled by Thy1 Regulatory Elements. In: *Cold Spring Harbor protocols* 2015 (10), S. 875–882. DOI: 10.1101/pdb.top087668.
- Martin, Natalia; Jaubert, Jean; Gounon, Pierre; Salido, Eduardo; Haase, Georg; Szatanik, Marek; Guénet, Jean-Louis (2002): A missense mutation in *Tbce* causes progressive motor neuronopathy in mice. In: *Nature genetics* 32 (3), S. 443–447. DOI: 10.1038/ng1016.
- Martín, Mauricio G.; Pfrieder, Frank; Dotti, Carlos G. (2014): Cholesterol in brain disease: sometimes determinant and frequently implicated. In: *EMBO reports* 15 (10), S. 1036–1052. DOI: 10.15252/embr.201439225.
- Michailidou, Iliana; Jongejan, Aldo; Vreijling, Jeroen P.; Georgakopoulou, Theodosia; Wissel, Marit B. de; Wolterman, Ruud A. et al. (2018): Systemic inhibition of the membrane attack complex impedes neuroinflammation in chronic relapsing experimental autoimmune encephalomyelitis. In: *Acta neuropathologica communications* 6 (1), S. 36. DOI: 10.1186/s40478-018-0536-y.
- Michalak, M.; Robert Parker, J. M.; Opas, M. (2002): Ca<sup>2+</sup> signaling and calcium binding chaperones of the endoplasmic reticulum. In: *Cell calcium* 32 (5-6), S. 269–278.
- Miller, David H.; Leary, Siobhan M. (2007): Primary-progressive multiple sclerosis. In: *The Lancet. Neurology* 6 (10), S. 903–912. DOI: 10.1016/S1474-4422(07)70243-0.
- Miller, S. D.; Vanderlugt, C. L.; Begolka, W. S.; Pao, W.; Yauch, R. L.; Neville, K. L. et al. (1997): Persistent infection with Theiler's virus leads to CNS autoimmunity via epitope spreading. In: *Nature medicine* 3 (10), S. 1133–1136.
- Misgeld, Thomas; Kerschensteiner, Martin (2006): In vivo imaging of the diseased nervous system. In: *Nature reviews. Neuroscience* 7 (6), S. 449–463. DOI: 10.1038/nrn1905.
- Miyawaki, A.; Llopis, J.; Heim, R.; McCaffery, J. M.; Adams, J. A.; Ikura, M.; Tsien, R. Y. (1997): Fluorescent indicators for Ca<sup>2+</sup> based on green fluorescent proteins and calmodulin. In: *Nature* 388 (6645), S. 882–887. DOI: 10.1038/42264.

- Miyazaki, Kenichi; Manita, Satoshi; Ross, William N. (2012): Developmental profile of localized spontaneous Ca(2+) release events in the dendrites of rat hippocampal pyramidal neurons. In: *Cell calcium* 52 (6), S. 422–432. DOI: 10.1016/j.ceca.2012.08.001.
- Mogami, H.; Gardner, J.; Gerasimenko, O. V.; Camello, P.; Petersen, O. H.; Tepikin, A. V. (1999): Calcium binding capacity of the cytosol and endoplasmic reticulum of mouse pancreatic acinar cells. In: *The Journal of physiology* 518 (Pt 2), S. 463–467.
- Montalban, Xavier; Hauser, Stephen L.; Kappos, Ludwig; Arnold, Douglas L.; Bar-Or, Amit; Comi, Giancarlo et al. (2017): Ocrelizumab versus Placebo in Primary Progressive Multiple Sclerosis. In: *The New England journal of medicine* 376 (3), S. 209–220. DOI: 10.1056/NEJMoa1606468.
- Murchison, David; Griffith, William H. (2007): Calcium buffering systems and calcium signaling in aged rat basal forebrain neurons. In: *Aging cell* 6 (3), S. 297–305. DOI: 10.1111/j.1474-9726.2007.00293.x.
- Nakai, J.; Ohkura, M.; Imoto, K. (2001): A high signal-to-noise Ca(2+) probe composed of a single green fluorescent protein. In: *Nature biotechnology* 19 (2), S. 137–141. DOI: 10.1038/84397.
- Nardone, Raffaele; Florea, Cristina; Höller, Yvonne; Brigo, Francesco; Versace, Viviana; Lochner, Piergiorgio et al. (2017): Rodent, large animal and non-human primate models of spinal cord injury. In: *Zoology (Jena, Germany)* 123, S. 101–114. DOI: 10.1016/j.zool.2017.06.004.
- Nashmi, R.; Fehlings, M.G (2001): Changes in axonal physiology and morphology after chronic compressive injury of the rat thoracic spinal cord. In: *Neuroscience* 104 (1), S. 235–251. DOI: 10.1016/S0306-4522(01)00009-4.
- Nielsen, Trine Rasmussen; Rostgaard, Klaus; Nielsen, Nete Munk; Koch-Henriksen, Nils; Haahr, Sven; Sørensen, Per Soelberg; Hjalgrim, Henrik (2007): Multiple sclerosis after infectious mononucleosis. In: *Archives of neurology* 64 (1), S. 72–75. DOI: 10.1001/archneur.64.1.72.
- Nikić, Ivana; Merkler, Doron; Sorbara, Catherine; Brinkoetter, Mary; Kreutzfeldt, Mario; Bareyre, Florence M. et al. (2011): A reversible form of axon damage in experimental autoimmune encephalomyelitis and multiple sclerosis. In: *Nature medicine* 17 (4), S. 495–499. DOI: 10.1038/nm.2324.
- Nikolaeva, Maria A.; Mukherjee, Ballari; Stys, Peter K. (2005): Na+-dependent sources of intra-axonal Ca2+ release in rat optic nerve during in vitro chemical ischemia. In: *The Journal of neuroscience : the official journal of the Society for Neuroscience* 25 (43), S. 9960–9967. DOI: 10.1523/JNEUROSCI.2003-05.2005.
- Onifer, Stephen M.; Smith, George M.; Fouad, Karim (2011): Plasticity After Spinal Cord Injury: Relevance to Recovery and Approaches to Facilitate It. In: *Neurotherapeutics* 8 (2), S. 283–293. DOI: 10.1007/s13311-011-0034-4.
- Orton, Sarah-Michelle; Herrera, Blanca M.; Yee, Irene M.; Valdar, William; Ramagopalan, Sreeram V.; Sadovnick, A. Dessa; Ebers, George C. (2006): Sex

- ratio of multiple sclerosis in Canada: a longitudinal study. In: *The Lancet. Neurology* 5 (11), S. 932–936. DOI: 10.1016/S1474-4422(06)70581-6.
- Ouardouz, Mohamed; Coderre, Elaine; Basak, Ajoy; Chen, Andrew; Zamponi, Gerald W.; Hameed, Shameed et al. (2009a): Glutamate receptors on myelinated spinal cord axons: I. GluR6 kainate receptors. In: *Annals of neurology* 65 (2), S. 151–159. DOI: 10.1002/ana.21533.
- Ouardouz, Mohamed; Coderre, Elaine; Zamponi, Gerald W.; Hameed, Shameed; Yin, Xinghua; Trapp, Bruce D.; Stys, Peter K. (2009b): Glutamate receptors on myelinated spinal cord axons: II. AMPA and GluR5 receptors. In: *Annals of neurology* 65 (2), S. 160–166. DOI: 10.1002/ana.21539.
- Ouardouz, Mohamed; Nikolaeva, Maria A.; Coderre, Elaine; Zamponi, Gerald W.; McRory, John E.; Trapp, Bruce D. et al. (2003): Depolarization-induced Ca<sup>2+</sup> release in ischemic spinal cord white matter involves L-type Ca<sup>2+</sup> channel activation of ryanodine receptors. In: *Neuron* 40 (1), S. 53–63. DOI: 10.1016/j.neuron.2003.08.016.
- Öztürk, Zeynep; O'Kane, Cahir J.; Pérez-Moreno, Juan José (2020): Axonal Endoplasmic Reticulum Dynamics and Its Roles in Neurodegeneration. In: *Frontiers in neuroscience* 14, S. 48. DOI: 10.3389/fnins.2020.00048.
- Palacios, Natalia; Alonso, Alvaro; Brønnum-Hansen, Henrik; Ascherio, Alberto (2011): Smoking and increased risk of multiple sclerosis: parallel trends in the sex ratio reinforce the evidence. In: *Annals of epidemiology* 21 (7), S. 536–542. DOI: 10.1016/j.annepidem.2011.03.001.
- Palay, S. L.; Palade, G. E. (1955): The fine structure of neurons. In: *The Journal of biophysical and biochemical cytology* 1 (1), S. 69–88.
- Palmer, Amy E.; Jin, Can; Reed, John C.; Tsien, Roger Y. (2004): Bcl-2-mediated alterations in endoplasmic reticulum Ca<sup>2+</sup> analyzed with an improved genetically encoded fluorescent sensor. In: *Proceedings of the National Academy of Sciences of the United States of America* 101 (50), S. 17404–17409. DOI: 10.1073/pnas.0408030101.
- Palmer, Amy E.; Qin, Yan; Park, Jungwon Genevieve; McCombs, Janet E. (2011): Design and application of genetically encoded biosensors. In: *Trends in biotechnology* 29 (3), S. 144–152. DOI: 10.1016/j.tibtech.2010.12.004.
- Pampliega, Olatz; Domercq, María; Villoslada, Pablo; Sepulcre, Jorge; Rodríguez-Antigüedad, Alfredo; Matute, Carlos (2008): Association of an EAAT2 polymorphism with higher glutamate concentration in relapsing multiple sclerosis. In: *Journal of neuroimmunology* 195 (1-2), S. 194–198. DOI: 10.1016/j.jneuroim.2008.01.011.
- Pearse, D. D.; Lo, T. P.; Cho, K. S.; Lynch, M. P.; Garg, M. S.; Marcillo, A. E. et al. (2005): Histopathological and behavioral characterization of a novel cervical spinal cord displacement contusion injury in the rat. In: *Journal of neurotrauma* 22 (6), S. 680–702. DOI: 10.1089/neu.2005.22.680.

- Petrova, Natalia; Carassiti, Daniele; Altmann, Daniel R.; Baker, David; Schmierer, Klaus (2018): Axonal loss in the multiple sclerosis spinal cord revisited. In: *Brain pathology (Zurich, Switzerland)* 28 (3), S. 334–348. DOI: 10.1111/bpa.12516.
- Pfriege, Frank W. (2003): Outsourcing in the brain: do neurons depend on cholesterol delivery by astrocytes? In: *BioEssays : news and reviews in molecular, cellular and developmental biology* 25 (1), S. 72–78. DOI: 10.1002/bies.10195.
- Pineau, Isabelle; Lacroix, Steve (2007): Proinflammatory cytokine synthesis in the injured mouse spinal cord: multiphasic expression pattern and identification of the cell types involved. In: *The Journal of comparative neurology* 500 (2), S. 267–285. DOI: 10.1002/cne.21149.
- Porter, K. R. (1953): Observations on a submicroscopic basophilic component of cytoplasm. In: *The Journal of experimental medicine* 97 (5), S. 727–750.
- Porter, K. R.; Claude, A.; Fullam, E. F. (1945): A STUDY OF TISSUE CULTURE CELLS BY ELECTRON MICROSCOPY : METHODS AND PRELIMINARY OBSERVATIONS. In: *The Journal of experimental medicine* 81 (3), S. 233–246.
- Puckett, W. R.; Hiester, E. D.; Norenberg, M. D.; Marcillo, A. E.; Bunge, R. P. (1997): The astroglial response to Wallerian degeneration after spinal cord injury in humans. In: *Experimental neurology* 148 (2), S. 424–432. DOI: 10.1006/exnr.1997.6692.
- Raeymaekers, Luc; Larivière, Els (2011): Vesicularization of the endoplasmic reticulum is a fast response to plasma membrane injury. In: *Biochemical and biophysical research communications* 414 (1), S. 246–251. DOI: 10.1016/j.bbrc.2011.09.065.
- Ramírez, Omar A.; Couve, Andrés (2011): The endoplasmic reticulum and protein trafficking in dendrites and axons. In: *Trends in cell biology* 21 (4), S. 219–227. DOI: 10.1016/j.tcb.2010.12.003.
- Ramírez, Omar A.; Vidal, René L.; Tello, Judith A.; Vargas, Karina J.; Kindler, Stefan; Härtel, Steffen; Couve, Andrés (2009): Dendritic assembly of heteromeric gamma-aminobutyric acid type B receptor subunits in hippocampal neurons. In: *The Journal of biological chemistry* 284 (19), S. 13077–13085. DOI: 10.1074/jbc.M900575200.
- Reddy, H.; Narayanan, S.; Arnoutelis, R.; Jenkinson, M.; Antel, J.; Matthews, P. M.; Arnold, D. L. (2000): Evidence for adaptive functional changes in the cerebral cortex with axonal injury from multiple sclerosis. In: *Brain : a journal of neurology* 123 (Pt 11), S. 2314–2320.
- Ridge, S. C.; Sloboda, A. E.; McReynolds, R. A.; Levine, S.; Oronsky, A. L.; Kerwar, S. S. (1985): Suppression of experimental allergic encephalomyelitis by mitoxantrone. In: *Clinical immunology and immunopathology* 35 (1), S. 35–42.
- Rizzuto, R.; Pinton, P.; Carrington, W.; Fay, F. S.; Fogarty, K. E.; Lifshitz, L. M. et al. (1998): Close contacts with the endoplasmic reticulum as determinants of mitochondrial Ca<sup>2+</sup> responses. In: *Science (New York, N.Y.)* 280 (5370), S. 1763–1766.

- Rizzuto, Rosario; Stefani, Diego de; Raffaello, Anna; Mammucari, Cristina (2012): Mitochondria as sensors and regulators of calcium signalling. In: *Nature reviews. Molecular cell biology* 13 (9), S. 566–578. DOI: 10.1038/nrm3412.
- Rodriguez-Garcia, Arancha; Rojo-Ruiz, Jonathan; Navas-Navarro, Paloma; Aulestia, Francisco Javier; Gallego-Sandin, Sonia; Garcia-Sancho, Javier; Alonso, Maria Teresa (2014): GAP, an aequorin-based fluorescent indicator for imaging Ca<sup>2+</sup> in organelles. In: *Proceedings of the National Academy of Sciences of the United States of America* 111 (7), S. 2584–2589. DOI: 10.1073/pnas.1316539111.
- Rogers, W. Kirke; Todd, Michael (2016): Acute spinal cord injury. In: *Best Practice & Research Clinical Anaesthesiology* 30 (1), S. 27–39. DOI: 10.1016/j.bpa.2015.11.003.
- Rosenbluth, J. (1962): Subsurface cisterns and their relationship to the neuronal plasma membrane. In: *The Journal of cell biology* 13, S. 405–421.
- Rowland, James W.; Hawryluk, Gregory W. J.; Kwon, Brian; Fehlings, Michael G. (2008): Current status of acute spinal cord injury pathophysiology and emerging therapies: promise on the horizon. In: *Neurosurgical focus* 25 (5), E2. DOI: 10.3171/FOC.2008.25.11.E2.
- Rungta, Ravi L.; Choi, Hyun B.; Tyson, John R.; Malik, Aqsa; Dissing-Olesen, Lasse; Lin, Paulo J. C. et al. (2015): The cellular mechanisms of neuronal swelling underlying cytotoxic edema. In: *Cell* 161 (3), S. 610–621. DOI: 10.1016/j.cell.2015.03.029.
- Salinas, Sara; Proukakis, Christos; Crosby, Andrew; Warner, Thomas T. (2008): Hereditary spastic paraplegia: clinical features and pathogenetic mechanisms. In: *The Lancet. Neurology* 7 (12), S. 1127–1138. DOI: 10.1016/S1474-4422(08)70258-8.
- Salter, M. W.; Hicks, J. L. (1995): ATP causes release of intracellular Ca<sup>2+</sup> via the phospholipase C beta/IP<sub>3</sub> pathway in astrocytes from the dorsal spinal cord. In: *The Journal of neuroscience : the official journal of the Society for Neuroscience* 15 (4), S. 2961–2971.
- Sarchielli, Paola; Greco, Laura; Floridi, Ardesio; Floridi, Alessandro; Gallai, Virgilio (2003): Excitatory amino acids and multiple sclerosis: evidence from cerebrospinal fluid. In: *Archives of neurology* 60 (8), S. 1082–1088. DOI: 10.1001/archneur.60.8.1082.
- Scalfari, Antonio; Neuhaus, Anneke; Degenhardt, Alexandra; Rice, George P.; Muraro, Paolo A.; Daumer, Martin; Ebers, George C. (2010): The natural history of multiple sclerosis: a geographically based study 10: relapses and long-term disability. In: *Brain : a journal of neurology* 133 (Pt 7), S. 1914–1929. DOI: 10.1093/brain/awq118.
- Schampel, Andrea; Volovitch, Oleg; Koeniger, Tobias; Scholz, Claus-Jürgen; Jörg, Stefanie; Linker, Ralf A. et al. (2017): Nimodipine fosters remyelination in a mouse model of multiple sclerosis and induces microglia-specific apoptosis. In:

*Proceedings of the National Academy of Sciences of the United States of America* 114 (16), E3295-E3304. DOI: 10.1073/pnas.1620052114.

- Scheiter, Alexander (2020): Die Dynamik des axoplasmatischen Retikulums in Modellen der Neuroinflammation und des spinalen Traumas. Unter Mitarbeit von Martin Kerschensteiner. München: Universitätsbibliothek der Ludwig-Maximilians-Universität.
- Schumacher, Adrian Minh (2016): The role of calcium in axonal degeneration in an animal model of multiple sclerosis. Dissertation. Universitätsbibliothek der Ludwig-Maximilians-Universität, München.
- Schwab, Jan M.; Zhang, Yi; Kopp, Marcel A.; Brommer, Benedikt; Popovich, Phillip G. (2014): The paradox of chronic neuroinflammation, systemic immune suppression, autoimmunity after traumatic chronic spinal cord injury. In: *Experimental neurology* 258, S. 121–129. DOI: 10.1016/j.expneurol.2014.04.023.
- Schwaller, Beat (2010): Cytosolic Ca<sup>2+</sup> buffers. In: *Cold Spring Harbor perspectives in biology* 2 (11), a004051. DOI: 10.1101/cshperspect.a004051.
- Sharif-Alhoseini, M.; Khormali, M.; Rezaei, M.; Safdarian, M.; Hajighadery, A.; Khalatbari, M. M. et al. (2017): Animal models of spinal cord injury: a systematic review. In: *Spinal cord* 55 (8), S. 714. DOI: 10.1038/sc.2016.187.
- Shibata, Yoko; Shemesh, Tom; Prinz, William A.; Palazzo, Alexander F.; Kozlov, Michael M.; Rapoport, Tom A. (2010): Mechanisms determining the morphology of the peripheral ER. In: *Cell* 143 (5), S. 774–788. DOI: 10.1016/j.cell.2010.11.007.
- Shigeoka, Toshiaki; Jung, Hosung; Jung, Jane; Turner-Bridger, Benita; Ohk, Jiyeon; Lin, Julie Qiaojin et al. (2016): Dynamic Axonal Translation in Developing and Mature Visual Circuits. In: *Cell* 166 (1), S. 181–192. DOI: 10.1016/j.cell.2016.05.029.
- Shimomura, O.; Johnson, F. H.; Saiga, Y. (1962): Extraction, purification and properties of aequorin, a bioluminescent protein from the luminous hydromedusan, *Aequorea*. In: *Journal of cellular and comparative physiology* 59, S. 223–239. DOI: 10.1002/jcp.1030590302.
- Singh, Anoushka; Tetreault, Lindsay; Kalsi-Ryan, Suhkvinder; Nouri, Aria; Fehlings, Michael G. (2014): Global prevalence and incidence of traumatic spinal cord injury. In: *Clinical epidemiology* 6, S. 309–331. DOI: 10.2147/CLEP.S68889.
- Sintzel, Martina B.; Rametta, Mark; Reder, Anthony T. (2018): Vitamin D and Multiple Sclerosis: A Comprehensive Review. In: *Neurology and therapy* 7 (1), S. 59–85. DOI: 10.1007/s40120-017-0086-4.
- Snapp, Erik L.; Hegde, Ramanujan S.; Francolini, Maura; Lombardo, Francesca; Colombo, Sara; Pedrazzini, Emanuela et al. (2003): Formation of stacked ER cisternae by low affinity protein interactions. In: *The Journal of cell biology* 163 (2), S. 257–269. DOI: 10.1083/jcb.200306020.
- Sorbara, Catherine Diamante; Wagner, Naomi Elizabeth; Ladwig, Anne; Nikić, Ivana; Merkler, Doron; Kleele, Tatjana et al. (2014): Pervasive axonal transport deficits in

- multiple sclerosis models. In: *Neuron* 84 (6), S. 1183–1190. DOI: 10.1016/j.neuron.2014.11.006.
- Spacek, J.; Harris, K. M. (1997): Three-dimensional organization of smooth endoplasmic reticulum in hippocampal CA1 dendrites and dendritic spines of the immature and mature rat. In: *The Journal of neuroscience : the official journal of the Society for Neuroscience* 17 (1), S. 190–203.
- Stagi, Massimiliano; Gorlovoy, Philipp; Larionov, Sergey; Takahashi, Kazuya; Neumann, Harald (2006): Unloading kinesin transported cargoes from the tubulin track via the inflammatory c-Jun N-terminal kinase pathway. In: *FASEB journal : official publication of the Federation of American Societies for Experimental Biology* 20 (14), S. 2573–2575. DOI: 10.1096/fj.06-6679fje.
- Stefan, Christopher J.; Manford, Andrew G.; Emr, Scott D. (2013): ER-PM connections: sites of information transfer and inter-organelle communication. In: *Current opinion in cell biology* 25 (4), S. 434–442. DOI: 10.1016/j.ceb.2013.02.020.
- Steinman, Lawrence; Zamvil, Scott (2003): Transcriptional analysis of targets in multiple sclerosis. In: *Nature reviews. Immunology* 3 (6), S. 483–492. DOI: 10.1038/nri1108.
- Stich, O.; Perera, S.; Berger, B.; Jarius, S.; Wildemann, B.; Baumgartner, A.; Rauer, S. (2016): Prevalence of neurofascin-155 antibodies in patients with multiple sclerosis. In: *Journal of the neurological sciences* 364, S. 29–32. DOI: 10.1016/j.jns.2016.03.004.
- Stirling, David P.; Cummins, Karen; Wayne Chen, S. R.; Stys, Peter (2014): Axoplasmic reticulum Ca(2+) release causes secondary degeneration of spinal axons. In: *Annals of neurology* 75 (2), S. 220–229. DOI: 10.1002/ana.24099.
- Stone, Sarrabeth; Lin, Wensheng (2015): The unfolded protein response in multiple sclerosis. In: *Frontiers in neuroscience* 9, S. 264. DOI: 10.3389/fnins.2015.00264.
- Stromnes, Ingunn M.; Goverman, Joan M. (2006a): Active induction of experimental allergic encephalomyelitis. In: *Nature protocols* 1 (4), S. 1810–1819. DOI: 10.1038/nprot.2006.285.
- Stromnes, Ingunn M.; Goverman, Joan M. (2006b): Passive induction of experimental allergic encephalomyelitis. In: *Nature protocols* 1 (4), S. 1952–1960. DOI: 10.1038/nprot.2006.284.
- Stys, P. K.; Waxman, S. G.; Ransom, B. R. (1992): Ionic mechanisms of anoxic injury in mammalian CNS white matter: role of Na<sup>+</sup> channels and Na<sup>(+)</sup>-Ca<sup>2+</sup> exchanger. In: *The Journal of neuroscience : the official journal of the Society for Neuroscience* 12 (2), S. 430–439.
- Stys, Peter K.; Zamponi, Gerald W.; van Minnen, Jan; Geurts, Jeroen J. G. (2012): Will the real multiple sclerosis please stand up? In: *Nature reviews. Neuroscience* 13 (7), S. 507–514. DOI: 10.1038/nrn3275.

- Subramanian, K.; Meyer, T. (1997): Calcium-induced restructuring of nuclear envelope and endoplasmic reticulum calcium stores. In: *Cell* 89 (6), S. 963–971.
- Sulkowski, Grzegorz; Dąbrowska-Bouta, Beata; Salińska, Elżbieta; Strużyńska, Lidia (2014): Modulation of glutamate transport and receptor binding by glutamate receptor antagonists in EAE rat brain. In: *PloS one* 9 (11), e113954. DOI: 10.1371/journal.pone.0113954.
- Sun, Xiaojia; Minohara, Motozumi; Kikuchi, Hitoshi; Ishizu, Takaaki; Tanaka, Masahito; Piao, Hua et al. (2006): The selective Rho-kinase inhibitor Fasudil is protective and therapeutic in experimental autoimmune encephalomyelitis. In: *Journal of neuroimmunology* 180 (1-2), S. 126–134. DOI: 10.1016/j.jneuroim.2006.06.027.
- Suzuki, Junji; Kanemaru, Kazunori; Ishii, Kuniaki; Ohkura, Masamichi; Okubo, Yohei; Iino, Masamitsu (2014): Imaging intraorganellar Ca<sup>2+</sup> at subcellular resolution using CEPIA. In: *Nature communications* 5, S. 4153. DOI: 10.1038/ncomms5153.
- Tadini-Buoninsegni, Francesco; Smeazzetto, Serena; Gualdani, Roberta; Moncelli, Maria Rosa (2018): Drug Interactions With the Ca<sup>2+</sup>-ATPase From Sarco(Endo)Plasmic Reticulum (SERCA). In: *Frontiers in molecular biosciences* 5, S. 36. DOI: 10.3389/fmolb.2018.00036.
- Tang, Shen; Wong, Hing-Cheung; Wang, Zhong-Min; Huang, Yun; Zou, Jin; Zhuo, You et al. (2011): Design and application of a class of sensors to monitor Ca<sup>2+</sup> dynamics in high Ca<sup>2+</sup> concentration cellular compartments. In: *Proceedings of the National Academy of Sciences of the United States of America* 108 (39), S. 16265–16270. DOI: 10.1073/pnas.1103015108.
- Tao-Cheng, Jung-Hwa (2018): Stimulation-induced structural changes at the nucleus, endoplasmic reticulum and mitochondria of hippocampal neurons. In: *Molecular brain* 11 (1), S. 44. DOI: 10.1186/s13041-018-0387-2.
- Terasaki, M.; Jaffe, L. A.; Hunnicutt, G. R.; Hammer, J. A. (1996): Structural change of the endoplasmic reticulum during fertilization: evidence for loss of membrane continuity using the green fluorescent protein. In: *Developmental biology* 179 (2), S. 320–328.
- Terasaki, M.; Slater, N. T.; Fein, A.; Schmidek, A.; Reese, T. S. (1994): Continuous network of endoplasmic reticulum in cerebellar Purkinje neurons. In: *Proceedings of the National Academy of Sciences of the United States of America* 91 (16), S. 7510–7514.
- Terasaki, Mark (2018): Axonal endoplasmic reticulum is very narrow. In: *Journal of cell science* 131 (4). DOI: 10.1242/jcs.210450.
- Thestrup, Thomas; Litzlbauer, Julia; Bartholomäus, Ingo; Mues, Marsilius; Russo, Luigi; Dana, Hod et al. (2014): Optimized ratiometric calcium sensors for functional in vivo imaging of neurons and T lymphocytes. In: *Nature methods* 11 (2), S. 175–182. DOI: 10.1038/nmeth.2773.
- Thompson, Alan J.; Banwell, Brenda L.; Barkhof, Frederik; Carroll, William M.; Coetzee, Timothy; Comi, Giancarlo et al. (2018): Diagnosis of multiple sclerosis:

- 2017 revisions of the McDonald criteria. In: *The Lancet. Neurology* 17 (2), S. 162–173. DOI: 10.1016/S1474-4422(17)30470-2.
- Tian, Lin; Hires, S. Andrew; Looger, Loren L. (2012): Imaging neuronal activity with genetically encoded calcium indicators. In: *Cold Spring Harbor protocols* 2012 (6), S. 647–656. DOI: 10.1101/pdb.top069609.
- Trapp, B. D.; Peterson, J.; Ransohoff, R. M.; Rudick, R.; Mörk, S.; Bö, L. (1998): Axonal transection in the lesions of multiple sclerosis. In: *The New England journal of medicine* 338 (5), S. 278–285. DOI: 10.1056/NEJM199801293380502.
- Trojano, M.; Paolicelli, D.; Bellacosa, A.; Cataldo, S. (2003): The transition from relapsing-remitting MS to irreversible disability: clinical evaluation. In: *Neurological sciences : official journal of the Italian Neurological Society and of the Italian Society of Clinical Neurophysiology* 24 Suppl 5, S268-70. DOI: 10.1007/s10072-003-0171-6.
- Tsien, R. Y. (1980): New calcium indicators and buffers with high selectivity against magnesium and protons: design, synthesis, and properties of prototype structures. In: *Biochemistry* 19 (11), S. 2396–2404. DOI: 10.1021/bi00552a018.
- Tsukita, S.; Ishikawa, H. (1980): The movement of membranous organelles in axons. Electron microscopic identification of anterogradely and retrogradely transported organelles. In: *The Journal of cell biology* 84 (3), S. 513–530.
- Tu, Huiping; Nelson, Omar; Bezprozvanny, Arseny; Wang, Zhengnan; Lee, Sheu-Fen; Hao, Yi-Heng et al. (2006): Presenilins form ER Ca<sup>2+</sup> leak channels, a function disrupted by familial Alzheimer's disease-linked mutations. In: *Cell* 126 (5), S. 981–993. DOI: 10.1016/j.cell.2006.06.059.
- Tzartos, John S.; Friese, Manuel A.; Craner, Matthew J.; Palace, Jackie; Newcombe, Jia; Esiri, Margaret M.; Fugger, Lars (2008): Interleukin-17 production in central nervous system-infiltrating T cells and glial cells is associated with active disease in multiple sclerosis. In: *The American journal of pathology* 172 (1), S. 146–155. DOI: 10.2353/ajpath.2008.070690.
- Ureshino, Rodrigo Portes; Erustes, Adolfo Garcia; Bassani, Taysa Bervian; Wachilewski, Patrícia; Guarache, Gabriel Cicolin; Nascimento, Ana Carolina et al. (2019): The Interplay between Ca<sup>2+</sup> Signaling Pathways and Neurodegeneration. In: *International journal of molecular sciences* 20 (23). DOI: 10.3390/ijms20236004.
- Vance, J. E. (1990): Phospholipid synthesis in a membrane fraction associated with mitochondria. In: *The Journal of biological chemistry* 265 (13), S. 7248–7256.
- Vance, J. E.; Pan, D.; Vance, D. E.; Campenot, R. B. (1991): Biosynthesis of membrane lipids in rat axons. In: *The Journal of cell biology* 115 (4), S. 1061–1068.
- Vanden Abeele, Fabien; Bidaux, Gabriel; Gordienko, Dmitri; Beck, Benjamin; Panchin, Yuri V.; Baranova, Ancha V. et al. (2006): Functional implications of calcium permeability of the channel formed by pannexin 1. In: *The Journal of cell biology* 174 (4), S. 535–546. DOI: 10.1083/jcb.200601115.

- Vierra, Nicholas C.; Kirmiz, Michael; van der List, Deborah; Santana, L. Fernando; Trimmer, James S. (2019): Kv2.1 mediates spatial and functional coupling of L-type calcium channels and ryanodine receptors in mammalian neurons. In: *eLife* 8. DOI: 10.7554/eLife.49953.
- Villegas, Rosario; Martinez, Nicolas W.; Lillo, Jorge; Pihan, Phillippe; Hernandez, Diego; Twiss, Jeffery L.; Court, Felipe A. (2014): Calcium release from intra-axonal endoplasmic reticulum leads to axon degeneration through mitochondrial dysfunction. In: *The Journal of neuroscience : the official journal of the Society for Neuroscience* 34 (21), S. 7179–7189. DOI: 10.1523/JNEUROSCI.4784-13.2014.
- Visavadiya, Nishant P.; Patel, Samir P.; VanRooyen, Jenna L.; Sullivan, Patrick G.; Rabchevsky, Alexander G. (2016): Cellular and subcellular oxidative stress parameters following severe spinal cord injury. In: *Redox biology* 8, S. 59–67. DOI: 10.1016/j.redox.2015.12.011.
- Wang, Songyu; Tukachinsky, Hanna; Romano, Fabian B.; Rapoport, Tom A. (2016): Cooperation of the ER-shaping proteins atlastin, lunapark, and reticulons to generate a tubular membrane network. In: *eLife* 5. DOI: 10.7554/eLife.18605.
- Warren, K. G.; Catz, I. (1994): Relative frequency of autoantibodies to myelin basic protein and proteolipid protein in optic neuritis and multiple sclerosis cerebrospinal fluid. In: *Journal of the neurological sciences* 121 (1), S. 66–73.
- Waterman-Storer, Clare M.; Salmon, E. D. (1998): Endoplasmic reticulum membrane tubules are distributed by microtubules in living cells using three distinct mechanisms. In: *Current Biology* 8 (14), S. 798–807. DOI: 10.1016/S0960-9822(98)70321-5.
- Watson, Charles; Paxinos, George; Kayalioglu, Gulgun (2009): The spinal cord. A Christopher and Dana Reeve Foundation text and atlas. 1. ed. Amsterdam, Boston: Elsevier/Academic Press. Online verfügbar unter <http://search.ebscohost.com/login.aspx?direct=true&scope=site&db=nlebk&db=nlabk&AN=248972>.
- Wegierski, Tomasz; Kuznicki, Jacek (2018): Neuronal calcium signaling via store-operated channels in health and disease. In: *Cell calcium* 74, S. 102–111. DOI: 10.1016/j.ceca.2018.07.001.
- Willer, C. J.; Dymont, D. A.; Risch, N. J.; Sadovnick, A. D.; Ebers, G. C. (2003): Twin concordance and sibling recurrence rates in multiple sclerosis. In: *Proceedings of the National Academy of Sciences of the United States of America* 100 (22), S. 12877–12882. DOI: 10.1073/pnas.1932604100.
- Williams, Philip R.; Marincu, Bogdan-Nicolae; Sorbara, Catherine D.; Mahler, Christoph F.; Schumacher, Adrian-Minh; Griesbeck, Oliver et al. (2014): A recoverable state of axon injury persists for hours after spinal cord contusion in vivo. In: *Nature communications* 5, S. 5683. DOI: 10.1038/ncomms6683.
- Witte, Maarten E.; Schumacher, Adrian-Minh; Mahler, Christoph F.; Bewersdorf, Jan P.; Lehmitz, Jonas; Scheiter, Alexander et al. (2019): Calcium Influx through

- Plasma-Membrane Nanoruptures Drives Axon Degeneration in a Model of Multiple Sclerosis. In: *Neuron* 101 (4), 615-624.e5. DOI: 10.1016/j.neuron.2018.12.023.
- Wolf, J. A.; Stys, P. K.; Lusardi, T.; Meaney, D.; Smith, D. H. (2001): Traumatic axonal injury induces calcium influx modulated by tetrodotoxin-sensitive sodium channels. In: *The Journal of neuroscience : the official journal of the Society for Neuroscience* 21 (6), S. 1923–1930.
- Wu, Yumei; Whiteus, Christina; Xu, C. Shan; Hayworth, Kenneth J.; Weinberg, Richard J.; Hess, Harald F.; Camilli, Pietro de (2017): Contacts between the endoplasmic reticulum and other membranes in neurons. In: *Proceedings of the National Academy of Sciences of the United States of America* 114 (24), E4859-E4867. DOI: 10.1073/pnas.1701078114.
- Wucherpfennig, K. W.; Strominger, J. L. (1995): Molecular mimicry in T cell-mediated autoimmunity: viral peptides activate human T cell clones specific for myelin basic protein. In: *Cell* 80 (5), S. 695–705.
- Yahata, Naoki; Yuasa, Shigeki; Araki, Toshiyuki (2009): Nicotinamide mononucleotide adenylyltransferase expression in mitochondrial matrix delays Wallerian degeneration. In: *The Journal of neuroscience : the official journal of the Society for Neuroscience* 29 (19), S. 6276–6284. DOI: 10.1523/JNEUROSCI.4304-08.2009.
- Yan, Tingting; Feng, Yan; Zheng, Jin; Ge, Xinjian; Zhang, Yi; Wu, Dongmei et al. (2010): Nmnat2 delays axon degeneration in superior cervical ganglia dependent on its NAD synthesis activity. In: *Neurochemistry international* 56 (1), S. 101–106. DOI: 10.1016/j.neuint.2009.09.007.
- Yednock, T. A.; Cannon, C.; Fritz, L. C.; Sanchez-Madrid, F.; Steinman, L.; Karin, N. (1992): Prevention of experimental autoimmune encephalomyelitis by antibodies against alpha 4 beta 1 integrin. In: *Nature* 356 (6364), S. 63–66. DOI: 10.1038/356063a0.
- Yoshimura, Kazuhiro; Ueno, Masaki; Lee, Sachiko; Nakamura, Yuka; Sato, Akinobu; Yoshimura, Koichi et al. (2011): c-Jun N-terminal kinase induces axonal degeneration and limits motor recovery after spinal cord injury in mice. In: *Neuroscience research* 71 (3), S. 266–277. DOI: 10.1016/j.neures.2011.07.1830.
- Zeng, Bo; Chen, Gui-Lan; Daskoulidou, Nikoleta; Xu, Shang-Zhong (2014): The ryanodine receptor agonist 4-chloro-3-ethylphenol blocks ORAI store-operated channels. In: *British journal of pharmacology* 171 (5), S. 1250–1259. DOI: 10.1111/bph.12528.
- Zhang, Ning; Fang, Marong; Chen, Haohao; Gou, Fangming; Ding, Mingxing (2014): Evaluation of spinal cord injury animal models. In: *Neural Regeneration Research* 9 (22), S. 2008–2012. DOI: 10.4103/1673-5374.143436.
- Zhao, Yongxin; Araki, Satoko; Wu, Jiahui; Teramoto, Takayuki; Chang, Yu-Fen; Nakano, Masahiro et al. (2011): An expanded palette of genetically encoded Ca<sup>2+</sup> indicators. In: *Science (New York, N.Y.)* 333 (6051), S. 1888–1891. DOI: 10.1126/science.1208592.

## Acknowledgements

First, I would like to thank both of my supervisors, Prof. Martin Kerschensteiner (LMU) and Prof. Thomas Misgeld (TUM), for making such a unique research opportunity in their laboratories possible. I am grateful for learning from their wide knowledge in neuroscience and the general tools of research. From the beginning, they were open to support my ideas and suggestions for the future progress of my project. The friendly and coequal environment during all our project and non-project related discussions also kept me substantially motivated.

Besides my advisors, I really enjoyed working with all my colleagues in the two laboratories. I thank them for their intellectual and mental support throughout the whole year. Especially noteworthy was the assistance and friendship of Christoph Mahler and Adrian-Minh Schumacher who worked on the same project with me. I am also very grateful for all the funny chats, gaming nights and activities with my other “small lab” members – Tradite Neziraj, Marta Wesolowski, Stefan Syma and Saskia List – as well as Paula Sánchez, Yi-Heng Tai and Willi Ullrich. Thank you for enduring my stupid jokes, Man’s not hot singing and my endless talk about Serrano. The work on the ER project would never have been possible without Alexander Scheiter who started the whole project, taught me everything that I needed to know including how to draw sausages around axons and continuously supported me even when he went back to medical school. Without all of these people this year would not have been as memorable as it is to me now.

Finally, I would like to thank Birte, my family and all my friends for their emotional support, proofreading my manuscript and for even making my studies and this thesis possible.

# Affidavit / Eidesstattliche Versicherung



## Eidesstattliche Versicherung

Lehmitz, Jonas

Name, Vorname

Ich erkläre hiermit an Eides statt,  
dass ich die vorliegende Dissertation mit dem Titel

**Calcium and structural dynamics of the axonal endoplasmic reticulum in animal models of spinal cord injury and multiple sclerosis**

Selbstständig verfasst, mich außer der angegebenen keiner weiteren Hilfsmittel bedient und alle Erkenntnisse, die aus dem Schrifttum ganz oder annähernd übernommen sind, als solche kenntlich gemacht und nach ihrer Herkunft unter Bezeichnung der Fundstelle einzeln nachgewiesen habe.

Ich erkläre des Weiteren, dass die hier vorgelegte Dissertation nicht in gleicher oder in ähnlicher Form bei einer anderen Stelle zur Erlangung eines akademischen Grades eingereicht wurde.

Aachen, 20.12.2021

Ort, Datum

Jonas Lehmitz

Unterschrift Doktorand